

FAMU-FSU College of Engineering
Department of Electrical and Computer Engineering
System Level Design and Review



Solar Flare

EEL4911C – ECE Senior Design Project I

Project title: FAMU-FSU Shell Eco-Marathon Solar Car 2014

Team #: 2

Student team members:

- **Fritz Jeanty**, electrical engineering (Email: Fj08c@my.fsu.edu)
- **James Croasmun**, mechanical engineering (Email: Jgc10c@my.fsu.edu)
- **Zachary Barr**, electrical engineering (Email: Zacharywbarr@gmail.com)
- **Julia Clarke**, electrical engineering (Email: Julia1.clarke@famu.edu)
- **David Jolicoeur**, mechanical engineering (Email: David1.jolicoeur@famu.edu)
- **Jose Cardenal**, industrial & manufacturing engineering (Email: jic09c@eng.fsu.edu)
- **Wael Nabulsi**, electrical engineering (Email: wn11@my.fsu.edu)
- **Francois Wolmarans**, industrial & manufacturing engineering (Email: fw07@my.fsu.edu)

Senior Design Project Instructor: **Dr. Edrington, Chris**

- **Dr. Frank, Michael**
- **Dr. Amin, Kamal**
- **Dr. Hollis, Patrick**
- **Dr. Okoli, Okenwa**

Submitted in partial fulfillment of the requirements for
EEL4911C – ECE Senior Design Project I

November 15, 2013

Project Executive Summary

The Shell Eco-marathon is a long standing competition, in which Shell challenges students and enthusiasts from around the world to push the envelope for energy efficient vehicle designs. The competition gives teams the opportunity to design, build, and test their vehicles in a competitive winner-take-all environment. There are several different categories to compete in depending on the source of power of the vehicle. The current FAMU-FSU College of Engineering 2014 Solar Car team will participate in the solar car division.

The competition has two classes (each with their own rules and regulations) in which teams can compete: Urban Concept and Prototype. The Urban Concept class promotes building a practical vehicle that can operate under normal road driving conditions. Alternatively, the Prototype class encourages participants to stretch the boundaries of efficiency by making ergonomic trade-offs. For both vehicle classes, competitors will use as many attempts as possible in order to see how far the vehicle can run on the equivalent of one liter of fuel. The competition requires that all vehicles have a fixed speed and number of laps. A winner will be named for each class and fuel type, with additional prizes going to teams with a strong consideration for safety, teamwork, design, and technical innovation. The FAMU-FSU 2014 Solar Car team will participate in the prototype class, with a solar-based fuel source.

Over a period of several days, teams will be given several attempts in order to test the vehicles using a pre-determined asphalt track in Houston, Texas. The competition organizers will measure the efficiency of each run, and will then use the best run among the set in order to determine the winners for each class and energy source.

The FAMU-FSU 2014 Solar Car team plans to build a Prototype-class vehicle with a sleek profile, which minimizes nose area in order to minimize the drag on the car. The chassis will consist of carbon fiber due to its low weight and high strength. Additionally, we hope to use lightweight metals (such as aluminum) to build the seat, support structures, and mechanical parts. Based on the rules and regulations of the competition, the team will have several fireproof compartments (separated by bulkheads) in order to protect the driver. A strong consideration is given to safety, including features such as a 5-point safety harness, a roll bar, and an emergency shutdown button.

The team's primary goal is to place in the top 3 for its class and energy source division. Additionally, the team intends on being strong competitors for the safety, teamwork, and design prizes. Winning teams are awarded a prize of \$5000, which could be used by future FAMU-FSU Shell Eco-Challenge teams to improve upon future designs, and purchase high quality components. Furthermore, a prize-winning placement would establish FAMU-FSU as a serious competitor in the American division, and recognize the college and advisors who have invested time and money into the project.

Table of Contents

Project Executive Summary	2
Table of Contents.....	4
Table of Figures.....	8
Table of Tables	10
1 Introduction	11
1.1 Acknowledgements.....	11
1.2 Problem Statement.....	11
General Problem Statement	11
General Solution Approach	12
1.3 Operating Environment	13
1.4 Intended Use(s) and Intended User(s).....	13
1.5 Assumptions and Limitations	14
1.6 Expected End Product and Other Deliverables.....	15
2 System design.....	16
2.1 Mechanical Overview of the System.....	16
2.2 Major Components and Requirements of the Mechanical Systems.....	17
Chassis.....	17
Roll Bar and Rear Wheel Mount	17
Roll Hoop	18
Steering System	18
Braking System.....	18
Seat	19
Wheel Systems	19
Bulk Head.....	19
2.3 Electrical Overview of the System	20
2.4 Major Components and Requirements of the Electrical Systems.....	20
Solar Panel System	20
Battery System.....	21
Isolated DC-DC Converter	21
Motor Controller.....	22
Single Board Computer	23
Gate Driver	24
DC-DC Converter.....	26
2.5 Performance Assessment and Measurements	28
Center of Gravity (COG) Calculations	28

Weight Ratios Calculations30

Static Vertical Wheel Load Calculations31

Turning Radius and Tie Rod Calculations32

2.6 Design Process.....38

 Concept Selection Criteria.....38

 Concept Selection Criteria Prioritization38

 Design Selection40

3 Design of Major Component Subsystems.....41

 3.1 Chassis41

 3.2 Roll Bar & Rear Motor Mount42

 3.3 Roll Hoop44

 3.4 Steering System45

 Front Wheel Mount.....47

 Front Wheel Arm48

 Ball Bearings49

 Tie Rods.....50

 Rack and Pinion51

 U-Joint52

 Steering Column53

 Steering Wheel54

 3.5 Braking Systems55

 Rear Braking.....56

 Front Braking57

 Caliper58

 Caliper Mount.....59

 Front Wheel Arm60

 Rotor61

 3.6 Seat62

 3.7 Front Wheel Systems63

 3.8 Solar Panel System64

 Solar Array64

 3.9 Battery System and Isolated DC-DC Converter69

 Battery and Battery Management System (BMS).....69

 Isolated DC-DC Converter70

 3.10 Motor Controller72

 Single Board Computer72

 Gate Driver73

3.11 DC-DC Converter	74
SUBSYSTEM: ISV005V2	75
SUBSYSTEM: Texas Instruments LM5000	75
4 Schedule	79
5 Budget.....	82
Materials Budget Summary	83
Personnel Budget Summary	86
Miscellaneous Budget Summary	87
Overview Budget Summary	89
6 Overall Risk Assessment	90
6.1 Technical Risks.....	90
Competition Requirements	90
Chassis Failure.....	90
Steering Failure.....	91
Braking Failure	91
Bulkhead Design and Installation	91
Motor Controller Failure.....	92
Motor Controller Disqualification	92
DC-DC Conversion System.....	93
DC-DC Conversion Stage: ISV005V2	93
DC-DC Conversion Stage: LM5000.....	93
Battery Failure	93
Solar Panel Installation Failure.....	94
6.2 Schedule Risks.....	94
Ordered Parts	94
Required Equipment	94
Overlooked Designs	95
Testing Phase.....	95
6.3 Budget Risks.....	95
Funding Requests	95
Indirect Material Costs	96
Pricing Estimates	96
7 Conclusion.....	97
8 References	100
Appendix	102
A1: Fish Bone Analysis	102
A2: House of Quality.....	103

A3: Gantt chart	111
A4: Motor Controller Specs.....	112
A5: Chassis	117
A6: Roll Bar and Rear Wheel Mount	118
A7: Roll Hoop	119
A8: Front Wheel Arm.....	120
A9: Rack and Pinion.....	121
A10: Steering Wheel	122
A11: Calipers.....	123
A12: Caliper Mounts	124
A13: Front Wheel Arm.....	125
A14: Rotor	126
A15: Seat	127
A16: Front Wheels.....	128
A17: Rear Wheel	129
A18: Tie Rods.....	130
A19: Steering U-Joints	131
A20: Front Wheel Mounts	132
A21: Czochralski Process	133
A22 Solar Cell Technical Specifications	133
A23: Sanyo Denki Fan and Specifications	134
A24: Isolated DC-DC Converter Specifications.....	135
A25: LM5000 DataSheet.....	136

Table of Figures

Figure 1 Block diagram 1 of the mechanical system.....	16
Figure 2 Block diagram 2 of the Mechanical system	16
Figure 3 Block diagram 3 of the Mechanical System.....	17
Figure 4 Top Level Design of Electrical System [1]	20
Figure 5 Top level design of motor controller	22
Figure 6 TI TMS320F2808 [2]	23
Figure 7 Recommended Operating Environment [2].....	24
Figure 8 DRV8301DCA [3]	24
Figure 9 Function Block Diagram of TI DRV8301 [3]	25
Figure 10 Absolute Maximum Ratings of TI DRV8301 [3].....	26
Figure 11 Turning Radius Diagram [4]	33
Figure 12 Chassis.....	41
Figure 13 Roll Bar and Rear Wheel Mount	42
Figure 14 Roll Hoop	44
Figure 15 Steering System.....	45
Figure 16 Diagram of the steering System	46
Figure 17 Front Wheel Mount	47
Figure 18 Front Wheel Arm.....	48
Figure 19 Bearings [11]	49
Figure 20 Tie Rod	50
Figure 21 Rack and Pinion.....	51
Figure 22 U- Joint [11]	52
Figure 23 Steering Column.....	53
Figure 24 Steering Wheel	54
Figure 25 Braking System	56
Figure 26 Front Brakes	57
Figure 27 Calipers.....	58
Figure 28 Caliper Mount.....	59
Figure 29 Front Wheel Arm.....	60

Figure 30 Rotor	61
Figure 31 Seat	62
Figure 32 Front Wheel	63
Figure 33 Photo Of The Monocrystalline Solar Cells [1]	65
Figure 34 Solar Array Configuration Options [1]	66
Figure 35 The solar Junction Boxes used as Nodes [1]	67
Figure 36 Demonstration of Solar Panel Implementation [1]	68
Figure 37 Electric Ride LiFePO4 Battery Back [1]	69
Figure 38 Electric Ride LiFePO4 Battery Back [1]	70
Figure 39 Turnigy Watt Meter and Power Analyzer [1]	70
Figure 40 Turnigy Monitor Connections [1]	70
Figure 41 Isolated DC-DC Converter Configuration	71
Figure 42 LM25017 Isolated DC-DC Converter [5]	71
Figure 43 LM5000 [6]	75
Figure 44 LM5000 Internal circuit [6]	76
Figure 45 Voltage Divider Circuit [7]	77
Figure 46 ISV005V2 Board [8]	78
Figure 47 Design portion of the Gantt Chart	81
Figure 48 Diagram demonstrating the Czochralski process	133
Figure 49 Sanyo Denki Fan	134
Figure 50 Sanyo Denki Fan Specifications	134
Figure 51 Specifications for the LM25017 Isolated DC-DC Converter	135

Table of Tables

Table 1 Distance From the Part to the Roll Bar/Motor Mount	28
Table 2 Component Weights	29
Table 3 Moment Calculation Results.....	29
Table 4 Distance Front the Cars Center of Gravity to the Front of the Vehicle And to the Roll Bar.....	30
Table 5 Weight Ratios	31
Table 6 Static Vertical Wheel Loads	31
Table 7 Turning Radius Dimensions	34
Table 8 Turning Radiuses for various Wheel Widths.....	35
Table 9 Material quantity volume & Desired type	84
Table 10 aluminum Grade pricing	84
Table 11 Part Cost based on Aluminum type	85
Table 12 total part volume	86
Table 13 Polymer sheet prices	86
Table 14 Personnel budget.....	87
Table 15 miscellaneous budget.....	88
Table 16 remaining funds	88
Table 17 summary of direct costs (minus materials)	89
Table 18 total estimated cost (minus materials)	89
Table 19 Solar Cell Irradiation Profile.....	133
Table 20 Solar Cell Temperature Coefficients	133
Table 21 Solar Cell Electrical Performance.....	134

1 Introduction

1.1 Acknowledgements

The FAMU-FSU 2014 Solar Car team would like to thank the High Performance Materials Institute (HPMI) at Florida State University (FSU) for their generous donation of the materials necessary to build the vehicle. Additionally, we would also like to thank Dr. Edrington, Dr. Frank, and Dr. Amin for their technical support and guidance throughout the process. Their contributions have been invaluable allowing the team to make the necessary decisions which have carried the project forward. Additionally we would like to thank Dr. Liang, Dr. Okoli, Mr. Allen, and Mr. Horne for their role in the donation of materials and technical assistance in building the carbon fiber chassis.

1.2 Problem Statement

General Problem Statement

The team is required to build a solar-powered electrical vehicle which conforms to the rules and regulations of the Shell 2014 Eco-Challenge competition. The car is required to have several features which will ensure the safety of the driver and reduce the risk of mechanical or electrical failure. There are several dimension limitations including the height, width, ratio of height to track width, wheelbase, total length, and vehicle weight. Additionally, there are minimum standards established for the turning radius, and braking requirements. The primary concern for ranking in the competition is the efficiency of the vehicle, which will be determined by the organizer's evaluation. The largest problem that has to be solved is striking a balance between the necessary trade-offs for the weight, the cost, and the safety of vehicle.

General Solution Approach

This project is a large and complex undertaking. In order to determine where and how to begin, the team performed a house of quality analysis with the input of all 3 engineering disciplines. Using the competition rules and regulations as customer requirements and tentative components as quality characteristics used to fulfill those customer requirements; we were able to get a better understanding of how to prioritize objectives. Based on the results, we determined that the cost, weight, and safety of the vehicle were going to be the areas of concern. Ergonomic considerations also ranked high, but due to the nature of the prototype division, there is room for slack in this area.

Cost was kept as a primary concern to ensure that we stayed on (or below) budget. With this in mind we set out to minimize the weight of the overall design. The largest contributor to the weight was the chassis due to its relatively large size. In order to minimize weight it was decided that a low weight yet high strength material was necessary. After consulting with faculty, the 2013 team decided to build the chassis using carbon fiber donated by the High Performance Materials Institute. This decision was made after alternatives were eliminated due to cost or technical difficulty.

Additionally, the team has decided to use aluminum for additional mechanical parts, as well as stationary parts, such as the seat and roll bar. All design specifications fell within the ranges necessary for participation in the competition. The mechanical engineers were able to design a steering mechanism which would allow for separation of the driver from the mechanical and electrical components, and yield the minimum turning radius. For braking, the team decided to implement a regenerative braking system and a dual front/back braking system.

1.3 Operating Environment

The vehicle will operate on an asphalt track which has been set aside for use for the Shell 2014 Eco-Challenge marathon. The race will take place during the summer months in Houston, Texas. Based on our research, we have determined that dusty conditions and heat could be a concern. Additionally, due to the competition being held during the summer months, there exists a possibility of rainfall. The team has planned for the worst by including a comprehensive terrain and weather test in order to ensure that the vehicle is able to operate in adverse conditions.

1.4 Intended Use(s) and Intended User(s)

Due to the nature of the competition (race) ergonomic design considerations will be made for two drivers. The team has nominated Julia Clarke as the driver for the competition. In the event of an emergency, they have nominated Jose Cardenal as the backup driver. Using anthropometric data for individuals fitting their description, we will design the internal compartments to maximize their safety, accessibility, and field of vision. By performing an analysis of the user's anthropometry, posture, and repetitive motion, the team will be able to build a vehicle with tailor-fit ergonomic design. The goal is ensure a good fit for both drivers, which will lead to decreased fatigue and discomfort when operating the vehicle.

The vehicle will be used to compete in the 2014 Shell Eco-Challenge marathon. It will be raced on an asphalt track with the equivalent of 1 liter of fuel in order to determine the efficiency. Based on the regulations of the competition, the team does not intend for the car to exceed a speed of 15 mph. The turning radius will not be smaller than 8 meters at any given time. It is possible that the vehicle could be operated in a high heat or rainy environment.

1.5 Assumptions and Limitations

Various assumptions will be made in order to design and construct the vehicle. Each major component of the vehicle has been broken down into three parts. The first part of each component is the “design and analysis” phase. The team will design and analyze each major component within 9 days of the designated starting point. The second part of each component is the manufacturing of major parts. The team will manufacture in-house parts within 21 days of the designated starting point. The team will manufacture parts which require ordered materials, or components within 30 days of the designated starting point in order to provide a 9 day ordering/shipping period for each part. The third part of each major component is the installation. The team will install each major component of the vehicle within two days of the designated start date.

The team will build the following parts in house: front wheel mount, steering wheel, seat, seat mount rail, front bulkhead, and rear bulkhead. These parts will be built in house in order to minimize the cost of the vehicle while building parts that conform to the competitions rules and requirements. The front wheel, rear view mirrors, steering column, braking system, wiring necessities and, board and accessory battery will be purchased. These parts will be purchased in order to assure quality and reliability.

The team shall not exceed an overall cost of \$6,000 in the design and manufacturing phase of the vehicle. Once the design and manufacturing phase is completed the car will be up to date with all competition rules and requirements. Furthermore, costs such as competition transportation will come from department funding.

Due to the rules and regulations of the competition the vehicle will have various limitations. Based on the competitions safety regulations the car will have a roll bar which rises a minimum of 5cm over the driver’s head, an escape plan exceeding no more than 10 seconds, fire redundant

compartments which separate the driver from all electrical components and from the driving transmission, a 180 degree field of vision, and an emergency shutdown button which turns off all electrical components. Furthermore, based on the dimension and weight limitations placed by the competition the car will have a maximum height less than 100 cm, a minimum vehicle width of 50 cm and a maximum width of 130 cm from the point where the outermost tires touch the ground, a ratio of height divided by track width less than 1.25, a maximum length of 350cm, and a weight less than 140kg. Based on cost limitations, the team shall not exceed \$6,000. This limitation is set by the amount of money provided through the project funding.

1.6 Expected End Product and Other Deliverables

The expected end product is a completed and functioning solar-electric powered vehicle which adheres to the rules and regulations of the Shell Eco-Challenge. Additionally the team will produce a technical manual containing the specifications and safety features of the car for Phase II registration by the December deadline. This manual is a check on the team to ensure that they are in compliance with the rules and regulations of the competition.

2 System design

2.1 Mechanical Overview of the System

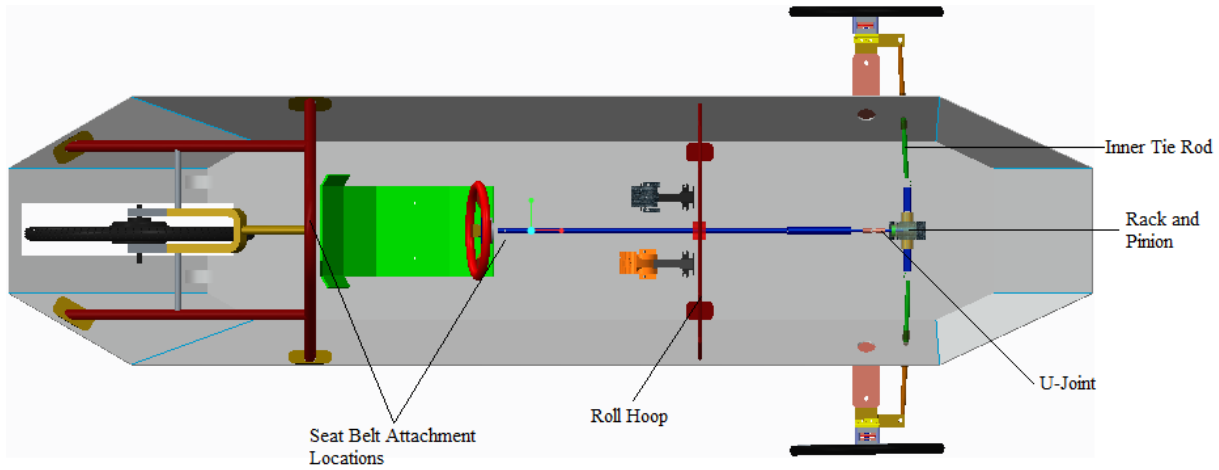


FIGURE 1 BLOCK DIAGRAM 1 OF THE MECHANICAL SYSTEM

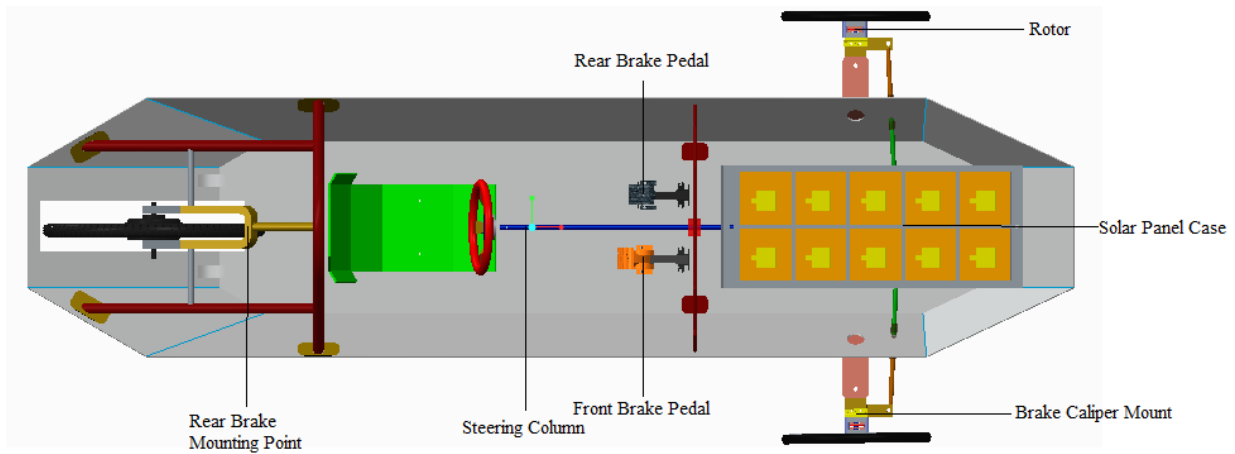


FIGURE 2 BLOCK DIAGRAM 2 OF THE MECHANICAL SYSTEM

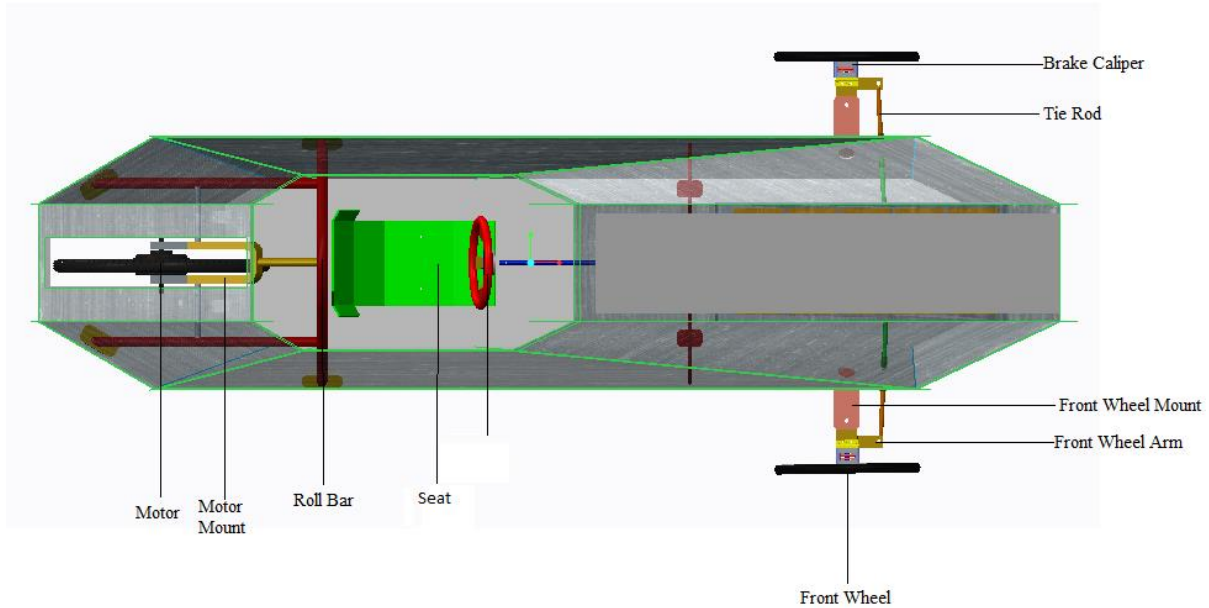


FIGURE 3 BLOCK DIAGRAM 3 OF THE MECHANICAL SYSTEM

2.2 Major Components and Requirements of the Mechanical Systems

Chassis

The rules mandated by Shell Eco-Marathon require that the chassis support the full load of the driver and structural components without deformation. The vehicle's body must retain its shape during gusts of rain, winds, and any environmental effects that can occur. The vehicle's body must also be designed with a drag coefficient less than or equal to 0.15. A reduction in the coefficient of drag will increase the overall efficiency and performance.

Roll Bar and Rear Wheel Mount

The roll bar and rear motor mount must be in compliance with the requirements issued by the Shell Eco-Marathon competition. The requirements state that the roll bar must be 5cm above the drivers head when fully seated, and approximately 2cm from the shoulders on each side. The

roll bar must also be capable of withstanding a static load of 700N in any direction without deformation.

Roll Hoop

The roll hoop protects the driver's legs and the front portion of the chassis during a roll over. If the car were to flip the roll hoop would be the second place on the car that would come in contact with the ground. By using a sturdy roll hoop the team will assure that the car is not deformed leaving the driver trapped inside in the case of an emergency. Furthermore, it will allow the mass of the steering column and wheel to be supported. The use of a roll hoop increases the safety of the design and the structural integrity of the chassis.

Steering System

The Shell Eco-Marathon Competition requires the vehicle to have an 8 meter turning radius which must be properly installed and implemented in order to ensure safety when maneuvering along the track. The steering system includes the front wheel steering assemblies, rack and pinion, steering column, and steering wheel.

Braking System

The Shell Eco-Marathon Competition has various braking requirements which must be met in order for team to compete. The vehicle must have two independent braking systems one for the front wheels the other for the back wheels. Each braking system must be capable of holding the vehicle in place when engaged on a 20 degree incline. The front braking system will use a disc and caliper system and the rear braking system will use a bicycle braking system. Each braking system will be engaged by individual foot pedals.

Seat

Comfort, safety, and convenience are important factors in the ergonomic functionality of the car seat design. The Shell Eco-Marathon Competition has required that the seat must be designed so that the driver's head will remain at least 5 centimeters below the top of the roll bar. The seat must be positioned so that the driver can see clearly over the steering wheel, as well as reach the accelerator and brake pedals. In addition, the driver's seat must be equipped with an effective safety harness having at least five mounting points to keep the driver in the seat. The 5-point harness must be firmly attached to the vehicle's chassis and fitted into a single buckle.

Wheel Systems

All types of wheels and tires are permitted however wheels located in the vehicle body must be isolated from the driver by fire-retardant bulkheads. The three wheels must support the full load of the car and driver; furthermore, they must remain in contact with the ground at all times. Based on input from various advisors the teams current proposed design is to use bicycle or wheelchair hubs and rims. These types of wheels will have low weights and small surface contact areas which will lead to smaller values for the static and kinetic frictions. The main difference between the two is that the support rod which runs through the hub is generally larger for wheelchairs than for bicycles.

Bulk Head

The bulkhead must be made from fire retardant material. It will separate the driver from all moving parts, wires, and electrical components. It is required by the Shell Eco-Marathon Competition to have one installed in the chassis in order to pass the safety regulations.

2.3 Electrical Overview of the System

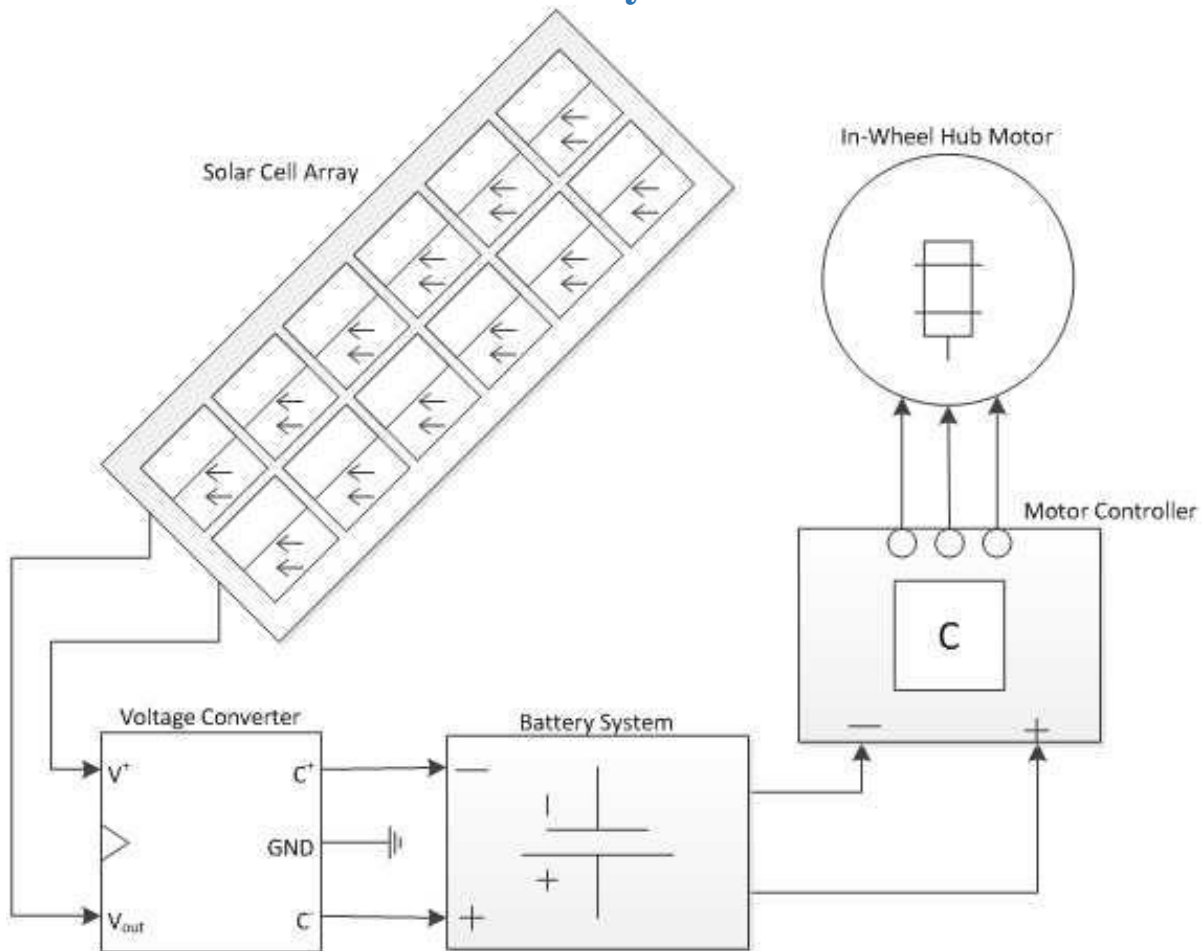


FIGURE 4 TOP LEVEL DESIGN OF ELECTRICAL SYSTEM [1]

2.4 Major Components and Requirements of the Electrical Systems

Solar Panel System

The Shell Eco – Marathon Competition states the allowable amount of solar energy is 20% of the total propulsion energy consumed; and the total combined surface area of solar cells will be less than 0.17m^2 . The solar arrays must not protrude from the vehicle. A third diode will be used to serve as protection from unwanted current flow into the modules. $125 \times 125\text{mm}$ Monocrystalline solar cells will be used to provide a high electrical efficiency.

Battery System

Shell Eco-Marathon competition states that the vehicle must have one lithium ion battery with a battery management system (BMS). The battery must be in a separated from other compartments by a flame retardant bulk head. A 24V, 20Ah battery pack LiFePO₄ battery from electric rider is being used to power the car. The battery pack purchased from Electric Rider contains a BMS that will meet the requirements of the competition and will protect and monitor the entire battery pack as well as individual cells.

Isolated DC-DC Converter

An accessory battery was originally going to be used to power all of the instrumentation. After consulting with Dr. Edrington, it was decided that instead of an accessory battery an isolated DC-DC converter would be used to power the instrumentation. An isolated DC-DC converter was chosen because of its built in transformer which provides an added safety feature.

When choosing an isolated DC-DC converter it is important to get the voltage rating for the input, and voltage and current ratings for the output so the right converter can be selected. If the converter picked does not fall within the specifications for the component a problem could arise. The team made sure that all the specifications for the component that would be hooked up to the converter matched the converter so no problems would occur. The LM25017 was the isolated DC-DC converter that was chosen.

Motor Controller

Competition requirements state that students design their own motor controller. The motor controller has been broken up into three components. The single board controller, driver stage and power stage.

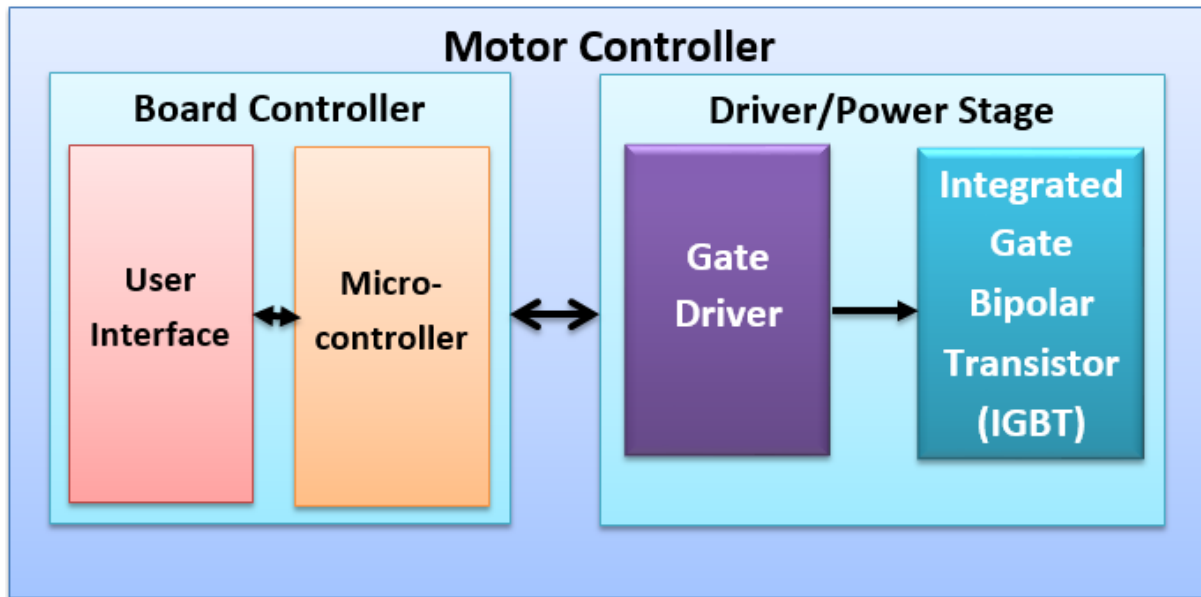


FIGURE 5 TOP LEVEL DESIGN OF MOTOR CONTROLLER

For competition purposes, the main blocks of the motor controller's top level block diagram are the single board controller, driver stage and power stage as illustrated in Figure 5. The user interface communicates over a standard or proprietary field bus that generates the proper switching patterns to control the motor's motion based on feedback from the host. The gate drivers generate the necessary voltage and current required to accurately and efficiently drive the Insulated Gate Bipolar Transistor (IGBT) in the power stage.

After developing an understanding for the control requirements of the Magic Pie Motor, a single board controller was decided upon in order to develop the interface between the driven and power stage of the motor controller and the motor, a gate driver to generate the necessary voltage

and current required to accurately and efficiently drive the power stage and an IGBT was chosen to regulate the current flow in the power stage to prevent excess current to the motor.

Single Board Computer



FIGURE 6 TI TMS320F2808 [2]

The single board controller that will be used to develop the interface between the driver and power stage of the motor controller is the TI TMS320F2808. The TI TMS320F2808 has 56 I/O pins that can be used in the implementation of the horn or shutdown system. Figure 7 shows the recommended operating conditions

over operating free-air temperature range (unless otherwise noted)

		MIN	NOM	MAX	UNIT
Device supply voltage, I/O, V_{DDIO}		3.14	3.3	3.47	V
Device supply voltage CPU, V_{DD}		1.71	1.8	1.89	V
Supply ground, V_{SS} , V_{SSIO}		0			V
ADC supply voltage (3.3 V), V_{DDA2} , V_{DDAIO}		3.14	3.3	3.47	V
ADC supply voltage (1.8 V), V_{DD1A18} , V_{DD2A18}		1.71	1.8	1.89	V
Flash supply voltage, V_{DD3VFL}		3.14	3.3	3.47	V
Device clock frequency (system clock), $f_{SYSCLKOUT}$	100-MHz devices	2		100	MHz
	60-MHz devices	2		60	MHz
High-level input voltage, V_{IH}	All inputs except X1	2		$V_{DDIO} + 0.3$	V
	X1	$0.7 * V_{DD} - 0.05$		V_{DD}	
Low-level input voltage, V_{IL}	All inputs except X1	$V_{SS} - 0.3$		0.8	V
	X1			$0.3 * V_{DD} + 0.05$	
High-level output source current, $V_{OH} = 2.4 V$, I_{OH}	All I/Os except Group 2			-4	mA
	Group 2 ⁽¹⁾			-8	
Low-level output sink current, $V_{OL} = V_{OL MAX}$, I_{OL}	All I/Os except Group 2			4	mA
	Group 2 ⁽¹⁾			8	
Ambient temperature, T_A	A version	-40		85	°C
	S version	-40		125	
	Q version (Q100 Qualification)	-40		125	

FIGURE 7 RECOMMENDED OPERATING ENVIRONMENT [2]

Gate Driver



[3] FIGURE 8 DRV8301DCA

The gate driver that will be used is the Texas Instrument DRV8301. The operating supply voltage for the DRV8301 is between 0-70V. It also has a maximum supply current of 15mA. Being that the motor will be operating for an extended period of time, it is imperative to note that the DRV8301 operate at temperatures ranging from -40C (-40F) to 125C (257F). In addition, the user has independent control of up to 6 Pulse Width Modulation Inputs. Figure 9 and Figure 10

show the Function Block Diagram and Absolute Maximum Ratings of the TI DRV8301 respectively.

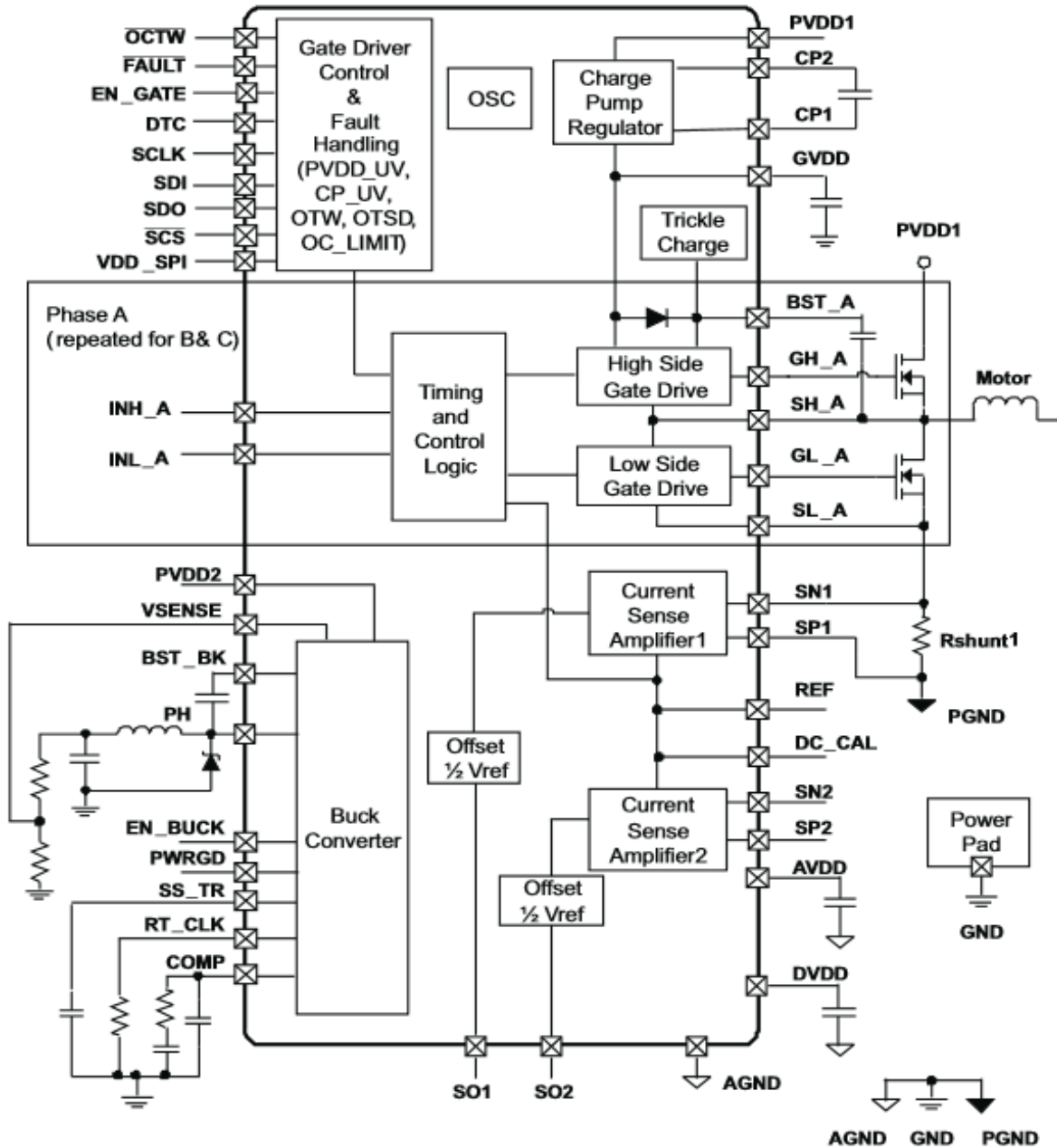


FIGURE 9 FUNCTION BLOCK DIAGRAM OF TI DRV8301 [3]

			VALUE		UNITS
			MIN	MAX	
PVDD	Supply voltage range including transient	Relative to PGND	-0.3	70	V
PVDD _{RAMP}	Maximum supply voltage ramp rate	Voltage rising up to PVDD _{MAX}		1	V/ μ S
V _{PGND}	Maximum voltage between PGND and GND		± 0.3		V
I _{IN_MAX}	Maximum current for all digital and analog inputs (INH_A, INL_A, INH_B, INL_B, INH_C, INL_C, SCLK, SCS, SDI, EN_GATE, DC_CAL, DTC)		± 1		mA
I _{IN_OD_MAX}	Maximum sinking current for open drain pins ($\overline{\text{FAULT}}$ and $\overline{\text{OCTW}}$ Pins)		7		mA
V _{OPA_IN}	Voltage range for SPx and SNx pins		± 0.6		V
V _{LOGIC}	Input voltage range for logic/digital pins (INH_A, INL_A, INH_B, INL_B, INH_C, INL_C, EN_GATE, SCLK, SDI, SCS, DC_CAL)		-0.3	7	V
V _{GVDD}	Maximum voltage for GVDD Pin		13.2		V
V _{AVDD}	Maximum voltage for AVDD Pin		8		V
V _{DVDD}	Maximum voltage for DVDD Pin		3.6		V
V _{VDD_SPI}	Maximum voltage for VDD_SPI Pin		7		V
V _{SDO}	Maximum voltage for SDO Pin		VDD_SPI +0.3		V
V _{REF}	Maximum reference voltage for current amplifier		7		V
I _{REF}	Maximum current for REF Pin		100		μ A
T _J	Maximum operating junction temperature range		-40	150	$^{\circ}$ C
T _{STORAGE}	Storage temperature range		-55	150	$^{\circ}$ C
	Capacitive discharge model		500		V
	Human body model		2000		V

FIGURE 10 ABSOLUTE MAXIMUM RATINGS OF TI DRV8301 [3]

DC-DC Converter

The requirement for the DC-DC conversion system as a whole is the transfer of DC power generated at the solar panels and conversion of this DC power in to a suitable voltage level capable of charging the battery while the car is in use. This was not accomplished last year because the highest voltage level achieved for the DC-DC converter was approximately 24V in the most favorable of conditions.

The ISV005V2 board is currently being used however it is not successful in charging the battery. A part replacement or addition is required to get the ISV005V2 to charge the battery. Initially, a proposed solution was to replace several of the resistors to get the ISV005V2 to charge the battery. However, a second DC-DC boosting stage will be implemented after the existing ISV005V2 board. The product selected to accomplish this task will be the Texas instruments LM5000.

Thus, the requirements this year is to further boost this voltage to a level of approximately 26V and sufficiently charge the battery while the car is in use. This will be achieved through 2 stages of DC-DC conversion. These stages must be able to properly boost the DC power created by the solar panels and sufficiently charge the battery to be considered successful.

Requirements specifications: Subsystem: ISV005V2

According to the previous year's final report testing plan, the ISV005V2 was able to boost the DC generated in the solar panels to a voltage of 24V. However, this was assuming that the car would always be under the most ideal conditions of sunlight. In order to remedy this design flaw, a second DC-DC conversion stage is to be implemented.

Thus, the ISV005V2 will be the first stage of DC-DC conversion after the solar panels. This is in order to take full advantage of the MPPT algorithm inside of the ISV005V2 board. The requirements of this stage are to boost the voltage to a respectable level of at least 10V. This value is based off of a test that was conducted in a cloudy weather environment and as such is considered the worst case scenario voltage to leave the first stage of DC-DC conversion. The test voltage during cloudy weather had an exit voltage of 11.5V so a value of 10V leaving the first stage of DC-DC conversion is not unreasonable.

Requirements specifications: Subsystem: LM5000

The second DC-DC Converter will need to operate as a secondary power boost after the initial DC boost occurs. More specifically, the DC power originates in the solar panel, is boosted using the MPPT algorithm located in the ISV005V2 to the highest possible voltage, and then boosted once again using the newly implemented DC-DC converter.

Thus, the requirements for the LM5000 DC-DC converter is to boost the voltage to a safe level that will be able to charge the battery when in use. This must be accomplished using only the voltage generated from the ISV005V2 DC-DC converter (minimum 10V). The necessary voltage in order to charge the battery while the car is in use is 26V. This will be considered the minimum allowable output voltage of the secondary stage DC-DC converter.

2.5 Performance Assessment and Measurements

Center of Gravity (COG) Calculations

In order to determine the weight ratios for the chassis and normal maximum static loads for each wheel the theoretical center of gravity was calculated. The process was started by first measuring the distance distances from the roll bar/motor mount to each components center of gravity is shown in Table 1. The parts and components which have been considered in the measurements are the larger heavier parts which cause large moments on the chassis.

Part:	Distance taken from roll bar (in)
Battery	85
Front Mounts	69.5
Rack and Pinion	61
Petals	56
Driver	21
Roll bar/ Rear Motor Mount	0

TABLE 1 DISTANCE FROM THE PART TO THE ROLL BAR/MOTOR MOUNT

The next step in the calculation required the weight of each component. Although the majority of these values were known, some values were estimated due to the uncertainty of the materials used for those components. The weight of each component considered in the calculation can be seen in Table 2 Component Weights.

Part:	Weight (lbs)
Battery	20
Front Mounts	20
Rack and Pinion	2.6
Petals	1.51
Driver	170
Roll bar/ Rear Motor Mount	20

TABLE 2 COMPONENT WEIGHTS

The moment for each part was then calculated from the roll bar using the Equation 1. The results for these calculations can be seen in Table 3.

EQUATION 1

$$\text{Moment (lbs * in)} = \text{Weight (lbs)} * \text{Length from roll bar (in)}$$

Part:	Moment (lbs.*in):
Battery	1700
Front Mounts	1390
Rack and Pinion	158.6
Petals	84.56
Driver	3570
Roll bar/ Rear Motor Mount	0

TABLE 3 MOMENT CALCULATION RESULTS

The distance to the car's center of gravity from the roll bar was calculated using Equation 2 and the values for its distance from the roll bar and the front of the chassis are displayed in Table 4.

$$\text{EQUATION 2 } \textit{Distance from roll bar (in)} = \frac{\textit{Sum of the moments (lbs*in)}}{\textit{Sum of weights (lbs)}}$$

Location:	Distance taken from roll bar (in):	Distance from the front x(0) (in):
Car's COG	14.237	82.762

TABLE 4 DISTANCE FRONT THE CARS CENTER OF GRAVITY TO THE FRONT OF THE VEHICLE AND TO THE ROLL BAR

Weight Ratios Calculations

Once the center of gravity was determined, the team used those values in order to calculate the weight ratios. The weight were determined using the cars center of gravity from the motor mount and the measured wheel base as shown in Equation 3 and in Equation 4.

$$\text{EQUATION 3 } \textit{Front Weight Ratio} = \frac{\textit{Distance from the Car's COG to motor mount}}{\textit{The measured wheel base}}$$

$$\text{EQUATION 4 } \textit{Rear Weight Ratio} = \frac{\textit{Distance from the car's COG to the front wheel mounts}}{\textit{The measured wheel base}}$$

The distance used in Equation 3 is not equal to the distance from the car's COG to the roll bar/motor mounts COG because the rear wheel is located further back in the chassis than its center of gravity. The calculated weight ratios can be seen in Table 5.

Weight Ratios	
Front:	.354
Rear	0.646

TABLE 5 WEIGHT RATIOS

Static Vertical Wheel Load Calculations

The static vertical wheel loads were calculated using Equation 5 and Equation 6 . The results can be seen in Table 6.

EQUATION 5

$$\begin{aligned}
 & \textit{Front Static Vertical Wheel Loads (lbs)} \\
 & = \frac{\textit{Maximum load (lbs)} * \textit{Distance from motor to COG}_{car}(\textit{in})}{\textit{Wheel Base (in)}}
 \end{aligned}$$

EQUATION 6

$$\begin{aligned}
 & \textit{Rear Static Vertical Wheel load(lbs)} \\
 & = \frac{\textit{Maximum load (lbs)} * \textit{Distance from front mounts to COG}_{car}(\textit{in})}{\textit{Wheel Base (in)}}
 \end{aligned}$$

Static Vertical Wheel Loads (lbs.)	
Front:	166.232
Rear	303.782

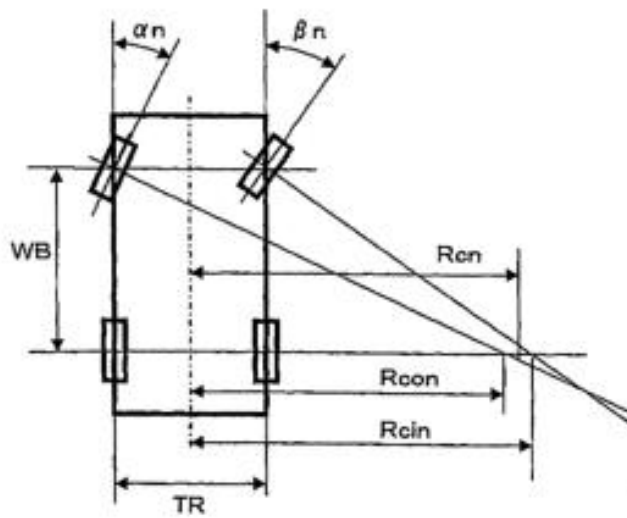
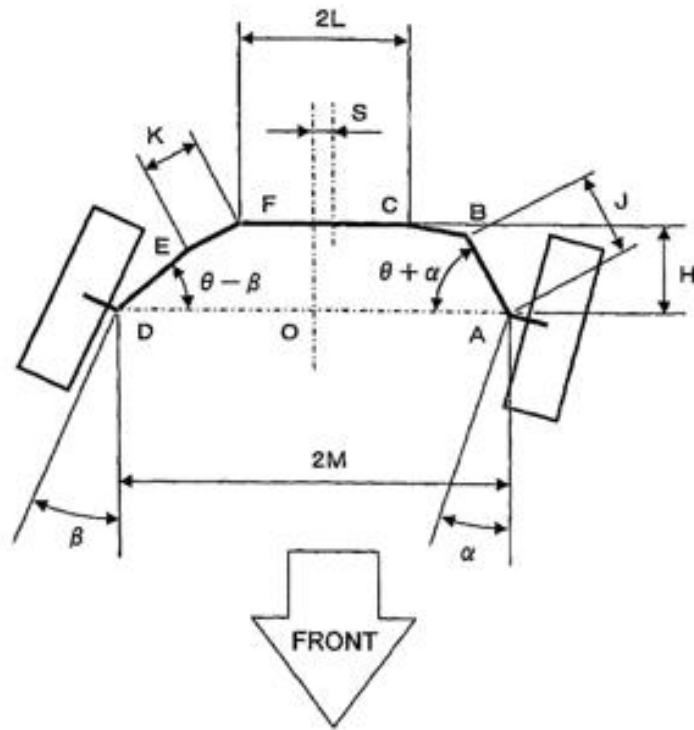
TABLE 6 STATIC VERTICAL WHEEL LOADS

These static vertical wheel loads are the maximum loads that will be imposed on the chassis at any given time. The maximum load used in the equation above was the maximum weight of the car allowed by the competition plus the weight of the driver assuming the driver weighs 160 lbs.

Although the full magnitude of these forces most likely never be reached the team used the maximum forces that could exist on the system in order to assure quality, safety, and reliability.

Turning Radius and Tie Rod Calculations

According to the competition rules and regulation the vehicle must have at least an 8m turning radius. [4] Figure 11 illustrates how the turning radius of the vehicle was calculated.



[4] FIGURE 11 TURNING RADIUS DIAGRAM

The known variables in the above diagrams are M and WB . WB is our measured wheel base for our chassis which is approximately 85.5 in (2.17 m). M is the distance from the center neutral axis of the chassis to the kingpin which the steering assemblies rotate around. These distances for various rim sizes are shown in Table 7.

Wheel Width (in):	M Distance (in):	M (meters)
12	16	0.406
14	16.708	0.424
16	17.416	0.442
18	18.125	0.4603
20	18.833	0.478
22	19.542	0.496

TABLE 7 TURNING RADIUS DIMENSIONS

The values shown in Table 7 were used along with Equation 7, Equation 8, and Equation 9 to determine the turning radius for a desired maximum turning angle $\alpha\eta$ and $\beta\eta$. These turning angles in our calculations $\alpha\eta$ and $\beta\eta$ are both equal to 35° .

$$\text{EQUATION 7 } R_{cin} = \frac{WB}{\tan(\beta\eta) + M}$$

$$\text{EQUATION 8 } R_{con} = \frac{WB}{\tan(\alpha\eta) - M}$$

$$\text{EQUATION 9 } \textit{Turning Radius } R_{cn} = \frac{R_{cin} + R_{con}}{2}$$

The team calculated the turning radiuses for various rim sizes with wheel widths ranging from 12-22 inches in order to assure that the best possible turning radius was achieved. The results for these calculations can be seen in Table 8.

Wheel Width (in):	Turning Radius (meters):
12	4.676
14	4.902
16	5.161
18	5.463
20	5.816
22	6.235

TABLE 8 TURNING RADIUSSES FOR VARIOUS WHEEL WIDTHS

From the results illustrated in Table 8, it is clear that the turning radius is increasing with rim size. The turning radius increases with rim size because the value of M must increase as the rim increases in order to prevent the wheels from rubbing on the chassis. With the desired maximum turning angle known the tie rod travel distance could be calculated using Equation 10.

$$\text{EQUATION 10 } \textit{Tie rod travel distance} = \text{Sin}(\alpha\eta) * (L)$$

L in Equation 10 is the length from the kingpin to the tie rod connection point on the front wheel arm. Previous equations show that $\alpha\eta$ is equal to $\beta\eta$; therefore, the tie rod travel distance was calculated to be 2.44 in which corresponds to a total rack travel distance of 4.87in.

Force and Factor of Safety Calculations for Front Mount and Wheel Hub Rod:

The team began to calculate the load per front wheel using Equation 11. Once the load per wheel was calculated the moment was then calculated for the wheel hub and front mount using Equation 11. The length for the front mount in Equation 12 corresponds to the length from the chassis to the kingpin. The length for the bicycle hub bolt in Equation 12 corresponds to the distance from the chassis to the point on the front wheel arm where the wheel hub rod attaches.

$$\text{EQUATION 11 } \textit{Normal Force Per Front Wheel (lbs)} = \frac{\textit{Front Static Vertical Wheel Load}}{\textit{\# of Wheels}}$$

$$\text{EQUATION 12 } \textit{Bending Moment M (lbs * in)} = \textit{Force * Length}$$

The team then calculated the area for square tubing in order to find the direct shear force on the front wheel mount as shown in Equation 13. The area for the circle was then calculated in order to find the direct shear force for the wheel hub bolt as shown in Equation 14. Next the moment of inertia for square tubing was calculated to find the bending stress on the front wheel mount as shown in Equation 15. The moment of inertia for the circle was then calculated in order to find the bending stress for the front wheel hub bolt as shown in Equation 16.

$$\text{EQUATION 13 } \textit{Area for Square tubing} = l_{outer}^2 - l_{inner}^2$$

$$\text{EQUATION 14 } \textit{Area for circle} = \pi * r^2$$

$$\text{EQUATION 15 } \textit{Moment of Inertia for Square Tubing} = \frac{1}{12} * l_{outer}^4 - \frac{1}{12} * l_{inner}^4$$

$$\text{EQUATION 16 } \textit{Moment of Inertia for Circle} = \frac{1}{4} * \pi * r^4$$

Once the moments and the moment of inertia were calculated the team found the bending moments using **Error! Not a valid bookmark self-reference.**, where y is the distance from the neutral axis to the surface.

$$\text{EQUATION 17 } \sigma_y = \frac{M*y}{I}$$

The direct shear force for each part was then calculated using Equation 18.

$$\text{EQUATION 18 } \tau_{xy} = \frac{P}{A_{shear}}$$

Once the direct shear force was calculated as shown in Equation 18 and normal force was calculated as shown in Equation 17 the principle stresses were calculated using Equation 19. Next the maximum shear force in the plane was calculated as shown in Equation 20. In Equation 17, Equation 19, and Equation 20 σ_x is equal to zero because the force acting on each part is acting in the normal axis. Once the car is in motion there will be a σ_x however it will be relatively small in comparison to σ_y .

$$\text{EQUATION 19 } \sigma_{1,2} = \left(\frac{\sigma_x + \sigma_y}{2} \right) \pm \left(\left(\frac{\sigma_x - \sigma_y}{2} \right)^2 + \tau_{xy}^2 \right)^{0.5}$$

$$\text{EQUATION 20 } \tau_{\max \text{ in plane}} = \left(\left(\frac{\sigma_x - \sigma_y}{2} \right)^2 + \tau_{xy}^2 \right)^{0.5}$$

$$\text{EQUATION 21 } \sigma_{avg} = \frac{\sigma_x + \sigma_y}{2}$$

Once the maximum shear force in the plane was calculated the factor of safety per material was determined by using Equation 22. The shear yield strength per material was determined from material strength tables in “*Mechanics of Materials*” text book. Shear yield strength which were not found in the tables were approximated using Equation 24.

$$\text{EQUATION 22 } \textit{Factor of Safety} = \frac{\textit{Yield Shear Strenght}}{\tau_{\text{max in plane}}}$$

$$\text{EQUATION 23 } \tau_y = \frac{\sigma_y}{\sqrt{3}}$$

All calculation results and constants can be seen in the tables located in appendix A27.

2.6 Design Process

Concept Selection Criteria

In order to develop the overall concept design for the vehicle, the team employed a fishbone analysis and a house of quality assessment. The fishbone diagram allows for an iterative approach to determining the causes of a series of defined effects. In the case of the solar vehicle, it allowed the team to split the customer requirements into 5 different categories: design limitations, efficiency, operator comfort, safety requirements, and steering & handling.

Using these 5 categories to further clarify the voice of the customer, the team was able to brainstorm ideas on how to approach the design of the vehicle. This process was completed by all of the engineers working on the project in order to promote a concurrent engineering design philosophy. By using a concurrent engineering approach the team will reduce the risk of having a failure or defect in the vehicle once the design phase of the project is completed. Eliminating these errors will reduce the overall cost in the long run.

The fishbone analysis can be found in Appendix A1 Fish bone Analysis.

Concept Selection Criteria Prioritization

Using the house of quality, the group determined the significant factors in the design the vehicle. More importantly, the group determined how the customer requirements and design factors would interact with each other, by establishing whether or not relationships existed between

them. Each of these relationships was ranked as being a weak, medium, or strong relationship; scores of 1, 3, and 9 were assigned respectively.

After establishing the existence and strength of the relationships between the customer requirements and the design factors (quality characteristics on HOQ), the team ranked the importance of each customer requirement. Each customer requirement was ranked equally (max score) because the competition requires teams to satisfy all rules and regulations in order to participate; based on this it was determined that no preference should be given to one customer requirement over another.

The team then ranked each of the design factors as needing to be maximized, minimized, or being on target. Based on this optimization ranking, the team then determined the level and direction of correlation between each design factor. Each pair was given a rating of being either a positive or negative correlation, with a strength of either weak or strong. By determining the correlation between each design factor, the team was then able to prioritize design factors for the optimization process.

The team then assigned a target value for each of the design factors based on the voice of the customer (Shell rules and regulations), and a difficulty score based on the cost and time necessary to implement each design factor. This allowed the team to determine how to optimize the vehicle by prioritizing design factors. The team will optimize the vehicle by making trade-offs in order to enhance a desired component/quality of a system or process. Using these factors, the team decided that the cost, weight, safety, ergonomic design, and regenerative braking were the most important design factors.

Finally, a competitor analysis was performed using the FAMU-FSU 2011 Solar Car as competitor. Ideally the team would have liked to rank the design against other universities, but due

to the competitive nature of the project this was not possible. The proposed design ranked as a 5 for each of the Demanded Quality variables, because we have to satisfy each of these requirements in order to compete in the 2014 Shell Eco-Challenge. The former FAMU-FSU car scored low in several categories because their design team was not as multi-disciplinary as the 2014 team, and the competition regulations have become stricter since their entry.

The completed house of quality and reasoning can be found in Appendix A2.

Design Selection

Once the HOQ was completed the team created a comparison matrix template using the most significant factors, in order to rank components against their alternatives in the design selection phase. The comparison matrix was created by assigning normalized percentage weight values, which were derived from our HOQ analysis, to each ranking criteria. Next an optimization legend was created, in order to determine which design was the most optimal for the vehicle. Each component was assigned a ranking relative to its alternatives. A higher score indicates a more optimal solution, while a score of 1 indicates the least optimal solution. The weights were then applied to the relative rankings, which gave us insight into which components best fit the customer's requirements. The alternative designs were generated based on input received from various advisors and professionals in the respective fields.

3 Design of Major Component Subsystems

3.1 Chassis

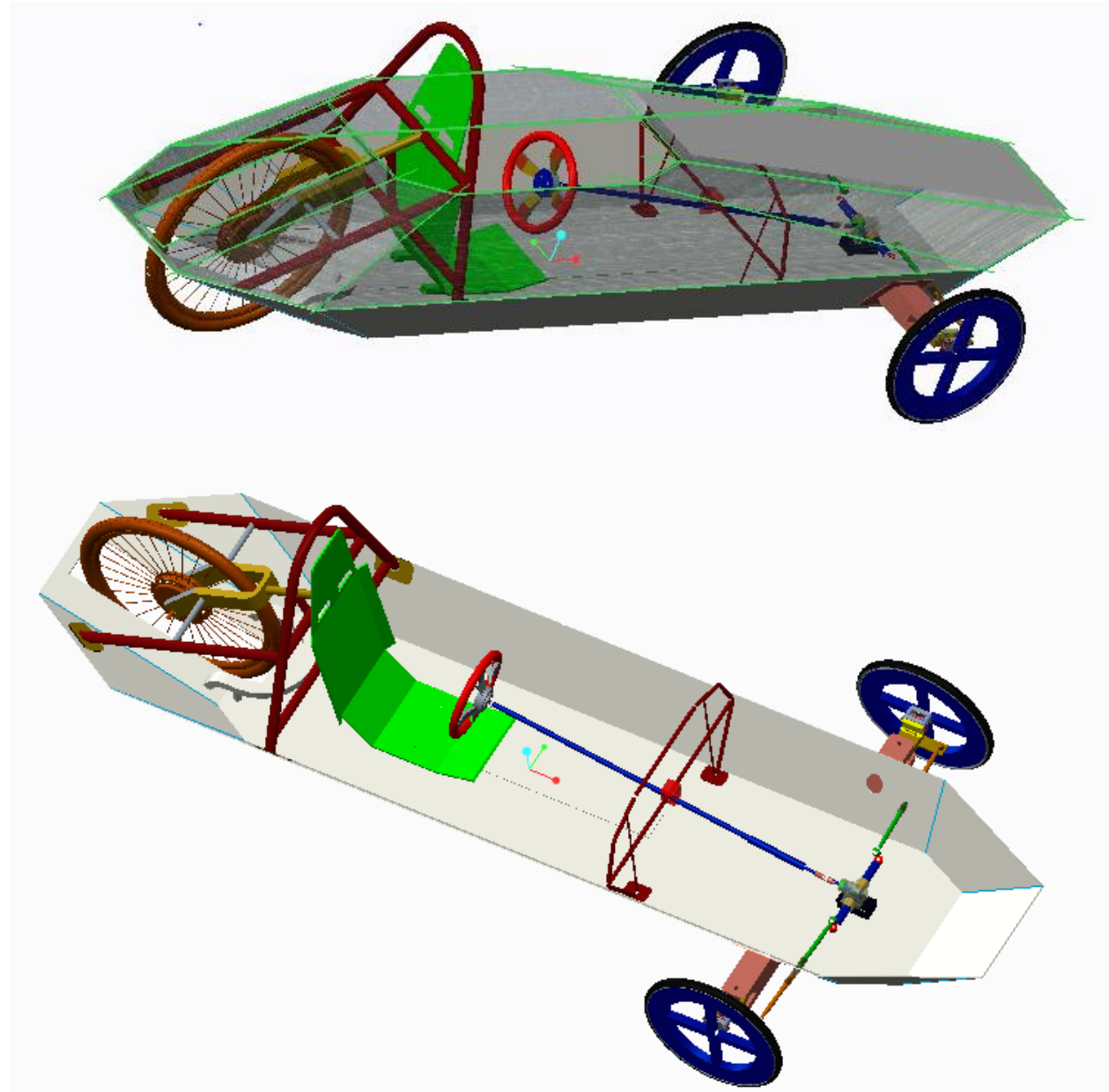


FIGURE 12 CHASSIS

The chassis is a carbon fiber molded structure that is responsible for supporting the full load of the car, which can be seen in Figure 12. This includes the driver, seat assembly, roll bar, wheel mount, solar panels, batteries, and all the electrical components. PVC has been added along

the bottom and sides of the chassis with balsa wood, in order to increase the rigidity of the structure. The top cover is also part of the chassis, however, the only weight it will support is the solar panel encapsulation box. It has been aerodynamically designed by last year's senior design team to minimize coefficient of drag. The chassis dimensions and specifications can be seen in Appendix A5.

Advantages:

- Light weight carbon fiber structure will decrease energy consumption.
- Rigidity and strength of structure is enhanced by the PVC pipes.
- Balsa wood will support the full load of the front and rear wheel assemblies.
- Manufacturing and digital analysis is completed

3.2 Roll Bar & Rear Motor Mount

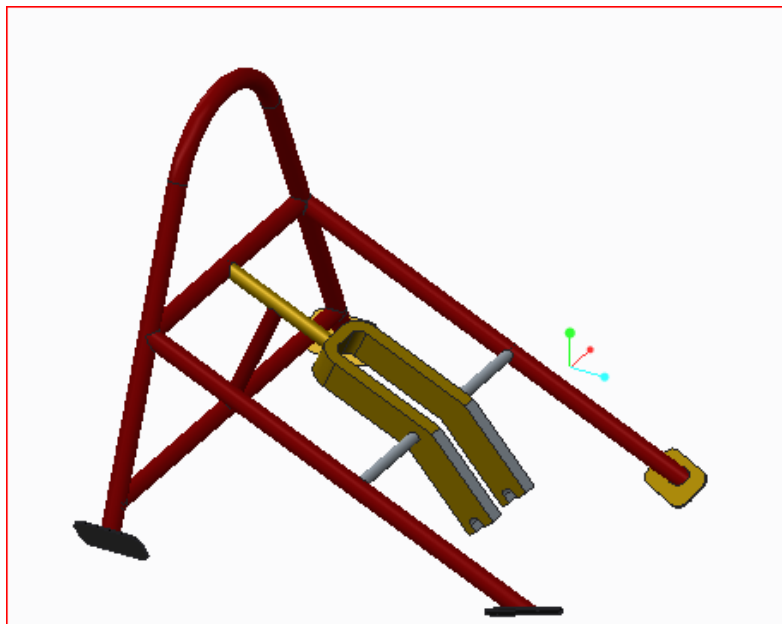


FIGURE 13 ROLL BAR AND REAR WHEEL MOUNT

The roll bar is responsible for keeping the driver safe at all times during the competition. This involves protecting the driver from a roll over, and supporting the normal and thrust loads

from the motor. The designs for the roll bar and rear wheel mount must comply with the regulations issued by the Shell Eco-Challenge Marathon Competition. The roll bar must be capable of withstanding a static load of 700 N in any direction without deforming. The dimensions of the roll bar will be 5 cm above the drivers head when fully seated, and approximately 2 cm from the shoulders on each side. The intention of this year's design team is to choose the lightest and strongest material, which will ensure the safety of the driver and meet the financial requirements of the project. The roll bar has been modified from last year's design by adding longer support arms, which will allow a 20° declined race seat to be used as seen in Figure 13. The motor mount is similar to the front frame of a bicycle, which the hub motor was originally designed for. The full dimensions and specifications for the roll bar and rear wheel mount can be seen in Appendix A6.

Advantages:

- Meets all the requirements set by Shell Eco-Challenge Marathon Competition.
- Allows the motor to be mounted in its intended operating environment.
- The structure of the roll bar will not deform during roll overs.
- The rear wheel mount will be capable of supporting the rear load of the car.

3.3 Roll Hoop

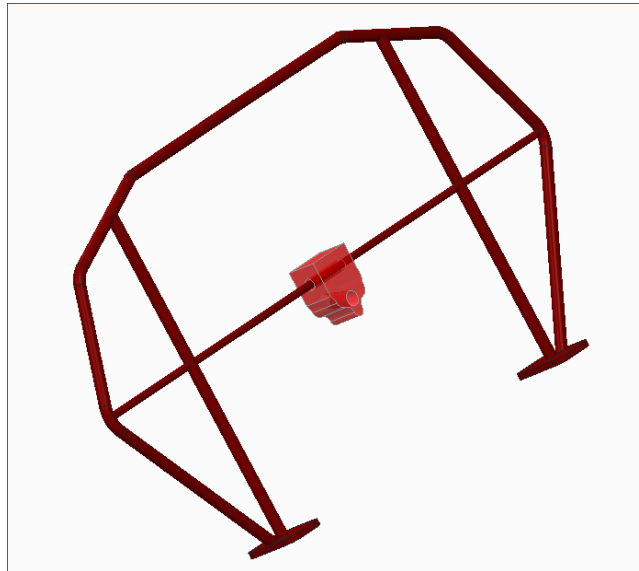


FIGURE 14 ROLL HOOP

The roll hoop will be mounted in the front of the solar car, and it will support the steering assembly. This part was added after the design error was pointed out by the mechanical engineering adviser Dr. Hollis. Without the part, there would be a point towards the front end of the car that would make contact with the ground in the event of a roll over. In the event of a roll over, the driver's legs will be protected because the roll hoop is the next highest point on the chassis after the roll bar. The two points on the car that will suffer the most from a roll over will be the roll hoop and the roll bar, because those are the only points making contact with the ground. The full dimensions and specifications for the roll hoop and rear wheel mount can be seen in Appendix A7.

Advantages:

- Prevents the driver's body from coming in contact with the ground if the car were to roll over.
- The mass of the steering column and steering wheel can be supported from the roll hoop.
- Increases the safety of the vehicle and integrity of the chassis.

3.4 Steering System

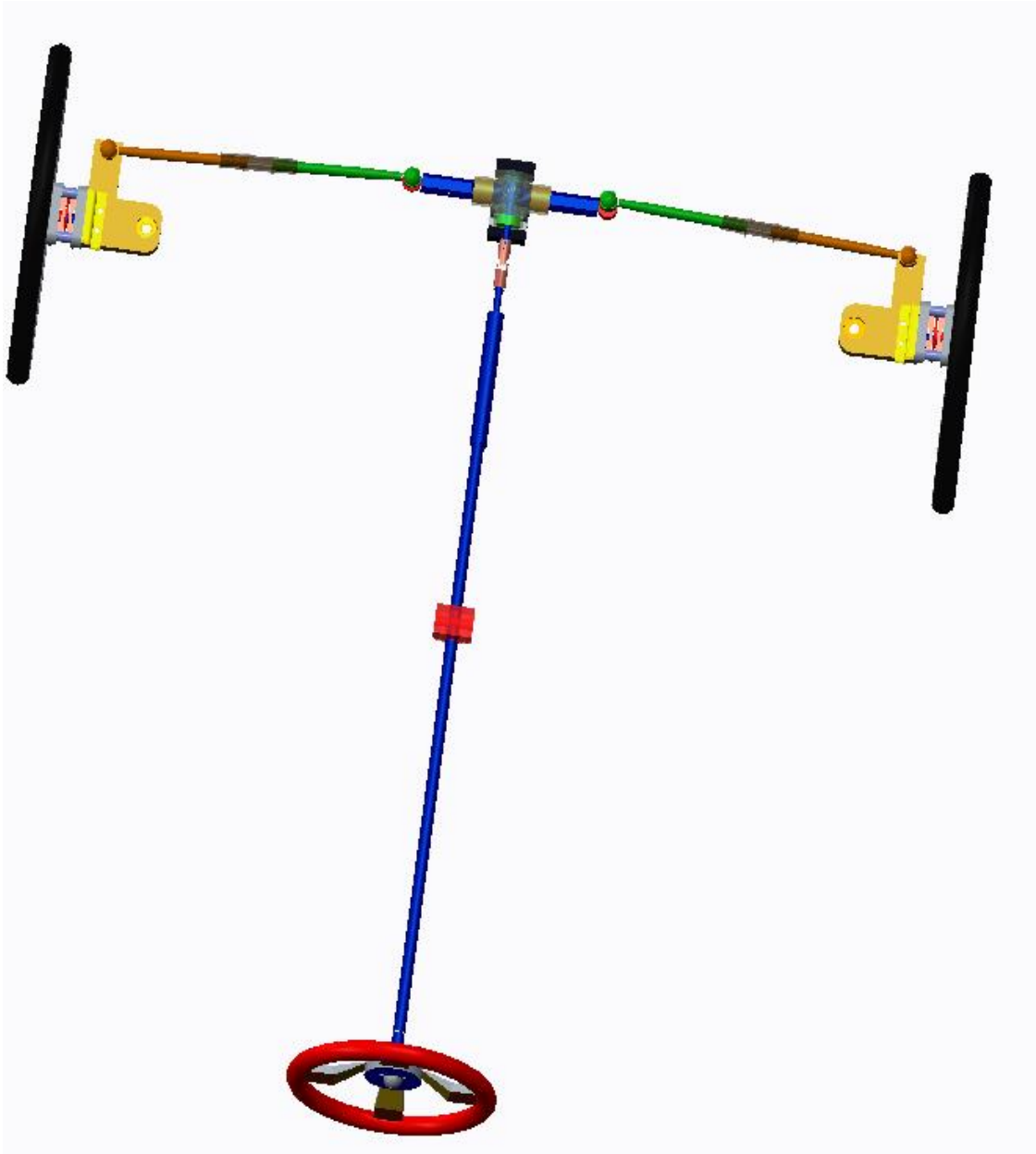
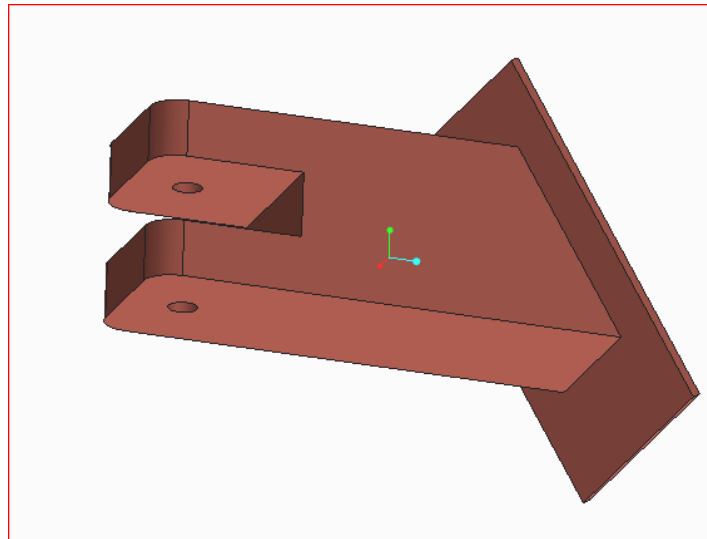


FIGURE 15 STEERING SYSTEM

The steering system for the vehicle will allow the design to meet the Shell Eco-Challenge Marathon requirement of a maximum turning radius of 8 meters. It contains seven subcomponents and is connected to the front wheel mount by a single bolt. The system incorporates a rack and pinion steering system, which decreases the amount of force required to turn the wheel, and thus

Advantages:

- Less force is required to steer the car.
- Will meet the steering requirements set by the competition.
- Components are relatively cheap and several can be machined in shop.
- High safety factors will ensure failure does not occur at connection points.

Front Wheel Mount**FIGURE 17 FRONT WHEEL MOUNT**

The front wheel mount houses the front wheel arm which allows the car to be steered. It is constructed of square tube piping with a C-bracket attached to the end which will be welded into place. The front wheel arm will fit into the C-bracket and will be held in place by the kingpin. The full dimensions and specifications can be seen in Appendix A20.

Advantages:

- Simple design allows the part to be machined in house.

- High safety factors minimizes the chances for failure

Front Wheel Arm

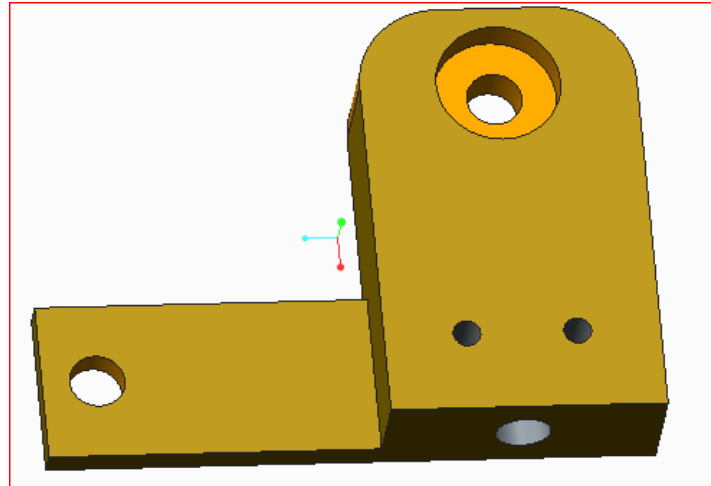


FIGURE 18 FRONT WHEEL ARM

The Front Wheel Arm is the part that connects the steering assembly and front braking systems to the chassis. It contains two ball bearings, which will allow it to rotate within the front wheel mount housing with a minimum amount of force. The rod from the wheel hub is screwed into the Front Wheel Arm. The tie rods are then connected to the arms, and then to the rack and pinion. The Full dimensions and specifications can be seen in Appendix A8.

Advantages:

- Simple design will allow the part to be machined in house.
- Capable of withstanding the force exerted onto it by the chassis.
- Will allow the car to meet the turning radius requirement.

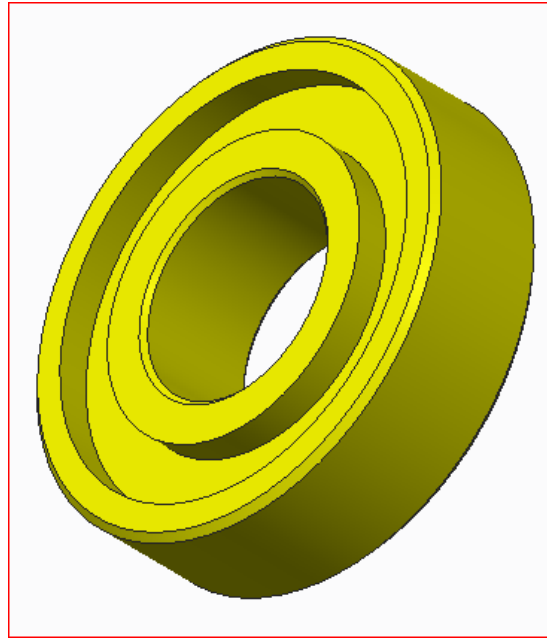
Ball Bearings

FIGURE 19 BEARINGS [11]

There will be four bearings within the steering system. Each front wheel arm will contain two bearings that will allow it to rotate around the kingpin smoothly with the minimum amount of force. These bearing will be able to withstand the forces associated with the Front Wheel Arm.

Advantages:

- Reduces the force required to turn the car.
- Makes the car more maneuverable and safe.
- Cheap component.

Tie Rods

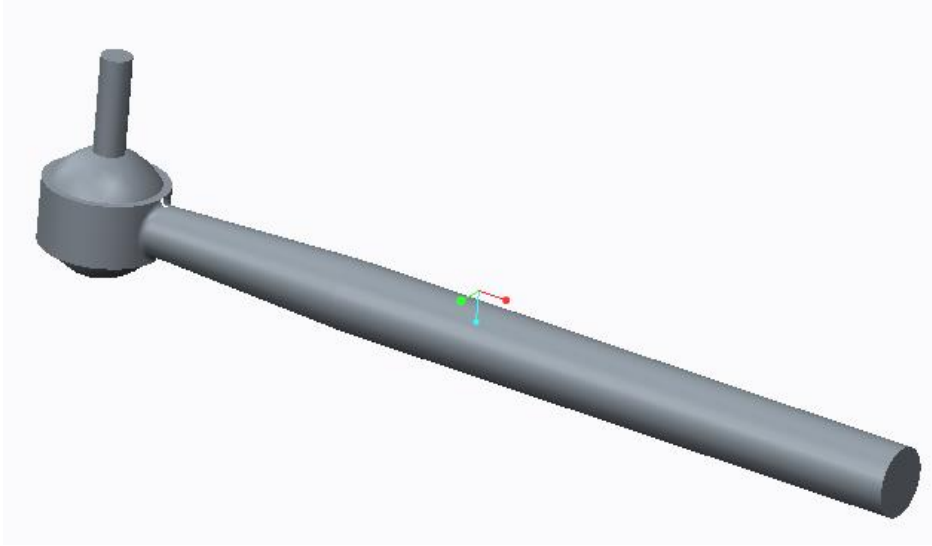


FIGURE 20 TIE ROD

The tie rods connect the front wheel arm to the rack and pinion. When the driver turns the steering wheel it causes the rack and pinion to pull the first tie rod and push the second which steers the car. The full dimensions and specifications can be seen in Appendix A18.

Advantages:

- Easily adjustable
- Cheap component

Rack and Pinion

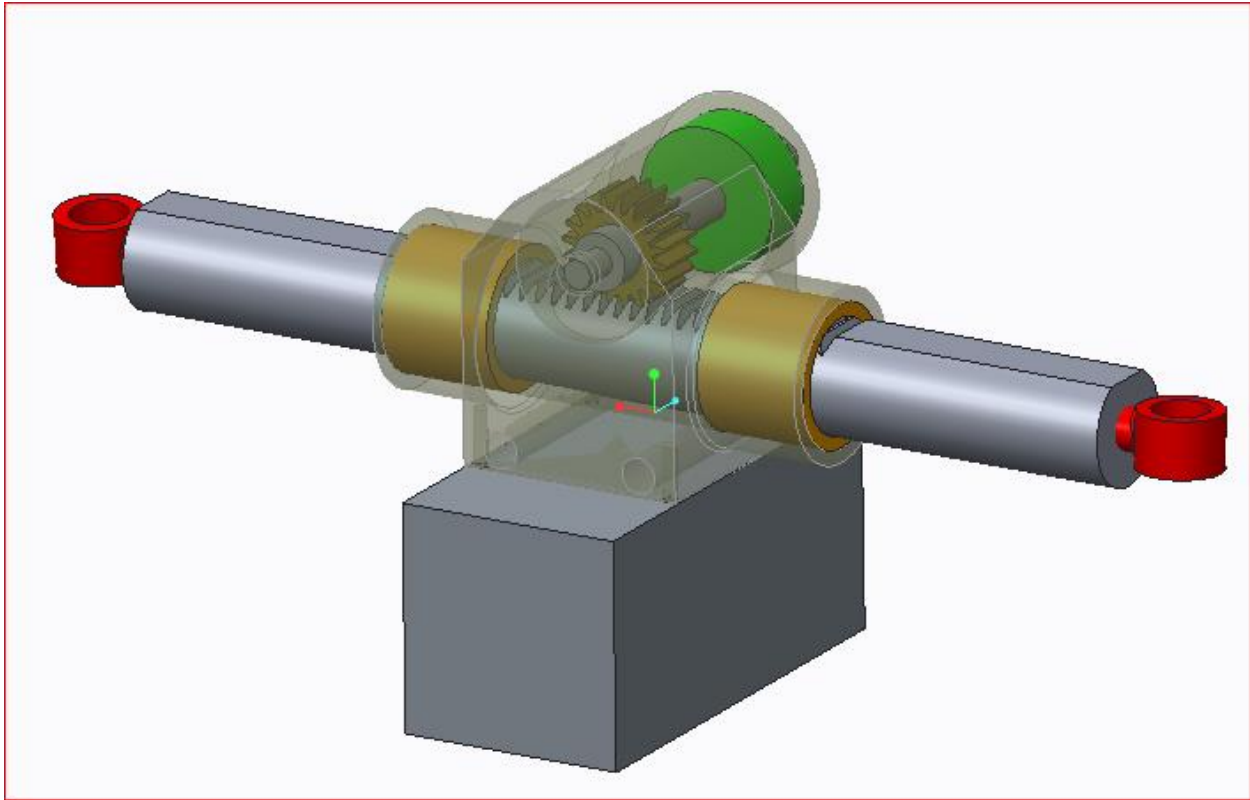


FIGURE 21 RACK AND PINION

The rack and pinion takes the input from the driver turning the steering wheels, and either pushes or pulls the corresponding tie rod. The use of a rack and pinion will make steering smoother and require less input force from the driver on the steering wheel to maneuver the vehicle. They are cheap and the required rack travel distance is easy to calculate per desired turning radiuses. The full dimensions and specifications for the rack and pinion can be seen in Appendix A9.

Advantages:

- Required rack travel distance is easy to calculate.
- Reduces input force from the driver to steer the vehicle.

- Smoother steering and overall maneuverability of the vehicle.

U-Joint

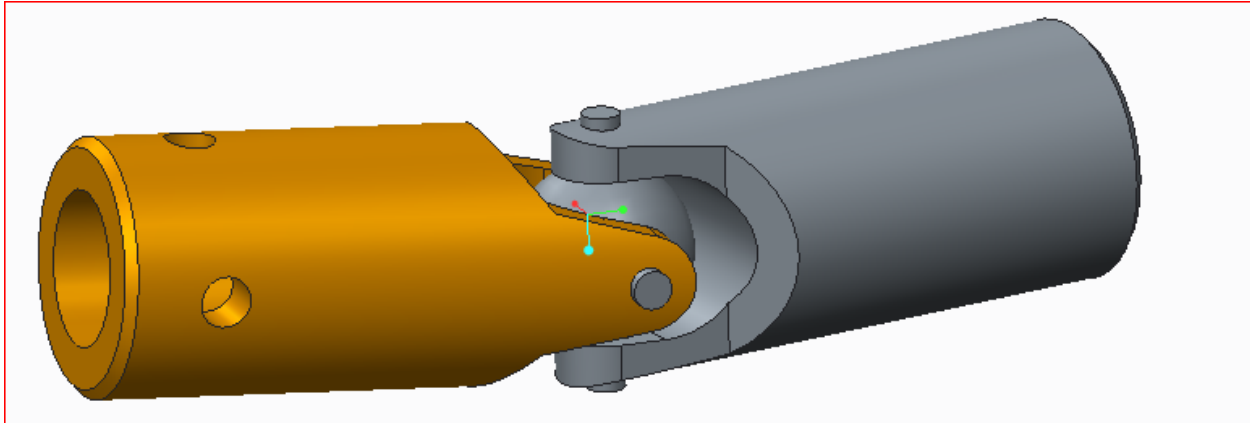


FIGURE 22 U- JOINT [11]

The u-joint allows the steering wheel to be angled towards the driver. It connects the rack and pinion to the steering column and the steering column to the steering wheel. The full u-joint dimensions and specifications can be seen in Appendix A19.

Advantages:

- Ergonomic friendly design.
- Allows the angle of the steering column to be adjusted.
- Will allow the team to use the roll hoop to support the steering column and wheel.

Steering Column

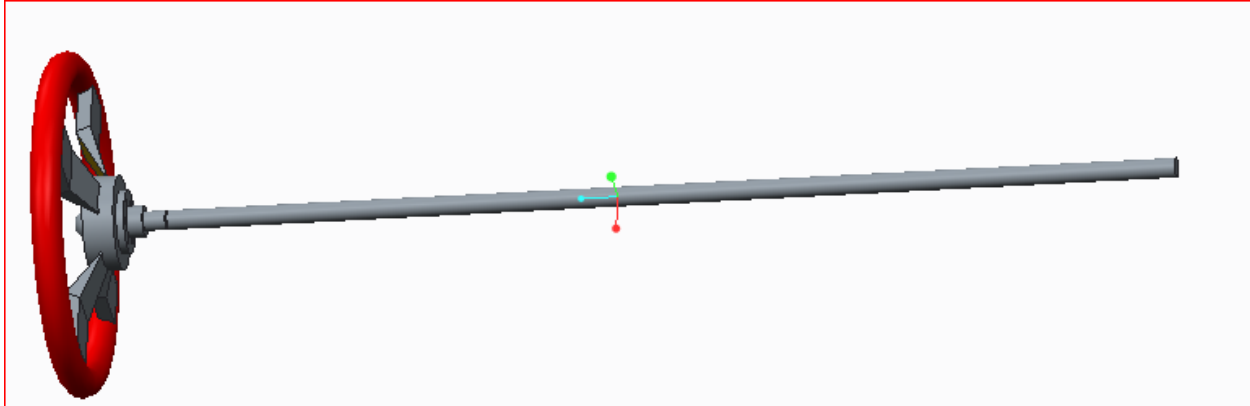


FIGURE 23 STEERING COLUMN

The steering column takes the input rotational force from the driver on the steering wheel, and transfers that force to the rack and pinion. It is a straight shaft that the team is considering constructing from carbon fiber.

Advantages:

- Cheap to purchase or construct
- Simple design
- Materials and technical expertise are being donated by HPMI

Steering Wheel

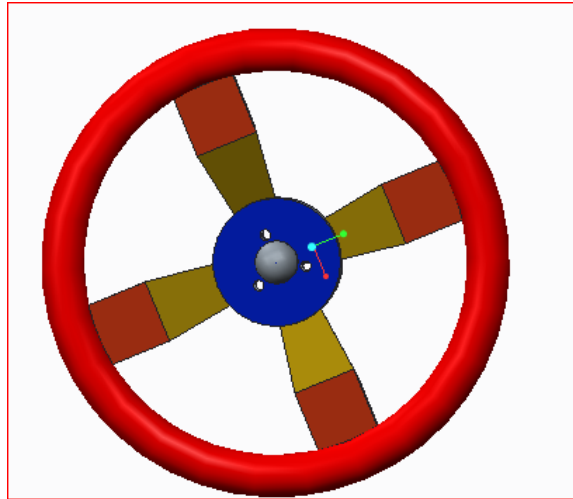


FIGURE 24 STEERING WHEEL

Takes the input from the driver and transfers it to the steering column. The steering wheel sits within comfortable reach of the driver and can be turned fully from lock to lock, with the driver fully strapped into the seat. The full steering wheel dimensions and specifications can be seen in Appendix A10.

Advantages:

- Can be constructed of many different materials
- Familiar for both daily and casual drivers
- Easily implemented into our system.

3.5 Braking Systems

The braking systems incorporated in the solar car are two independently functioning systems that will be tested and modified on a 20° incline. Each braking system will be applied separately and must immobilize the car on the 20° incline in order to meet the Shell Eco-Challenge Marathon requirements. Each system must also have its own pedal that can be engaged without the driver having to remove their hands from the steering wheel. For the rear braking system the team decided to utilize bicycle brakes since they are inexpensive and easy to incorporate into the system. Furthermore, the shoe size on the brakes can be easily changed to increase or decrease the stopping force applied. The pressure applied by the rear brakes can also be adjusted by changing the cable tension when the braking pedal is fully engaged.

For the front brakes, the hydraulic braking system with calipers and shoes was chosen. The front braking system will be the primary braking system. The competition rules stipulate that the primary braking system needs to be reliable, and be able to stop the vehicle in a reasonable time frame. Hydraulic braking systems are the standard for automobiles and high performance cars, and are a perfect fit for our application. If the force applied by the calipers is less than desired, the shoes can be replaced with ones with a higher surface area that would meet the standards for the vehicle.

Rear Braking



FIGURE 25 BRAKING SYSTEM

The rear brakes will be controlled by its own pedal in the car. They will be directly mounted on the wheel mount assembly. Bicycle brakes were chosen for the rear braking system.

The required stopping force will be supplied by using slightly larger brake shoes. Larger area also means less pressure is required when activating the brake pedal. Some complications that will be encountered in the installation process is the tilting of the brake shoe to the same angle as the wheel mount. This can be done by adding extra links or spacers to accomplish the most effective orientation of the stopping mechanism on the tilted wheel.

Advantages:

- Simple to install and adjust to meet requirements.
- Light weight mechanism that will mount to the motor mount easily.
- Cost is cheap and the parts can also be machined in house.

Front Braking

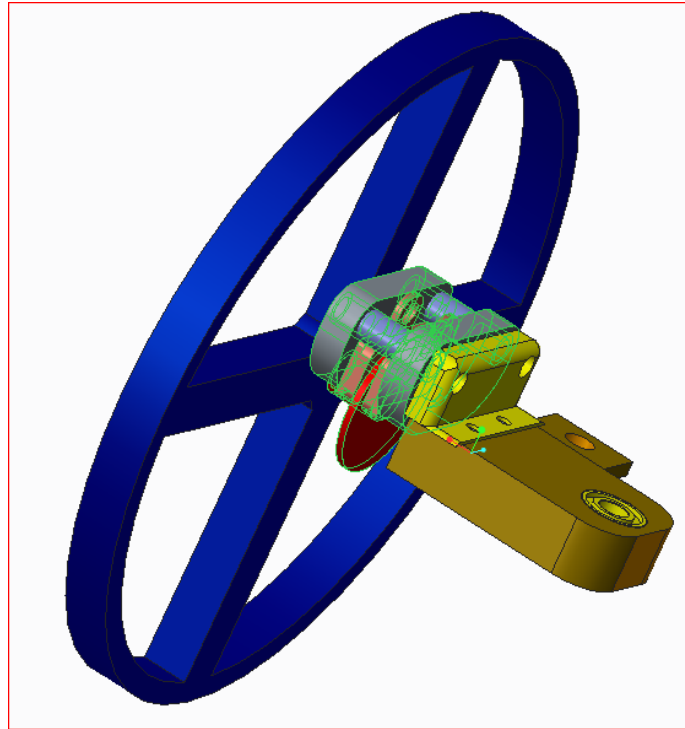


FIGURE 26 FRONT BRAKES

Front brake design incorporates a hydraulically engaged caliper/shoe combo and a simple piston, which will apply stopping force through pressurized fluid cables when activated. Hydraulic brakes are used on motorcycles, cars, and most high speed transportation. Even though the Shell Eco-Challenge Completion only measures the cars efficiency and not speed, having hydraulic brakes will allow the car to stop immediately at low speeds for safety reasons. When the brake pedal is engaged the hydraulic fluid will engage the pistons in the braking system, which will cause the braking shoes attached to the calipers to press down onto the rotor, thereby slowing and eventually stopping the vehicle. The housing used to support the braking system is a sleeve that goes over the wheel mount arm and can be welded or bolted in place.

Advantages:

- Different sizes of shoes and calipers can be chosen for the vehicle depending on the required braking force.
- Can stop heavier loads than bike brakes.

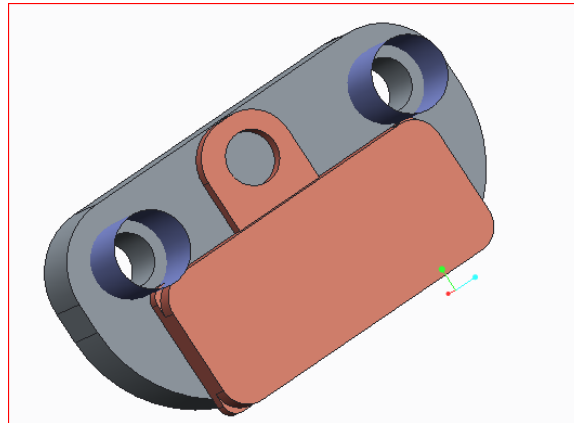
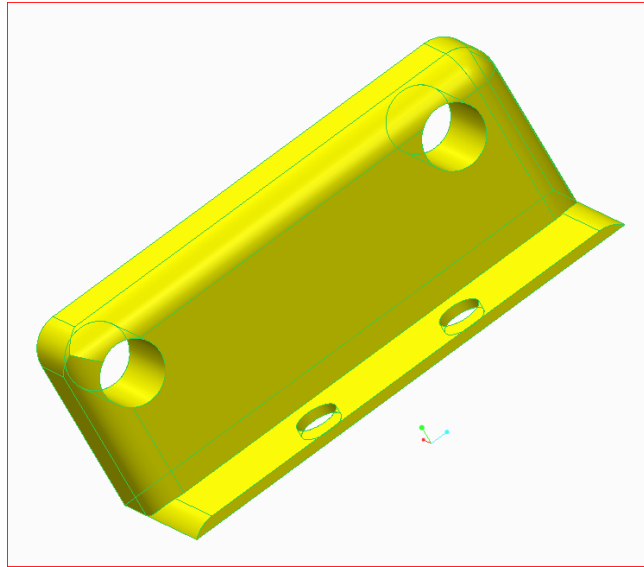
Caliper

FIGURE 27 CALIPERS

The caliper (with its attached shoe) is what stops the vehicle. When the brake pedal is engaged, hydraulic fluid pushes the piston which presses the shoes into the rotor, which slows and eventually stops the car. The full caliper dimensions and specifications can be found in Appendix A11.

Advantages:

- Higher stopping forces than bicycle brakes
- Utilizes a simple mounting system.

Caliper Mount**FIGURE 28 CALIPER MOUNT**

Holds the caliper in place around the wheel's rotor. The full dimensions and specifications can be found in Appendix A12.

Advantages:

- Simple design to machine and install
- Small volume component means it will be cheaper and take less gross material.

Front Wheel Arm

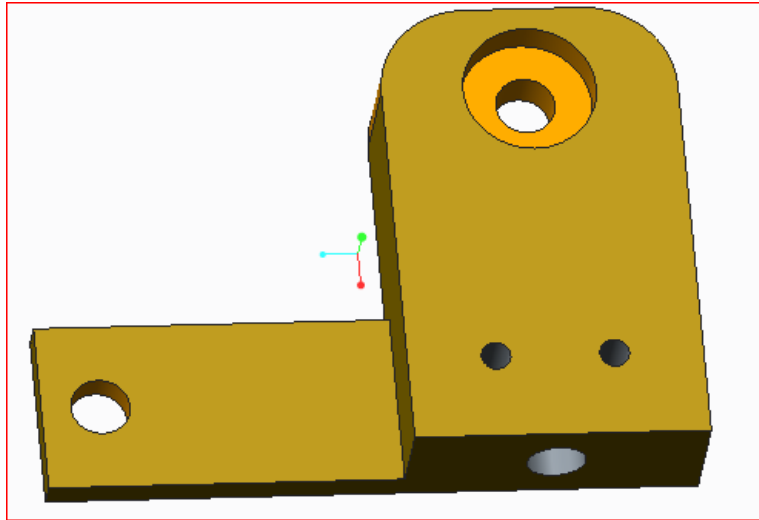
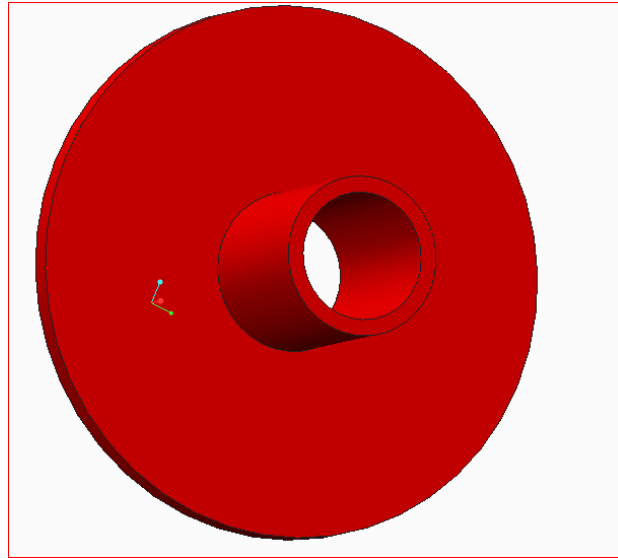


FIGURE 29 FRONT WHEEL ARM

The caliper mount will be connected on top of the front wheel arm. It will maintain the height and orientation of the caliper around the rotor. The full dimensions and specifications can be seen in Appendix A13.

Advantages:

- Small size and simple design.
- Allows the team to incorporate hydraulic brakes on the front wheels.
- Can be machined in house.

Rotor**FIGURE 30 ROTOR**

The rotor will be secured to the front wheel hub. As the front wheel spins, so too will the attached rotor. When the brake pedal is engaged, the calipers will close around the rotor which will slow and eventually stop the front wheels. The full rotor dimension and specifications can be seen in Appendix A14.

Advantages:

- Simple design to machine and install
- Some wheelchair hubs and bicycle wheels come with pre-attached rotors.

3.6 Seat

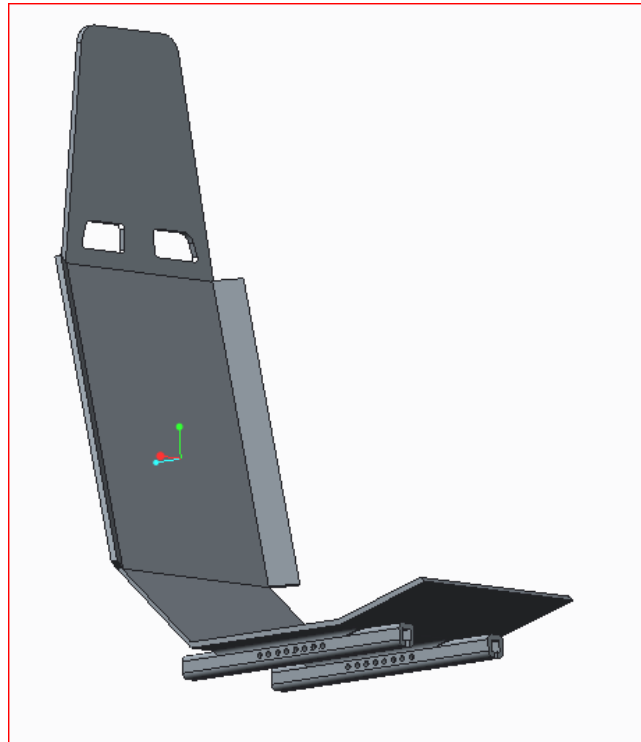


FIGURE 31 SEAT

Comfort, safety, and convenience are all important factors in the ergonomic considerations of the car seat design. The seat must be designed so that the driver's head will remain at least 5 centimeters below the top of the roll bar. The seat must be positioned so that it will allow the driver to see clearly over the steering wheel as well as reach the accelerator and brake pedals. In addition, the driver's seat must be equipped with an effective safety harness having at least five mounting points to keep the driver in the seat. The 5-point harness must be firmly attached to the vehicle's chassis and fitted into a single buckle. The design of the seat will be optimized so that individuals ranging from 4 ½ feet to 6 feet will be able to drive the vehicle. The seat design chosen for the application was the seat with the 20° decline. The use of this style of seat will require the team to cut the top of the chassis. Implementation of this part will slightly increase the drag coefficient, however it will not be significant enough to alter the intended operating speed. This will allow the

team to easily meet the vision requirements set by the competition, and will allow the vehicle to be driven by each team member. If the top was not cut, the only members of the team that would have fit into the chassis would have been the driver and backup driver. The full seat dimensions and specifications can be seen in Appendix A15.

Advantages:

- This design for the seat will be mounted on rails that will allow the seat to slide forward and backward.
- Each unique driver will enter and exit the vehicle with less resistance.
- All team members will be capable of driving the vehicle.
- Vision requirements set by the Shell Eco-Challenge Marathon will be met.

3.7 Front Wheel Systems

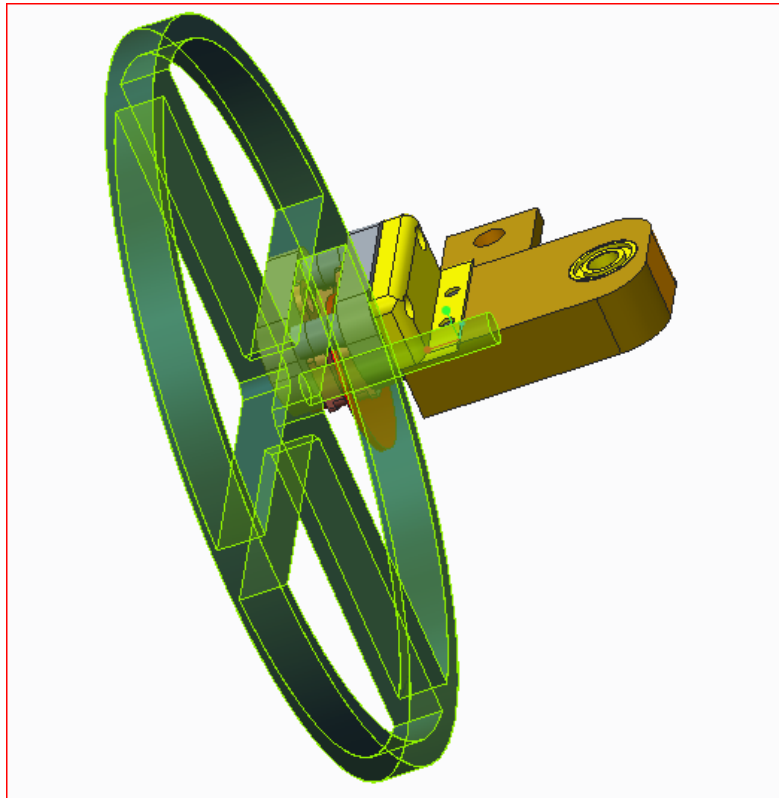


FIGURE 32 FRONT WHEEL

The team has considered using both bicycle or wheelchair hubs and rims. These types of hubs come equipped with bearings, and usually require minimum amounts of force to spin. This will require less power from the motor to move the vehicle. Wheelchair hubs might be better equipped for this application because they are designed to withstand a force on only one side of the wheel, whereas with bicycle wheels the force is split on either side of the wheel. The hub rods are connected to our system by screwing into the front wheel arm of the steering assembly.

Each front wheel must be capable of withstanding 81.3 lbs. which is common for both bicycle and wheelchair wheels. If a failure were to occur between the wheel and our front wheel arm (the piece the wheel screws into), the hub bolt would need to be replaced with one of the same dimensions but made from stronger material. This would be a cheap easy fix and the chance of failure is low, because the forces have been calculated for this connection point. The full wheel dimensions and specifications can be found in Appendix A16.

Advantages:

- The front wheel hubs can be purchased with installed bearings and rims.
- Connects easily to our steering assembly.
- Depending on the forces the size of the components can be adjusted to minimize the stress and moments on the wheel hub shaft.

3.8 Solar Panel System

Solar Array

The majority of the decision-making and selection for the solar array was completed by the 2012 FAMU-FSU solar car team, this section will serve as a reiteration of their findings. The 2013 FAMU-FSU team added discussion on the mounting solution, the installation, and provided an

explanation of the array's implementation in the electrical system. Performance curves for the spectral response (SR) and current-voltage (IV) curve are given.

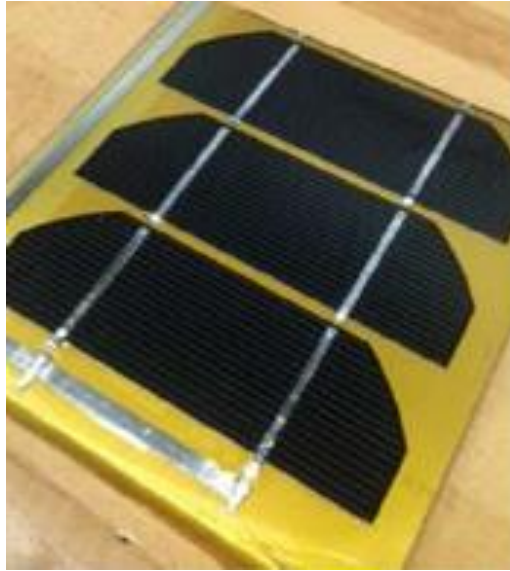


FIGURE 33 PHOTO OF THE MONOCRYSTALLINE SOLAR CELLS [1]

The 2014 team consulted with the engineering college faculty during the selection process in order to narrow down choices until a final decision was made. Three different types of solar panels were considered: monocrystalline, polycrystalline, and thin film solar panels. After the faculty consultation, it was decided that monocrystalline was the best fit for the project. The term monocrystalline is self-explanatory; the cell consists of a single silicon crystal. Monocrystalline cells are the most efficient of the available panel types, because their production process (Czochralski method, see Appendix) forms an almost perfect crystal lattice which minimizes interference of the electron flow through the material.

By minimizing the interference of the electron flow, monocrystalline panels have the highest efficiency (15-20%) among the possible selections. The largest drawback is the cost because of the expensive production process involved with drawing out the silicon ingot. Although monocrystalline is more expensive, it was selected because of the superior efficiency which is the

main criteria used for ranking in the competition. Polycrystalline and thin film (amorphous) solar panels were ruled out because their efficiencies are typically in the range of 12-14% and 6-8%, respectively. Another consideration in selecting the solar array was the space limitations imposed by the Shell organization. The solar panels have to fit into a limited area (no larger than 0.17 m²), so it made sense to maximize the efficiency in the small allotted area by selecting the monocrystalline.

The solar cell was cut into three pieces using a high intensity laser beam. The cutting process allowed the team to arrange the solar cells into an array which would increase the voltage by a factor of 3, and reduce the current by a factor of 3. This resulted in a voltage rating of 1.8V and a current rating of 1.7A. The 2012 solar car team considered 2 different configurations based on the advice of the electrical engineering project advisors. The first configuration consisted of 10 modules in series, and calculations put the voltage supplied at 18V with a current rating of 1.7A. The second configuration consisting of two parallel rows of 5 modules connected in series, which supplied 9V and had a current rating of 3.4A. The configurations can be seen in the figure below. Regardless of the configuration, the theoretical power supplied by the system totals to 25W of power. This assumption will be confirmed during the testing phase.

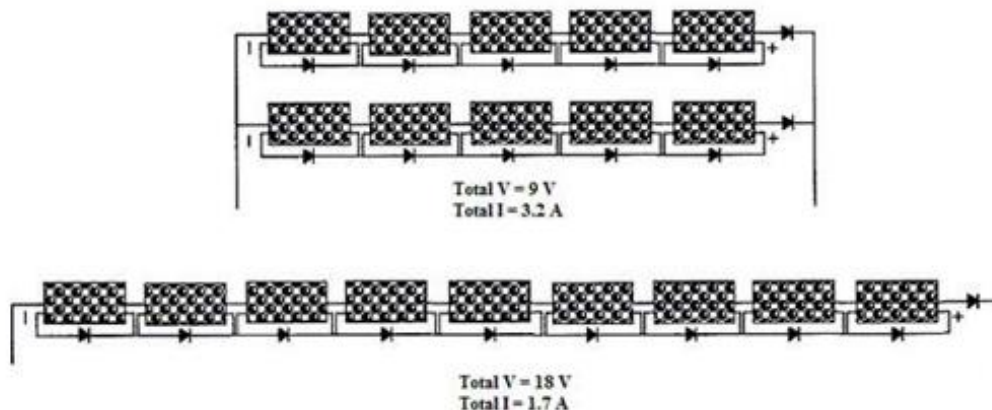


FIGURE 34 SOLAR ARRAY CONFIGURATION OPTIONS [1]

The 2012 solar car team made the decision to include a “solar junction box” for each module, which consisting of a diode. This component was used to solve problems related to partial shading of the cells and to correct loss of power. Another diode was added to the end terminal of the solar array, which serves as a protection diode for unwanted back current flow into the modules array.¹ The junction box can be seen in the figure below.



FIGURE 35 THE SOLAR JUNCTION BOXES USED AS NODES [1]

The solar array will be mounted on the top-front chassis of the car, as demonstrated by the dark grey area depicted in the image of the vehicle below. This location was picked because it is the area of the car which maximized the incidence angle of light hitting the solar panel. The alternatives were the back or side of the car, which both had severe limitations for setting up the solar array in the desired configuration. Additionally, mounting the solar panels on the rear or side of the car would lead to non-optimal angle of incidence, which lead to a lower power output. A special mounting bracket was created to host the solar panel array, which can be found in the relevant mechanical engineering section.

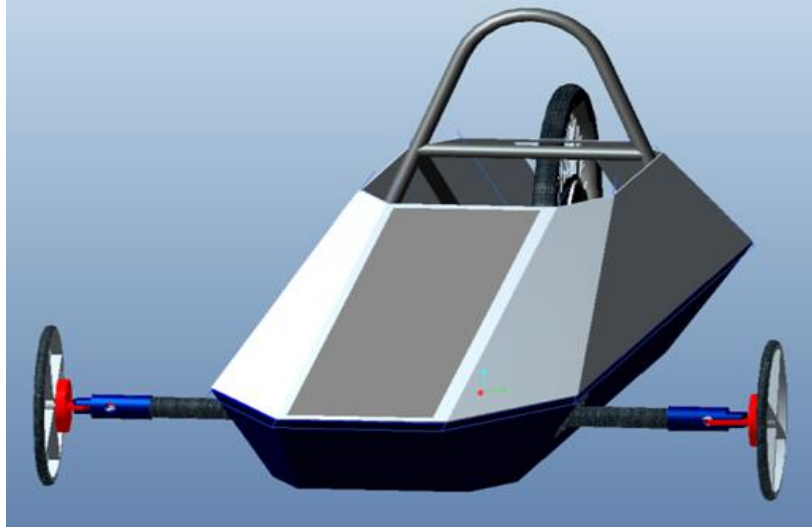


FIGURE 36 DEMONSTRATION OF SOLAR PANEL IMPLEMENTATION [1]

Some risks are associated with the solar panel implementation and testing schedule. The largest concern is that the 2012 solar car team was never able to get the battery to charge using the solar array and DC-DC converter. The team suspected that the problem lays with the DC-DC converter, and the group is currently in the process of reviewing the propulsion system design. Additionally, the competition rules concerning solar panel mounting has changed from 2012, so as to not allow independent structures; that is to say that the solar panels have to sit flush with the chassis. The team is currently working with HPMI to solve this problem, and expects it to be resolved before the 20th November.

Current work on the solar array will consist of verifying calculations and assumptions with the team's project advisor. After the design has been verified, the team will start the implementation process and then proceed with the testing schedule as outlined in the Gantt chart. Additional technical specifications (electrical performance, irradiation profile, and temperature coefficients) for the solar panels can be found in the Appendix section.

3.9 Battery System and Isolated DC-DC Converter

Battery and Battery Management System (BMS)

After consulting with faculty for guidance on the battery selection and by using a decision matrix; the lithium iron phosphate battery from Electric Rider was chosen because of its small size, low weight, and cost being under \$500 (including shipping). The selected battery is 6x10.25x3.5 inches, 24V, 20Ah and a weight of 10 lbs. The battery can be seen in Figure 37.

As previously stated, the Shell Eco-Marathon competition requires that all batteries have a battery management system. The BMS is required to have cell under/over voltage limits, over current limits, and over temperature limits. The battery pack purchased from Electric Rider contains a BMS that will meet the requirements of the competition, and will protect and monitor the entire battery pack as well as individual cells. After consulting with faculty the 2012-2013 solar car team also decided to purchase a watt meter which can be seen in and a power analyzer which can be seen in Figure 39. These two components will be used as a visual display of the batteries health and performance level during the car operation. The 130A-watt meter and power analyzer was purchased from Turnigy. The device rating is 60V, 130A, 6554W and 65Ah which is within the range of the battery specification. Figure 39 shows the device display and Figure 40 shows the connection with the battery and motor.



FIGURE 37 ELECTRIC RIDE LiFePO4 BATTERY BACK [1]



FIGURE 38 ELECTRIC RIDE LiFePO4 BATTERY BACK [1]



FIGURE 39 TURNIGY WATT METER AND POWER ANALYZER [1]

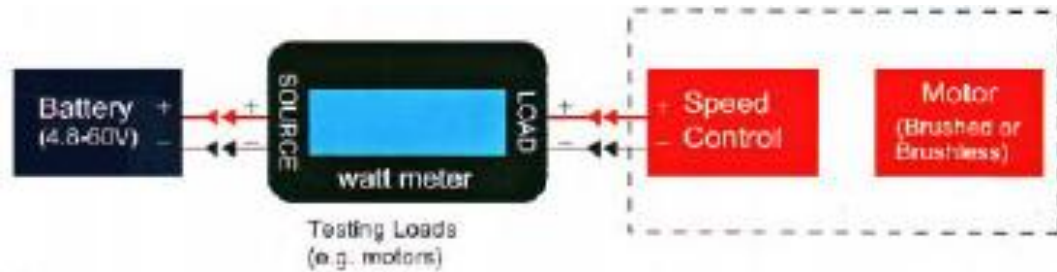


FIGURE 40 TURNIGY MONITOR CONNECTIONS [1]

Isolated DC-DC Converter

The team came together to discuss which components would be attached to the isolated DC-DC. After consulting with various advisors it was decided that the ventilation system, and the odometer would be connected to the isolated DC-DC converter. In the event the team attaches an odometer, the isolated DC-DC converter is subject to change. A block diagram of the isolated

DC-DC converter configuration is illustrated in Figure 41.36. The input to the converter is the 24V primary battery, and the output to the converter is the ventilation system. The Sanyo Denki fan was selected as a ventilation system due to its low price and appropriate specifications which can be seen in Appendix A23.

The appropriate DC-DC converter was selected by taking the fan's voltage rating of 12V and a current rating of 600mA into consideration. After taking the fan specifications and advisor consultations into consideration the team selected the Texas Instruments LM25017. This converter has a minimum input voltage of 9V and a maximum output voltage of 48V, which is well within the range of the battery. The minimum output voltage is 1.25V, the maximum output voltage is 40V, and the converter has a maximum output of 6.25A. All of these specifications fall within the appropriate ranges necessary in order to operate the ventilation system. The isolated DC-DC converter is relatively inexpensive with a cost of \$3.15. Specifications for the isolated DC-DC converter can be seen in Appendix A24.

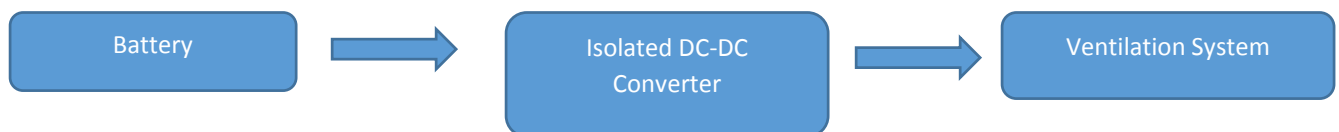


FIGURE 41 ISOLATED DC-DC CONVERTER CONFIGURATION



FIGURE 42 LM25017 ISOLATED DC-DC CONVERTER [5]

Advantages

- Low Cost
- Met all specifications of the battery and ventilation system

Many isolated DC-DC converters were compared but the converter that was chosen contained all the specifications the team needed. In the future the team would like to add an odometer. In the event an odometer is added, the selected isolated DC-DC converter is subject to change.

3.10 Motor Controller

Single Board Computer

The Single Board Controller will be the integrating tool between the selected components for the entire motor controller, including the gate driver and IGBT. The main approach when considering the board controller will be the board's compatibility with a 3 phase BLDC motor and Pulse Width Modulation for analog to digital conversions and speed control. The Board chosen was the TI TMS320F2808.

Advantages

- Low-Power Modes and Power Savings for less power consumption from propulsion battery
- Being familiar with the development tools included(C/C++) can make programming less time consuming
- The TI TMS320F28 will be borrowed from a professor at the University, helping to keep costs low

Several Single-Board Computers were considered. With competition rule restrictions in mind and after receiving expert advice from Dr. Chuy and Dr. Edrington, the TI RDK-BLDC, TI MSP430 Launch Pad, TI TMS320F2808, and the ATMEL ATAVRMC100 were amongst the final four board computer options. A decision matrix was then used to make a decision between the four board controllers. In the decision matrix, 4 factors were considered: safety, cost, efficiency, and implementation difficulty. Safety carried the most weight, followed by cost, efficiency and implementation, weighing at 0.432, 0.208, 0.187 and 0.173 respectively.

Initially, the TI RDK-BLDC scored the greatest score in the decision matrix. However, Article 67.A of the Shell Eco-marathon rules states “Modifications to purchased motor controllers are not acceptable.” Since the RDK-BLDC is accompanied with a motor, it is safe to assume disqualification. Therefore, TI TMS320F2808 became the next option primarily because it will be provided by a Professor from the College, hence decreasing the total cost of the project. Nevertheless, familiarity with the programming tools used for the TI TMS320F2808 makes implementation much easier.

Gate Driver

When choosing a gate driver, the same characteristics that were considered for the single board controller was also considered for the gate driver. The TIDRV8301DCA possessed features that will be convenient when integrating the electrical components of the motor controller.

Advantages

- Current Shunt amplifiers that support bi-directional current sensing
- Over current protection
- Specifically for three phase motor drive applications

Many gate drivers were initially considered. It is imperative that the gate driver selected was able to generate the necessary current to drive the IGBT. Using expert advice from Dr. Chuy and Dr. Edrington, the options for the gate driver was reduced to the International Rectifier IR3230SPF and Texas Instruments DRV8301DCA. From that point, a decision matrix similar to that used for the single board computer was used to make a decision between the two gate drivers. The same 4 factors were considered with the same weights applied: safety = 0.432, cost = 0.208, efficiency = 0.187 and implementation = 0.173. Although the DRV8301 was not the most cost efficient, it was the safest, efficient and easiest to implement with features such as over current protection and bi-directional current sensing.

3.11 DC-DC Converter

The purpose of the DC-DC converter is to take the DC power being transmitted from the solar panels and boost it using a MPPT (Maximum Power Point Tracking) algorithm such that it is able to charge the vehicles battery while in use. In order for this to happen, the output voltage from the DC-Dc converter must be constantly above the 24V of the lithium- ion battery. This will not always be the case as the output voltage on a cloudy day would be very close to the measured 11.5V.

Currently, the preexisting ISV005V2 board is rated to accept maximum voltages of up to 18V and output voltages of up to 28.8V. This is where the error lies in charging the battery. The solar panel inputs of 8-9V and 3-3.5A will only generate the output voltage of 24V because the input voltage is nowhere near its maximum.

Therefore, the design team has come to the conclusion that based on the ever-changing environments and thus ever-changing solar panel voltage levels that a second isolated DC-DC converter will need to be implemented. This design will ensure that the DC power leaving the solar

panels will enter the ISV005V2 board at the closest possible value to the maximum, which will ensure that the maximum output voltage of 28.8V can be achieved. Once this output voltage can be achieved, the battery can be properly charged while the car is in use.

SUBSYSTEM: ISV005V2

The ISV005V2 board is a DC-DC converter that was previously used in last year's senior design team. This component was not considered a success because it was unable to charge the battery when connected to a stiff voltage source.

However, under the most ideal conditions, the output of the ISV005V2 was measured to be 24V. Under a cloudy weather condition, the output voltage was measured to be 11.5V. The minimum voltage level leaving the first stage of DC-DC conversion is 10V based on this value, with some room to spare.

SUBSYSTEM: Texas Instruments LM5000

The purchase of the Texas Instruments LM5000 high voltage switch mode regulator. A computer generated image of the LM5000 is shown in Figure 43. This device operates differently as the ISV005V2 but the final results are the same. More specifically, the LM5000 does not operate using a MPPT algorithm but instead using Pulse Width Modulation.



FIGURE 43 LM5000 [6]

This product more than meets the necessary requirements for this stage in the design, it accepts a wide range of voltages (3.1V – 40V) and its adjustable output (1.259 V ~ 75 V) more than meets the requirements to charge the battery when in use. These values can be confirmed by the LM5000 datasheet in Appendix A25.

The circuit diagram for the LM5000 is shown in Figure 44. With this knowledge and more testing in all environments, the final output voltage can be achieved successfully. A testing plan would include using several different voltage dividing circuits to ensure that in most conditions met by the solar car, a successful stage 2 output voltage would be high enough to charge the battery when in use (>26V).

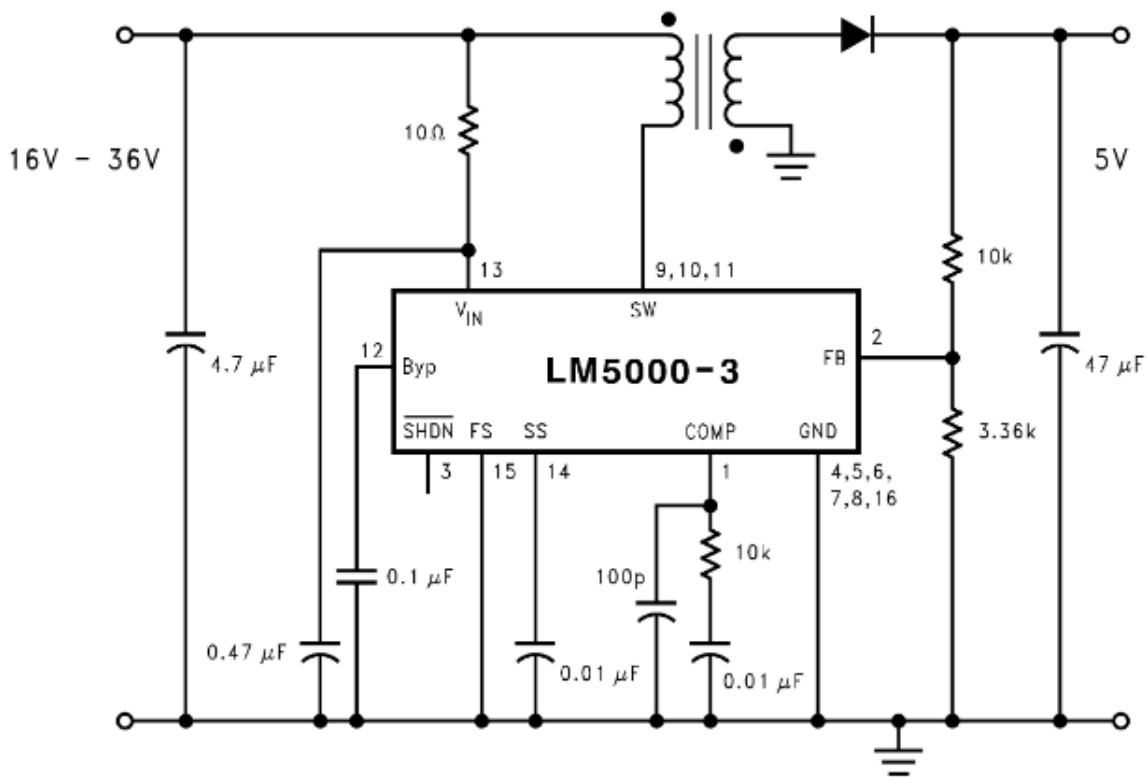


FIGURE 44 LM5000 INTERNAL CIRCUIT [6]

A typical voltage dividing circuit uses several resistor values to isolate the desired voltage across the load resistor. The load resistor in this case would be the charging lithium-ion battery. A circuit schematic of a typical voltage dividing circuit is shown in. Equation 24 governs the output voltage in a typical voltage divider. Using this relationship and the adjustable features of the LM5000, successfully charging the battery is possible.

$$\text{EQUATION 24 } V_{out} = V_{IN} \left(\frac{R_2}{R_1 + R_2} \right)$$

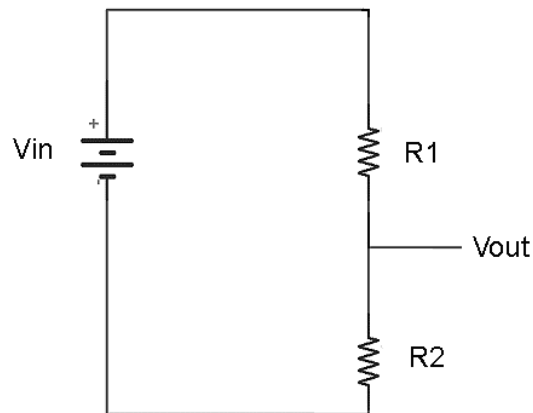


FIGURE 45 VOLTAGE DIVIDER CIRCUIT [7]

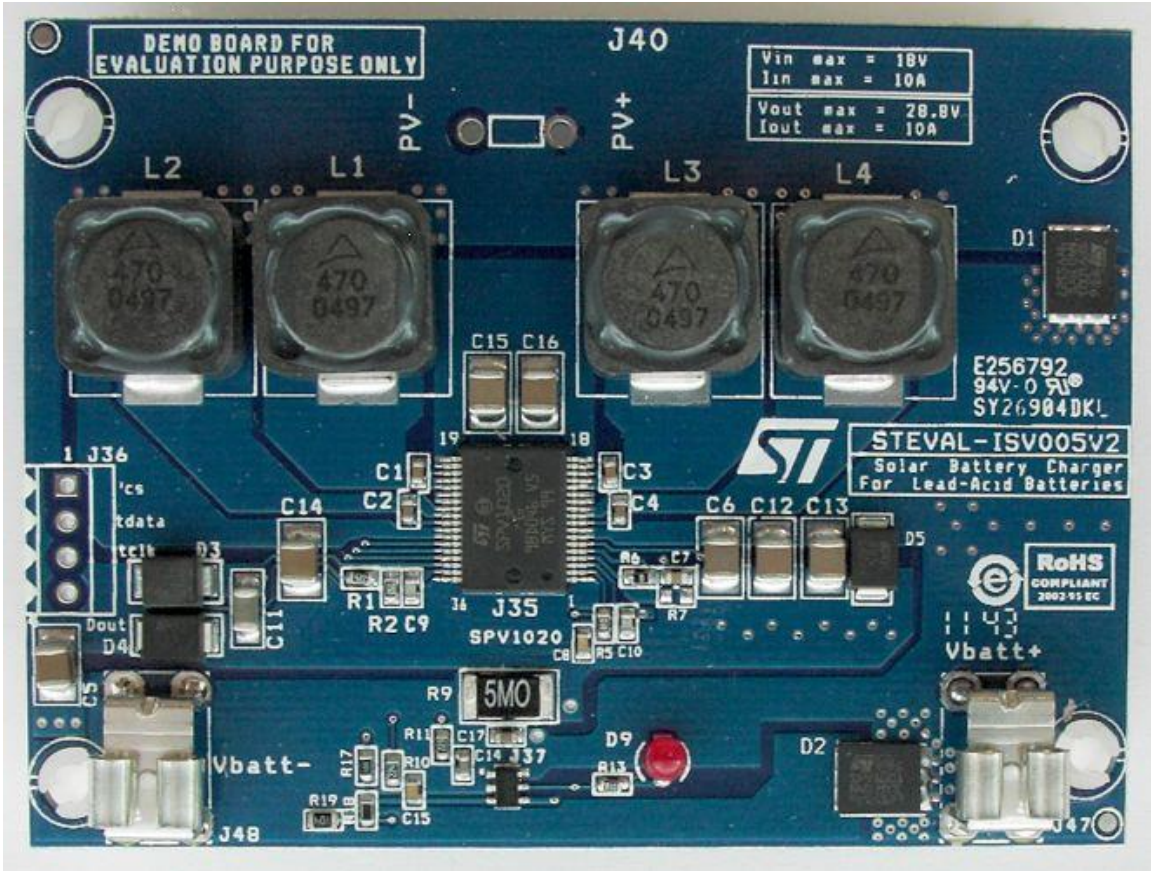


FIGURE 46 ISV005V2 BOARD [8]

4 Schedule

The team has created a Gantt chart to indicate the task by task scheduling from the project start to the project completion. The schedule has been broken down into four main sections: design, manufacturing, installation, and testing. All design aspects must be completed prior to the start of manufacturing in order to adhere to a concurrent engineering design philosophy. According to the Gantt chart schedule the design portion of the project will take place between October 14, 2013, and November 16, 2013. Once all design aspects have been completed the team will begin manufacturing each component of the vehicle according to the Gantt chart schedule. The manufacturing phase of the project will take place between December 16, 2013 and February 12, 2014. Once the manufacturing has been completed the team will begin the component installation which will last approximately 30 days. Once all components have been installed and the vehicle is fully functioning a 15 day testing period will take place. Based on the Gantt chart the following steps will be considered the critical path: front wheel mount design and analysis, front wheel steering design and analysis, front wheel brake design and analysis, tire manufacture, component installation, and testing. The team's completed Gantt chart can be found in Appendix A3 Gantt Chart.

The team has currently completed the design and analysis phase on time for major components listed in the Gantt chart including:

- Seat
- Roll bar
- Front wheel mount
- Front wheel steering

- Front wheel brake
- Rear wheel brake
- Battery compartment
- Tire
- DC-DC converter
- Resistor
- Accessory battery
- Pedals

The milestone 1 “Needs and Analysis” report and presentation have both been completed, moreover milestone 2 “Project Proposal” report and presentation have also been completed.

Due to an oversight the team has had to add a design and analysis for the roll hoop, and solar panel mounts in order to adhere to the rules and regulations. Although both additional parts have been designed and analyzed the additional time taken for these steps have set back the design for the bulk heads, rear view mirrors, and battery compartment. Although these designs have been set back none of them are critical tasks therefore they each have a slack time and will not set back the project completion dates. In order to remain on track the team will use part of the winter break which was included in the schedule to complete the design phase on time and commence the manufacturing phase of the project.

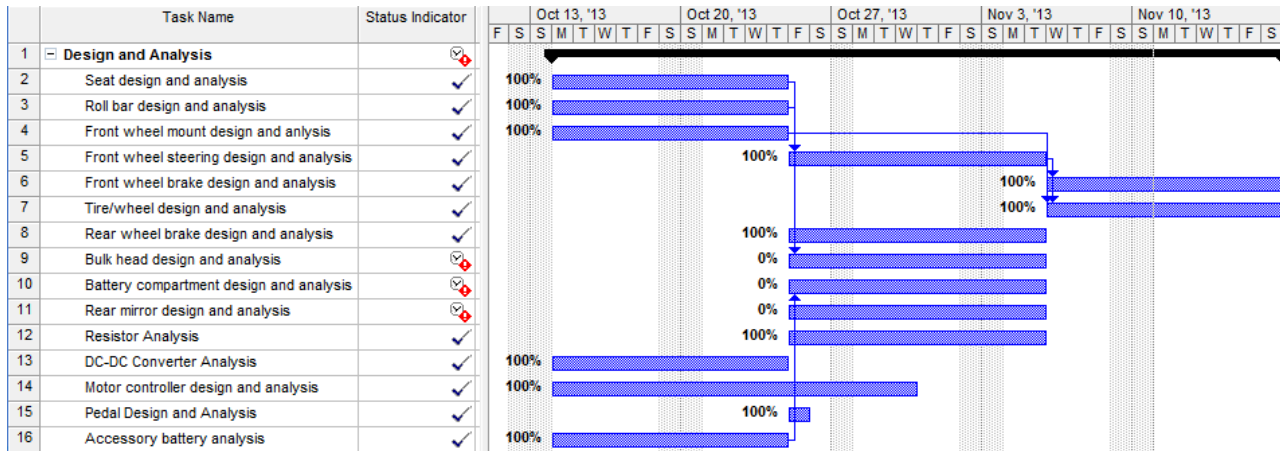


FIGURE 47 DESIGN PORTION OF THE GANTT CHART

Based on the team’s analysis of the accessory battery it has been decided that the option to use an accessory battery will be forgone. Since the accessory battery option will be forgone the manufacture 21 day manufacture time has been removed from the schedule which will allow additional recourses (team members) to be used during the manufacturing phase on any component which falls behind schedule.

5 Budget

Budgeting for the project was categorized into 3 main sections: material costs, personnel costs, and miscellaneous costs. Material costs include all costs associated with the materials necessary to manufacture remaining parts. Personnel costs were included per the request of the Electrical Engineering Department; these costs represent a simulation of the “real” cost of the project. Miscellaneous costs represents all costs not associated with materials and personnel.

Material costs were estimated by creating CAD models with engineered estimates of dimensions and tolerances. Several calculations for the estimates can be found in the Appendix section under the appropriate title. After the CAD models were created in the CREO, an analysis was done and the volume of each part was found. Using price estimates ($\$/\text{in}^3$) from a conglomerate of online materials providers [9], the total material cost was calculating by estimating the price of the total material volume. The estimates are tentative, and will be reviewed with HPMI engineering staff to determine their validity. Allowances will be made for possible scrap and re-work that may occur during manufacturing.

The mechanical engineering students decided during their design process that the bulk of the manufactured materials would consist of either aluminum or plastics. Their curriculum includes material science courses, so they are familiar with the material properties and desirable applications of these materials. Four different grades of aluminum were selected: 2011-T3, 2024-T3, 6061-T6, and 6262-T6511. These grades were selected for their range of machinability, strength, hardness, and surface finish.

The plastics were selected over a wide range as well. The selection included acrylic, nylon, polycarbonate, and polytetrafluoroethylene (Teflon). These plastics were selected for light weight, rigidity, strength, and low cost.

After the team's discussion with HPMI staff, and approval from all relevant parties, the team will be able to provide estimates for the remaining carbon fiber components. Until then the components are marked as to be determined (TBD). HPMI has generously offered to provide in-kind aid to the team, so we do not anticipate these costs to be high.

The personnel costs were calculating the criteria provided by the electrical engineering department. Personnel costs were calculated using a 32 week year with 12 hour work weeks, and hourly pay of \$30. We then calculated fringe benefits (perks) as 29% of yearly personnel pay which totaled to the sum of employee costs. Lastly, miscellaneous costs included expenditures of items that were not materials or personnel related, such as wiring, clamps, paint, etc.

Materials Budget Summary

Part:	Quantity:	Volume (in³)	Total Volume (in³)	Desired Material:
Front Brake Base	2	1.651	3.303	Aluminum
Front Wheel Mount	2	9.819	19.6395	Aluminum
Rotors	2	0.690	1.381	Aluminum
Front Mount	2	33.838	67.675	Aluminum
Rack and Pinion Base	1	15.951	15.951	Aluminum

Roll Bar	1	149.222	149.222	TBD
Petal Base	2	17.906	35.811	TBD
Petal Foot	2	3.538	7.077	TBD
Petal Pad	2	0.5407	1.081	TBD
Seat	1	121.497	121.497	TBD
Roll Hoop	1	21.24	21.24	TBD
Steering Column	1	2.209	2.209	Carbon Fiber
Steering Wheel	1	38.853	38.853	Carbon Fiber
Solar Panel Box	1	511.401	511.401	TBD

TABLE 9 MATERIAL QUANTITY VOLUME & DESIRED TYPE

<u>Aluminum Plate Price per 1 in³</u>				
Grade	2011-T3	2024-T3	6061-T6	6262-T6511
Price Estimate	\$1.47	1.84	\$0.96	\$0.96

TABLE 10 ALUMINUM GRADE PRICING

Part:	Volume (in³):	2011-T3	2024-T3	6061-T6	6262-T6511
Front Brake Base	3.303	\$4.86	\$6.08	\$3.17	\$3.17
Front Wheel Mount	19.639	\$28.87	\$36.14	\$18.85	\$18.85
Rotars	1.381	\$2.03	\$2.54	\$1.33	\$1.33
Front Mount	67.675	\$99.48	\$124.52	\$64.97	\$64.97
Rack and Pinion Base	15.951	\$23.45	\$29.35	\$15.31	\$15.31
Roll Bar	149.222	\$219.36	\$274.57	\$143.25	\$143.25
Petal Base	35.811	\$52.64	\$65.89	\$34.38	\$34.38
Petal Foot	7.077	\$10.40	\$13.02	\$6.79	\$6.79
Petal Pad	1.081	\$1.59	\$1.99	\$1.04	\$1.04
Seat	121.497	\$178.60	\$223.55	\$116.64	\$116.64
Roll Hoop	21.24	\$31.22	\$39.08	\$20.39	\$20.39
Steering Column	2.209	\$3.25	\$4.06	\$2.12	\$2.12
Steering Wheel	38.853	\$57.11	\$71.49	\$37.30	\$37.30
Totals	484.939	\$712.86	\$892.29	\$465.54	\$465.54

TABLE 11 PART COST BASED ON ALUMINUM TYPE

Part:	Total Volume (in³):
Petal Base	35.811
Petal Foot	7.077
Petal Pad	1.081
Solar Panel Casing	511.401
Total	555.370318

TABLE 12 TOTAL PART VOLUME

<u>Polymer Sheet Prices</u>				
	Acrylic	Nylon	Polycarbonate	PTFE
Price Estimate	\$9.35	\$57.99	\$14.84	\$60.22
Dimensions	12x24x0.125"	12x24x0.25"	12x24x0.236"	12x24x0.125"
Volume	36 in ³	72 in ³	68 in ³	36 in ³
Required Amount	16.00	8.00	9.00	16.00
Total Price	\$149.60	\$463.92	\$133.56	\$963.52

TABLE 13 POLYMER SHEET PRICES

Personnel Budget Summary

Name	Hours	Hourly Pay	Weekly Pay	Semesterly Pay¹	Yearly Pay²	Fringe Benefits³
Jose Cardenal	12	\$30.00	\$360.00	\$5,760.00	\$11,520.00	\$3,340.80

Francois Wolmarans	12	\$30.00	\$360.00	\$5,760.00	\$11,520.00	\$3,340.80
Zachary Barr	12	\$30.00	\$360.00	\$5,760.00	\$11,520.00	\$3,340.80
Fritz Jeanty	12	\$30.00	\$360.00	\$5,760.00	\$11,520.00	\$3,340.80
Julia Clarke	12	\$30.00	\$360.00	\$5,760.00	\$11,520.00	\$3,340.80
Wael Nabulsi	12	\$30.00	\$360.00	\$5,760.00	\$11,520.00	\$3,340.80
James Croasmun	12	\$30.00	\$360.00	\$5,760.00	\$11,520.00	\$3,340.80
David Jolicouer	12	\$30.00	\$360.00	\$5,760.00	\$11,520.00	\$3,340.80
TOTALS		\$240.00	\$2,880.00	\$46,080.00	\$92,160.00	\$26,726.40

TABLE 14 PERSONNEL BUDGET

¹ Based on 16 week semester

² Based on 32 week year

³ Calculated as 29% of yearly pay

Miscellaneous Budget Summary

Part #	Part Name	Number of Parts	Estimated Part Cost	Total Cost
1	Rear Wheel Tire	1	\$12.00	\$12.00
2	Wiring (Set)	1	\$50.00	\$50.00
3	Bolts (Set)	1	\$50.00	\$50.00
4	Clamps (Set)	1	\$20.00	\$20.00
5	Horn	1	\$10.00	\$10.00

6	Rear View Mirror Right	1	\$15.00	\$15.00
7	Rear View Mirror Left	1	\$15.00	\$15.00
8	Flame Retardant Suit	1	\$100.00	\$100.00
9	5 Point Harness (Seat Belt)	1	\$80.00	\$80.00
10	Helmet	1	\$30.00	\$30.00
11	Paint	1	\$120.00	\$120.00
12	Super Capacitor (Set)	1	\$50.00	\$50.00
13	Diode (Set)	1	\$10.00	\$10.00
14	Odometer (Set)	1	\$25.00	\$25.00
15	Resistor (Set)	1	\$10.00	\$10.00
Totals		15	\$597.00	\$597.00

TABLE 15 MISCELLANEOUS BUDGET

Starting Budget:	\$6,000.00
Expenditures:	\$597.00
Remaining Budget:	\$5,403.00

TABLE 16 REMAINING FUNDS

Overview Budget Summary

Expenditure	Cost
Personnel	\$92,160.00
Fringe Benefits	\$26,726.40
Expenses	\$597.00
Equipment ¹	\$0.00
Sub-Total	\$119,483.40

TABLE 17 SUMMARY OF DIRECT COSTS (MINUS MATERIALS)

Overhead Costs²	\$53,767.53
Total Estimated Project Cost	\$173,250.93

TABLE 18 TOTAL ESTIMATED COST (MINUS MATERIALS)

¹ Costs exceeding \$1000

² Calculated as 45% of direct costs

Materials estimates are excluded until design has been reviewed by HPMI.

6 Overall Risk Assessment

6.1 Technical Risks

Competition Requirements

In order to compete in the Shell Eco Challenge Marathon a technical write up for the vehicle is required. The technical write up must include a detailed description of the motor, motor controller, and all electrical and mechanical systems. Most of these components and systems are going to be built by the senior design team but the motor was left to them by last year's team. The motor that was purchased last year did not come with a technical description nor is one readily available online. The team member assigned to completing the technical write up will need to get in contact with the manufacture to obtain the details required for this competition.

Chassis Failure

The chassis to be used by this year's team was designed and manufactured by the previous year's senior design team. It is a monocoque structure and does not contain any internal frame work. The vehicle's shell must be able to support the full structural load of all the necessary components without any deformation occurring. If the chassis is not able to support the full load of the necessary components and the driver it will have to be redesigned and remanufactured. This could lead to a total project failure and the design team will not be able to compete in the competition. In order to not jeopardize the structural integrity of the vehicle any drilling into the chassis must be kept to a minimum.

Steering Failure

The competition requires the design team's vehicle to have an 8 meter turning radius. By designing the wheel mount and steering assemblies to be capable of a nearly 360 degree rotation the design team will use the steering component, either rack and pinion or plate steering, to limit the turning radius to the required 8 meters. The team will also test the vehicles turning radius prior to competition to ensure it is operating properly. This is a key requirement to compete in the competition and if the design team does not meet the requirement they will not be permitted to compete in the competition.

Braking Failure

The competition requires the vehicle to have two operating braking systems, one that acts of the front wheels and one that acts on the back wheels. The systems must be able to be engaged without having to remove a hand from the steering wheel. Each braking system must be capable of holding the vehicle in place on a 20 degree incline which will be tested at the competition. This will be a first time experience for the group members to design and install a fully functioning braking system. With the help of Dr. Hollis, and the knowledge of the required braking force needed to hold the car in place on the incline, the design team is confident they will be able to design and implement an efficient braking design.

Bulkhead Design and Installation

For the Shell Eco Challenge Marathon it requires that a permanent bulkhead be installed that separates the driver from all electrical and propulsion system components. The final layout of the electrical and mechanical systems has not been finalized and is likely to change during the design process which leads the design of the bulkhead to be put off till later in the design process.

Leaving a major component that is required to compete till later in the process is risky but by using materials available in the Engineering School machine shop and simple designs the engineering team hopes to minimize this risk. If the design team is not able to complete the bulkhead they will not be permitted to compete in the competition.

Motor Controller Failure

New for this year, the competition requires that each team construct their own motor controller. Building and programming a motor controller for a DC Brushless 3 phase motor is new to the design team. If they fail to properly construct the motor controller it could lead to a catastrophic design failure. The vehicle would likely not operate properly and could cause the motor to burn out or even overload the wires and circuits. By starting this process early in the design phase and using a mock motor during the testing phase the team hopes to minimize this risk.

Motor Controller Disqualification

In order to comply with competition rules and regulations the motor controller must be purpose built in a manner which demonstrates a clear understanding of the driver and power stage. The TI TMS320F2808 consists of a pre-soldered power stage, therefore an email was sent to a representative from the shell eco marathon competition in order to determine whether or not each team must purchase their board, driver, and power stage separately. According to the representative:

“Yes. The team does not need to purchase components from different suppliers. They must, however, integrate the components together into a MC system. This includes doing both hardware and software.”

Using the TI TMS320F2808 alone risks disqualification from the competition. Therefore, the alternative of designing a custom Printed Circuit Board (PCB) is being exercised by the team and advisors. This would allow the team to purpose build a motor-controller specifically for the motor.

DC-DC Conversion System

The risks associated with the DC-DC conversion system are minimal all things considered. For example, a failure of the system would only mean that the battery is not being charged simultaneously while it is being discharged. The different over voltage and over current protection implemented in the two stages of the DC-DC conversion system prevent the possibility of a power surge that could harm the battery.

DC-DC Conversion Stage: ISV005V2

The IDV005V2 has been tested during an extremely cloudy day and as such has been treated as the worst case scenario. This voltage was measured to be 11.5V, leading to the decision to make the minimum voltage leaving the first stage to be set at 10V.

DC-DC Conversion Stage: LM5000

The secondary DC-DC converter is implemented to compensate for the low voltages entering the ISV005V2. Thus, the risk is the same as the first stage of DC-DC conversion. Similar to the ISV005V2 board, the LM5000 stage has protection against over voltage and over current. One major risk associated with this stage is if a large enough voltage (>30V) were leaving, it would harm the battery. However, this isn't likely considering the input from the first DC-DC converter stage.

Battery Failure

The Shell Eco-Marathon competition states that lithium ion batteries must have a battery management system to protect cell under/over voltage limits, over current limit, over temperature limit, the individual cells as well as the entire pack. A malfunction in the BMS could result in a damaged battery. If the BMS fails and the battery is severely damaged the car will be inoperable. To ensure this does not happen the 2013-2014 solar car team will conduct a test to determine the protection limits and what occurs when the limit is reached.

Solar Panel Installation Failure

Shell Eco Challenge Marathon requires that the solar cells be installed and seated flush with the surface of the car. This is one area of the design process that the team has not yet addressed. The team will need to come up with a plan to meet this requirement. With the help of Dr. Hollis and the staff over at HPMI the team will be able come up with a process to properly seat and anchor our solar panels.

6.2 Schedule Risks

Ordered Parts

The team will have to order various parts and materials from suppliers. When ordering parts and materials from suppliers there is the additional risk of parts being delayed which can cause the manufacturing of a part to be delayed. If the manufacturing of a component which is part of the critical path is delayed the entire project can be delayed, and the team will run the risk of not completing the project by the designated deadline.

Required Equipment

Once the manufacturing phase commences the team will require access to various machines, tools, and technical equipment. If the team is unable to readily access any of these tools

it will delay the component completion. Similar to ordering delays if the component is part of the critical path it can cause the team to run the risk of not completing the project by the designated deadline.

Overlooked Designs

Building and designing a functional vehicle is a complex process. This process requires the design, manufacture, and installation of multiple components. In order to complete the vehicle in time for the competition each team member has been assigned specific tasks. If a component is overlooked due to the team's limited experience with vehicle design it will detract resources (team members) from their assigned tasks in order to complete the additional components. Detracting resources from specified tasks can cause those tasks to be delayed. If the component is part of the critical path it can cause the team to run the risk of not completing the project by the designated deadline.

Testing Phase

Throughout the design and manufacturing of each component the team will run extensive tests in order to assure quality, reliability, and safety. Although the team will run individual component tests and use simulations in order to test the entire vehicle before it is built the risk of failure when testing the completed vehicle is always present. If a major component such as the chassis fails, the team may not have enough time to rebuild the vehicle and correct the failure prior to the competition.

6.3 Budget Risks

Funding Requests

The team was told that a \$6000 budget was allocated to this project, however the money has not yet been appropriated. Now that the design has been finalized, and the material requirements and pricing has been determined, the team will be able to submit a formal request for funds. In the event of an emergency, such as the team not qualifying for the Eco-marathon, funding to this project may not be appropriated at the desired level.

Indirect Material Costs

Materials costs usually include more than the just the direct cost of the materials used to manufacture/assemble a product. Additional costs can include collateral costs, such as freight and insurance, as well as overruns, spoilage, and defective parts [10]. These types of costs are usually referred to as indirect material costs, and are defined as costs not directly identified with a single final cost objective. In the event of an error during manufacturing or material estimates, indirect material costs can quickly add up.

Pricing Estimates

Currently pricing of materials consists of estimates performed by calculating the volume of materials necessary to manufacture all necessary parts. The volume of materials was summed and then the price was estimated using a \$/in³ price from a major online materials provider. In the coming week, the team has arranged a meeting with Dr. Liang (Director of HPMI) and Mr. Jeremy Horne (Manufacturing engineer at HPMI); with their professional help, the material requirements and pricing estimates will be reviewed and corrected. However, until the team has secured their approval, there is some risk associated with the pricing estimates.

7 Conclusion

The team is required to build a solar-powered electrical vehicle which conforms to the rules and regulations of the Shell 2014 Eco-Challenge competition. The car is required to have several features which will ensure the safety of the driver and reduce the risk of mechanical or electrical failure. There are several dimension limitations including the height, width, ratio of height to track width, wheelbase, total length, and vehicle weight. Additionally, there are minimum standards established for the turning radius, and braking requirements.

After establishing the existence and strength of the relationships between the customer requirements and the design factors (quality characteristics on HOQ), the team ranked the importance of each customer requirement. Each customer requirement was ranked equally (max score) because the competition requires teams to satisfy all rules and regulations in order to participate; based on this it was determined that no preference should be given to one customer requirement over another. The primary concern for ranking in the competition is the efficiency of the vehicle, which will be determined by the organizer's evaluation.

Once the HOQ was completed the team created a comparison matrix template using the most significant factors, in order to rank components against their alternatives in the design selection phase. The comparison matrix was created by assigning normalized percentage weight values, which were derived from our HOQ analysis, to each ranking criteria. Next an optimization legend was created, in order to determine which design was the most optimal for the vehicle. Each component was assigned a ranking relative to its alternatives. A higher score indicates a more optimal solution, while a score of 1 indicates the least optimal solution. The weights were then applied to the relative rankings, which gave us insight into which components best fit the

customer's requirements. The alternative designs were generated based on input received from various advisors and professionals in the respective fields. The largest design problem that had to be solved was striking a balance between the necessary trade-offs for the weight, the cost, and the safety of vehicle.

The team decided to split the design work into two categories: mechanical and electrical components. After consulting with the advisors for the project on the status and validity of their designs, the team went to work simulating the mechanical and electrical behavior of the car's components. Various measurements were checked in order to ensure the safety, speed, low weight, and affordability of the vehicle. Mechanical components that were designed include: a roll bar and rear wheel mount, a roll hoop, a steering system, a braking system, a seat, the wheels, and a bulkhead. Electrical components that were designed include: the solar panel system, the propulsion system, the motor controller, the single board computer, and the DC-DC converter. Each component had its own unique design limitations which had to be considered before designs could be finalized.

Budgeting for the project was categorized into 3 main sections: material costs, personnel costs, and miscellaneous costs. Material costs include all costs associated with the materials necessary to manufacture remaining parts. Personnel costs were included per the request of the Electrical Engineering Department; these costs represent a simulation of the "real" cost of the project. Miscellaneous costs represents all costs not associated with materials and personnel.

Material costs were estimated by creating CAD models with engineered estimates of dimensions and tolerances. Several calculations for the estimates can be found in the Appendix section under the appropriate title. After the CAD models were created in the CREO, an analysis was done and the volume of each part was found. Using price estimates ($\$/\text{in}^3$) from a

conglomerate of online materials providers¹, the total material cost was calculating by estimating the price of the total material volume. The estimates are tentative, and will be reviewed with HPMI engineering staff to determine their validity. Allowances will be made for possible scrap and re-work that may occur during manufacturing.

The measurements performed by the team included a center of gravity calculations, a weight distribution, static vertical wheel load calculations, turning radius and tie rod calculations, and the turning radius calculation. These measurements will allow the team to finish the Measure step of their Define, Measure, Analyze, Design, Verify (DMADV) design process. In the next phase, the designs will be scrutinized by faculty members during the report and oral review. Once their approval has been earned, the team will then move on to analyzing the design for small improvements which could lead a cumulative gains in the efficiency of the vehicle.

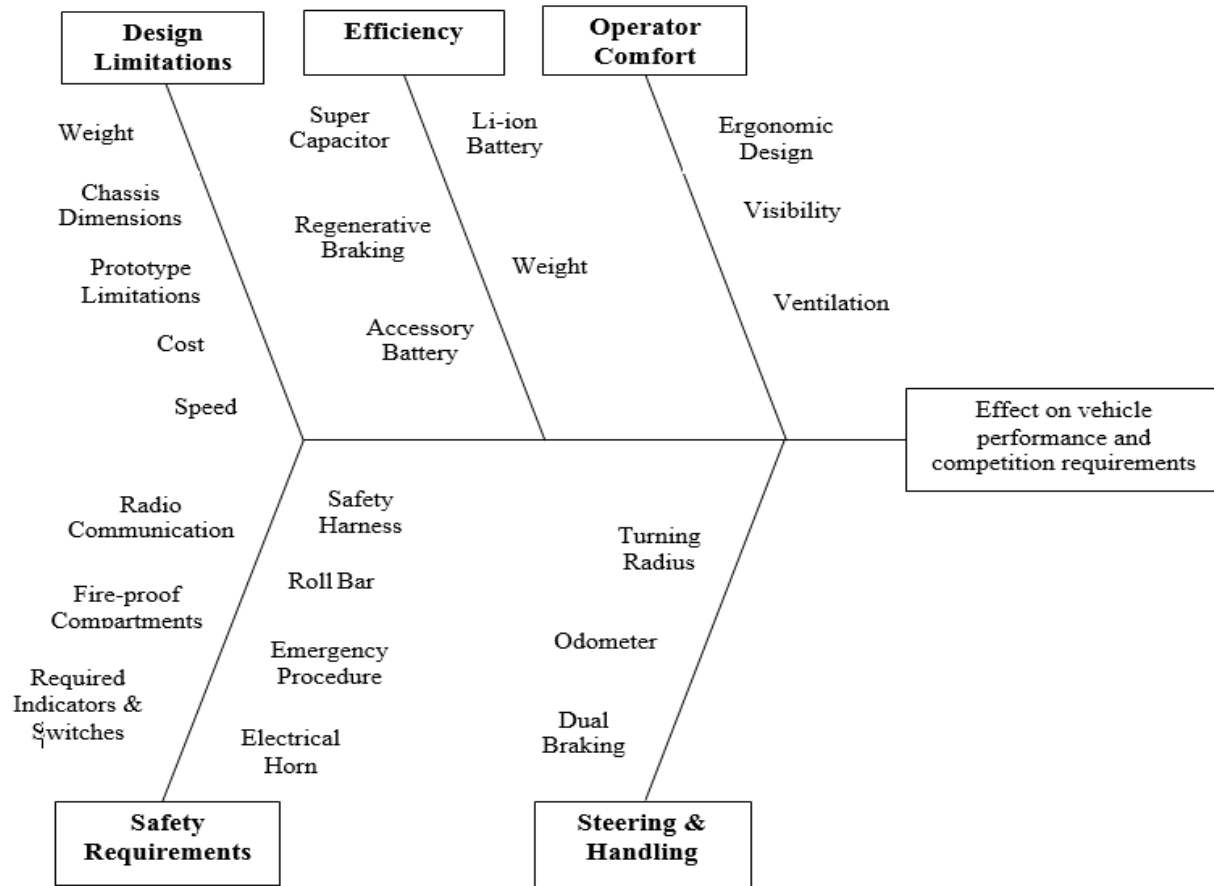
8 References

- [1] FAMU-FSU 2012 Solar Car Final System Design Review Report, Bosworth et al, April 2013.
- [2] "TMS320F2808." *Data Sheet*. Texas Instruments, n.d. Web. 14 Nov. 2013.
<<http://www.ti.com/lit/ds/symlink/tms320f2808.pdf>>.
- [3] " DRV8301." *Data Sheet*. Texas Instruments, n.d. Web. 14 Nov. 2013.
<<http://www.ti.com/lit/ds/symlink/tms320f2808.pdf>>.
- [4] "Turning Radius Calculation, Steering Assistance and Parking Assistance Employing Turning Radius Function." - *Patent #07706943*. N.p., n.d. Web. 14 Nov. 2013.
- [5] "LM25017(ACTIVE)48V, 650mA Wide Vin Synchronous Step-down Regulator with Integrated MOSFETs." *Converter (Integrated Switch)*. N.p., n.d. Web. 14 Nov. 2013.
- [6] *LM5000*. Digital image. *Www.ti.com*. Texas Instruments, n.d. Web. 14 Nov. 2013.
(<http://www.ti.com/lit/ds/symlink/lm5000.pdf>.)
- [7] "The Voltage Divider Rule." *The Voltage Divider Rule*. N.p., n.d. Web. 14 Nov. 2013.
<<http://www.aikenamps.com/VoltageDividerRule.htm>>.
- [8] "ISV005V2." *Data Sheet for ISV005V2*. Steval Microelectronics, n.d. Web. 14 Nov. 2013. <http://www.st.com/st-web-ui/static/active/en/resource/technical/document/data_brief/DM00047381.pdf>.
- [9] Online Metals store, Metals and Plastics, November 11, 2013.
(<http://www.onlinemetals.com/index.cfm>)
- [10] Defense Pricing and Acquisitions, Defence Pricing, July 23, 2013.
(http://www.acq.osd.mil/dpap/cpf/docs/contract_pricing_finance_guide/vol3_ch6.pdf)

- [11] "Small Mechanical Components: Precision Gears, Gear Assemblies, Timing Belts, Timing Belt Pulleys and Couplings - SDP/SI." *Small Mechanical Components: Precision Gears, Gear Assemblies, Timing Belts, Timing Belt Pulleys and Couplings - SDP/SI*. N.p., n.d. Web. 14 Nov. 2013. <<http://www.sdp-si.com/>>.
- [12] "SANYO DENKI - SANACE FANS - 109BF12HC2 - DC BLOWER, 120 X 32MM, 12V." *109BF12HC2*. N.p., n.d. Web. 14 Nov. 2013.

Appendix

A1: Fish Bone Analysis



The group began by comparing the required dual braking system to each of the thirteen quality characteristics. After careful analysis the following relationships were established:

- Strong relationship with safety, because having dual braking systems adds extra safety measures to the car.
- Weak relationship with weight, because adding a secondary braking system will slightly increase the cars weight.
- Moderate relationship with cost, because the dual braking system will moderately increase the cars cost.
- Strong relationship with regenerative braking system, because the braking systems will be directly related to regenerative braking.

The required safety features were then compared to each of the thirteen quality characteristics. A roll bar, 5 point seat belt, rear view mirrors, turning radius requirements, and bulkheads were considered when establishing the following relationships:

- Weak relationship with ventilation, because having a ventilation system will increase the operational safety when operating in extreme environments.
- Moderate relationship with speed, because adding these safety features moderately increases the vehicles weight which ultimately decreases the vehicles speed.
- Strong relationship with safety, because each of these safety features adds an extra level of operational safety.
- Moderate relationship with turning radius, because increased turning radius increases the cars maneuverability which affects the overall safety of the driver.
- Strong relationship with weight, because adding these safety features will significantly increase the cars weight.
- Strong relationship with visibility, because safety features such as the rear view mirrors will directly affect the driver's visibility.
- Weak relationship with ergonomic aspects of the car because implementing all of the safety features will make it more difficult to design the car in an ergonomic manner due to space restrictions.
- Strong relationship with cost, because implementing each safety feature will significantly increase the cost of the project.
- Weak relationship with a super capacitor, since the addition of a super capacitor increases the probability of an overload.

Required emergency procedures were compared to each of the thirteen quality characteristics. The addition of a ten second escape plan, and an electrical shutdown switch were considered when establishing the following relationships:

- Strong relationship with safety, including a ten second escape plan and having emergency shutdown switches will significantly increase the operational safety.
- Weak relationship with weight, because including these emergency procedures will slightly increase the cars weight due to extra parts.
- Strong relationship with ergonomic aspects, because including these emergency procedures will directly affect the ergonomic design of the car.
- Weak relationship with radio communication because having radio communication will make following emergency procedures easier at the time of an emergency.

- Moderate relationship with cost, because adding the extra parts necessary to incorporate these emergency procedures will moderately increase the cost of the project.

Required visibility was compared to each of the thirteen quality characteristics. The addition of rear view mirrors and a 180 degree field of vision were considered when establishing the following relationships:

- Strong relationship with safety because having the required visibility specs met significantly increases the operational safety of the vehicle.
- Strong relationship with visibility because having the required visibility specs met significantly increases the driver's visibility.
- Weak relationship with radio communication because radio communication will allow the pit crew to help the driver with their surroundings.
- Weak relationship with cost because having the required visibility specs met will slightly increase the project's cost. For example rear view mirrors will need to be purchased.

Required vehicle dimensions were compared to each of the thirteen quality characteristics. After careful analysis the following relationships were established:

- Weak relationship with ventilation, because the constricted size of the car limits the types of ventilation which can be used.
- Strong relationship with speed, because the vehicles dimensions directly affect the vehicles speed. The larger the vehicle, the slower it will run due to the limited engine size and energy capabilities.
- Strong relationship with safety, because the larger the car the more safe it will be. Inversely the smaller the car the less safe it will be.
- Strong relationship with turning radius because the turning radius is directly affected by the vehicle dimensions.
- Strong relationship with weight because the larger the car the more it will weigh, and vice versa, the smaller the car the less it will weigh.
- Strong relationship with visibility because the dimensions of the car will directly affect the drivers visibility. The shape and dimensions can also add blind spots in the driver's field of vision.
- Strong relationship with ergonomic aspects of the car dimension limits will directly affect the ergonomic design capabilities. The smaller the car the more difficult it will be to implement an ergonomic design.
- Strong relationship with cost because the larger the car the more material is used which increases the cost of the project, and vice versa the smaller the car the less material that is used, and the cheaper the cost of the project.

Separated fire proof compartments were compared to each of the thirteen quality characteristics. The fire retardant bulk heads were also considered when making these correlations. After careful analysis the following relationships were established:

- Weak relationship with ventilation, because the separate fire proof compartments make it more difficult to add ventilation to the car. Furthermore, the separated fire proof compartments take up a considerable amount of space which also decreases the ventilation possibilities.

- Strong relationship with safety, because having the separate fire proof compartments will directly increase the operational safety of the vehicle.
- Moderate relationship with weight, because adding the materials necessary to implement the separate fire proof compartments and the bulkheads will moderately increase the weight of the vehicle.
- Moderate relationship with cost, because adding the materials necessary to implement the separate fire proof compartments and the bulkheads will moderately increase the cost of the project.

Required indicators and switches were compared to each of the thirteen quality characteristics. The escape latch indicators and red arrows, the system shutdown switch, and the system shut down indicators were considered when establishing the following relationships:

- Strong relationship with safety, because the switches and indicators considered directly increase the operational safety during an emergency.
- Strong relationship with ergonomic design, because the location of the switches must be easily accessible to the driver of the car.
- Weak relationship with cost, because the switches and indicators considered should be fairly inexpensive to implement.
- Strong relationship with the odometer, because it is an indicator that is highly desired.
- Strong relationship with the accessory battery, because the accessory battery will power the additional indicators and switches.

The electric horn was compared to each of the thirteen quality characteristics. After careful analysis the following correlations were made:

- Strong relationship with safety, because having an electric horn will allow the driver to safely pass other vehicles on the track.
- Weak relationship with cost because the electric horn will be fairly inexpensive to implement.
- Strong relationship with the accessory battery, because the electric horn will be powered by the accessory battery.

The Li-Ion battery and the battery management system were compared to each of the thirteen quality characteristics. After careful analysis the following relationships were established:

- Strong relationship with speed, because the power which the battery produces, directly affects the vehicles speed.
- Strong relationship with safety, because implementing the battery and battery management system means having specialized safety precautions such as fire retardant bulk heads.
- Moderate relationship with weight because the battery weighs approximately 10lbs.
- Strong relationship with cost, because the Li-Ion Battery is one of the most expensive components in the vehicle.
- Strong relationship with a super capacitor, because the super capacitor will help charge the battery.
- Strong relationship with the regenerative braking, because the regenerative braking will help charge the battery.

The vehicles efficiency was compared to each of the thirteen quality characteristics. In terms of the competition the vehicles efficiency will be measured in km/kWh. After careful analysis the following relationships were established:

- Weak relationship with speed, because the speed at which the vehicle travels will affect the vehicles overall efficiency.
- Strong relationship with weight, because the vehicles weight will directly affect the efficiency. The lighter the vehicle the more efficient it will be.
- Strong relationship with a super capacitor, because the super capacitor will help charge the battery, thus increasing the distance traveled.
- Strong relationship with the regenerative braking, because the regenerative braking will help charge the battery, thus increasing the distance traveled.

Next it was determined that each functional requirement had to be ranked according to the HOQ optimization criteria. The direction of improvement for each variable was ranked as requiring minimization/maximization; in the case of a binary variable, each characteristic was simply marked to indicate that the requirement has been fulfilled. The results were as follows:

- Ventilation: Maximize
- Speed: Maximize
- Safety: Maximize
- Turning Radius: Minimize
- Weight: Minimize
- Visibility: Maximize
- Ergonomics: Maximize
- Radio Communication: On target
- Cost: Minimize
- Accessory Battery: On target
- Super capacitor: On target
- Odometer: On target
- Regenerative Braking: On target

The correlations between the quality characteristics was assessed based on the optimization criteria in order to determine the nature and strength of their relationship.

The ventilation variable shared the following correlations:

- A weak positive relationship with safety, because proper ventilation will help to ensure that the driver can operate the vehicle with full awareness of their surroundings.
- A strong positive relationship with ergonomics, because it ensures the comfort of the driver.
- A weak negative relationship with cost, because creating proper ventilation will require additional tool work and possibly procurement.
- A strong positive relationship with the accessory battery, because the ventilation may run off of the accessory battery.

The speed variable shared the following correlations:

- A strong negative relationship with the safety, because increasing the speed requires a reduction of materials used for the chassis, thereby reducing the overall safety of the driver in case of an accident.
- A strong positive relationship with the weight, because decreasing the weight will lead to a faster top speed.
- A weak negative relationship with ergonomics, because improving the ergonomics will require additional material which increases the weight.
- A strong positive relationship with the accessory battery, because the ventilation will run on the accessory battery.
- A strong negative relationship with cost, because increasing the speed will require additional mechanical and electrical parts.
- A weak positive relationship with the super capacitor, because the super capacitor will help to store additional power for the motor.
- A weak positive relationship with the regenerative braking, because it will help to generate additional power for the motor.

The safety variable shared the following correlations:

- A weak positive relationship with the turning radius, because the car needs to be able to safely navigate turns.
- A strong negative relationship with the weight, because the additional safety features will add additional weight to the car.
- A strong positive relationship with visibility, because the driver needs to be able to see everything within a 180 degree field of vision.
- A strong positive relationship with ergonomics, because it is directly related to all indicators and gauges that provide the operator with necessary information.
- A weak positive relationship with radio communication, because it will allow the pit crew to keep in contact with the operator in case of an emergency.
- A strong negative relationship with cost, because each additional safety consideration requires additional purchasing or modification.
- A weak positive relationship with the accessory battery, because the additional battery will power all of the safety components.
- A weak positive relationship with the super capacitor, because the super capacitor increases the risk of fire hazard.
- A weak positive relationship with the regenerative braking, because adding the additional components would increase the probability for mechanical error.

The turning radius variable shared the following correlations:

- A weak negative relationship with the weight, because adding the additional mechanical parts would cause a small increase in weight.
- A weak negative relationship with the cost, because procuring the additional parts would also increase the cost.

The weight variable shared the following correlations:

- A weak negative relationship with visibility, because adding the additional Plexiglas cover would increase the weight.

- A weak negative relationship with ergonomics, because adding additional material to increase the ergonomics would increase the weight.
- A strong positive relationship with cost, because reducing the weight would require much more expensive materials (i.e. Al honeycomb).
- A strong negative relationship with the accessory battery, because the additional battery adds significant weight to the vehicle.
- A weak negative relationship with the super capacitor, because it will add additional weight to the vehicle.
- A weak negative relationship with the odometer, because installing it will require additional parts which will add to the weight.
- A weak negative relationship with the regenerative braking, because the additional parts will increase the weight.

The visibility variable shared the following correlations:

- A strong positive relationship with ergonomics, because it allows for clear vision of the race track which is essential to human factors design.
- A weak negative relationship with the cost, because the Plexiglas cover and machining will cost additional money.

The ergonomics variable shared the following correlations:

- A strong negative relationship with cost, because increasing the comfort of use for the operator will increase costs.
- A weak positive relationship with the accessory battery, because some components (such as ventilation) will operate off of the additional battery.
- A weak positive relationship with odometer, because the odometer is an indicator which increases the safety of use for the operator.

The radio communication variable shared the following correlations:

- A weak negative relationship with the cost, because procuring the equipment will add to the costs.

The cost variable shared the following correlations:

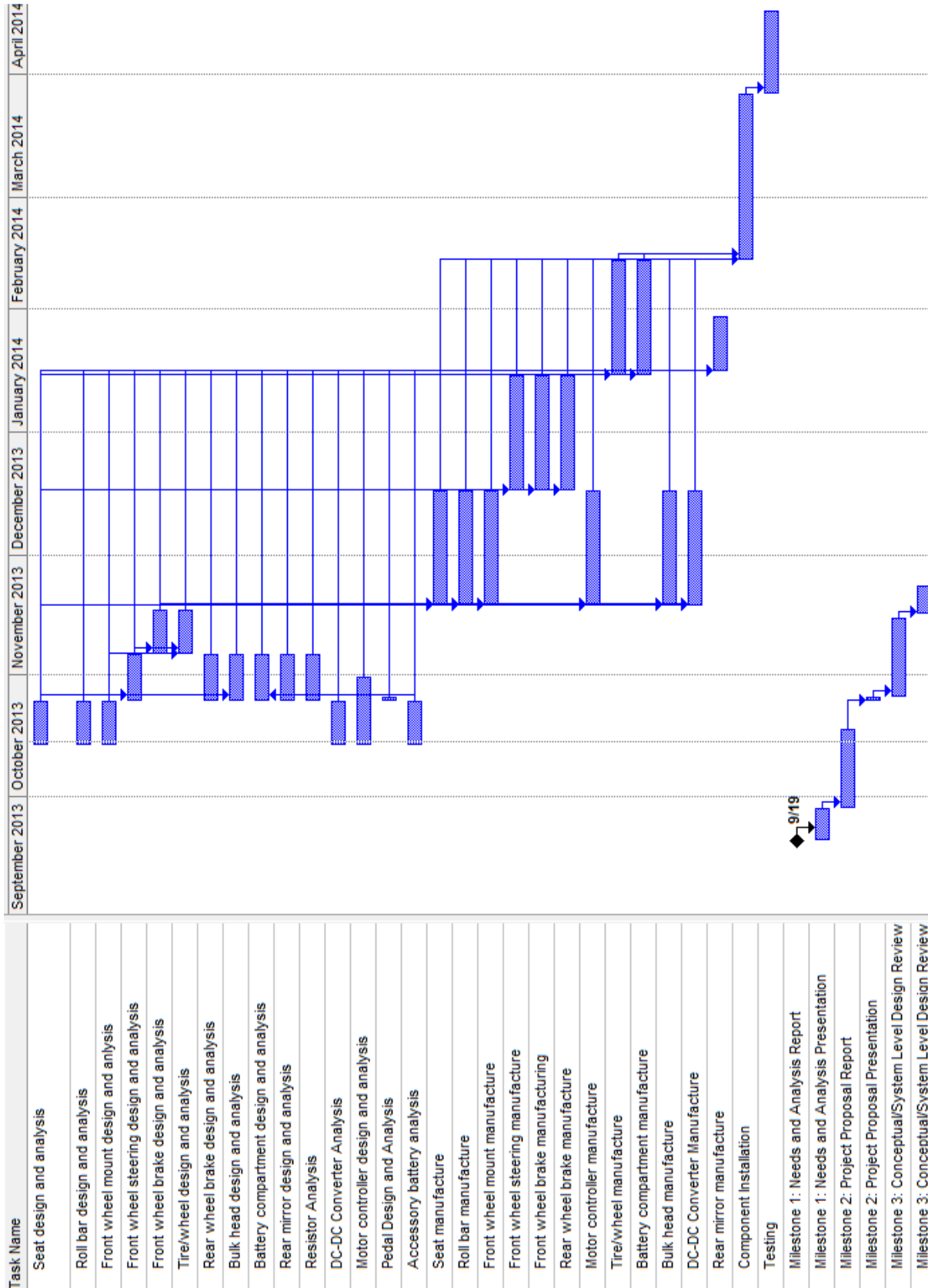
- A weak negative relationship with the accessory battery, because the additional battery will add to the cost.
- A weak negative relationship with the super capacitor, because the additional electrical parts will add to the cost.
- A weak negative relationship with the odometer, because the additional equipment will add to the cost.
- A weak negative relationship with the regenerative braking, because the additional mechanical equipment will add to the cost.

The accessory battery variable shared the following correlations:

- A strong positive relationship with the odometer, because the odometer will be powered using the additional battery.

Lastly, a competitor analysis was done using the FAMU-FSU 2011 solar car as a competitor. Using the requirements for participation in the 2014 Shell Eco-Solar challenge, we ranked both designs side by side. The 2014 solar car design scored a 5 in each category, and showed great improvement over the previous design.

A3: Gantt chart



A4: Motor Controller Specs

电机试验记录表

生产厂家:GoldenMotor.com 型号:MagicPie

编号:F0001150001

日期:2009年11月21日 操作者:

说明	转矩(N.m)	转速(r/min)	输出功率(W)	电压(V)	电流(A)	输入功率(W)	效率(%)
转矩(torque)Max	22.63	130	308.88	23.86	19.18	457.53	67.5
转速(revolution)Max	0.00	178	0.00	24.07	0.94	22.65	0.0
输出功率(Output)Max	22.63	130	308.88	23.86	19.18	457.53	67.5
电压(Voltage)Max	0.00	178	0.00	24.07	0.94	22.65	0.0
电流(Current)Max	22.63	130	308.88	23.86	19.18	457.53	67.5
输入功率(Input)Max	22.63	130	308.88	23.86	19.18	457.53	67.5
效率(efficiency)Max	8.94	159	148.78	23.99	8.14	195.38	76.1
1	0.00	178	0.00	24.07	0.94	22.65	0.0
2	0.13	177	2.43	24.07	1.05	25.19	9.7
3	0.26	177	4.86	24.07	1.15	27.73	17.5
4	0.39	177	7.27	24.07	1.26	30.27	24.0
5	0.52	176	9.68	24.07	1.36	32.81	29.5
6	0.66	176	12.09	24.07	1.47	35.35	34.2
7	0.79	176	14.48	24.07	1.57	37.89	38.2
8	0.92	176	16.87	24.06	1.68	40.43	41.7
9	1.05	175	19.25	24.06	1.79	42.96	44.8
10	1.18	175	21.62	24.06	1.89	45.50	47.5
11	1.31	175	23.99	24.06	2.00	48.04	49.9
12	1.22	175	22.36	24.06	1.92	46.30	48.3
13	1.17	175	21.46	24.06	1.88	45.33	47.3
14	1.09	175	20.01	24.06	1.82	43.78	45.7

15	1.01	175	18.56	24.06	1.75	42.23	44.0
16	0.92	176	16.92	24.06	1.68	40.48	41.8
17	0.84	176	15.47	24.07	1.62	38.93	39.7
18	0.81	176	14.92	24.07	1.59	38.35	38.9
19	0.72	176	13.28	24.07	1.52	36.61	36.3
20	0.64	176	11.81	24.07	1.46	35.06	33.7
21	0.53	176	9.79	24.07	1.37	32.93	29.7
22	0.44	177	8.14	24.07	1.30	31.18	26.1
23	0.31	177	5.74	24.07	1.19	28.66	20.0
24	0.18	177	3.34	24.07	1.09	26.14	12.8
25	0.10	177	1.86	24.07	1.02	24.59	7.6
26	0.00	178	0.00	24.07	0.94	22.65	0.0
27	0.09	177	1.67	24.07	1.01	24.40	6.9
28	0.28	177	5.19	24.07	1.17	28.08	18.5
29	0.39	177	7.22	24.07	1.26	30.21	23.9
30	0.55	176	10.16	24.07	1.38	33.31	30.5
31	0.65	176	12.00	24.07	1.46	35.25	34.0
32	0.86	176	15.83	24.07	1.63	39.32	40.3
33	1.09	175	20.01	24.06	1.82	43.78	45.7
34	1.05	175	19.29	24.06	1.79	43.00	44.8
35	1.21	175	22.18	24.06	1.92	46.10	48.1
36	1.50	174	27.40	24.06	2.15	51.72	53.0
37	1.74	174	31.70	24.06	2.34	56.37	56.2
38	1.65	174	30.09	24.06	2.27	54.62	55.1
39	1.86	174	33.83	24.06	2.44	58.69	57.6
40	2.12	173	38.44	24.05	2.65	63.72	60.3
41	2.22	173	40.21	24.05	2.73	65.66	61.2
42	2.38	173	43.02	24.05	2.86	68.76	62.6

说明	转矩(N.m)	转速(r/min)	输出功率(W)	电压(V)	电流(A)	输入功率(W)	效率(%)
----	---------	-----------	---------	-------	-------	---------	-------

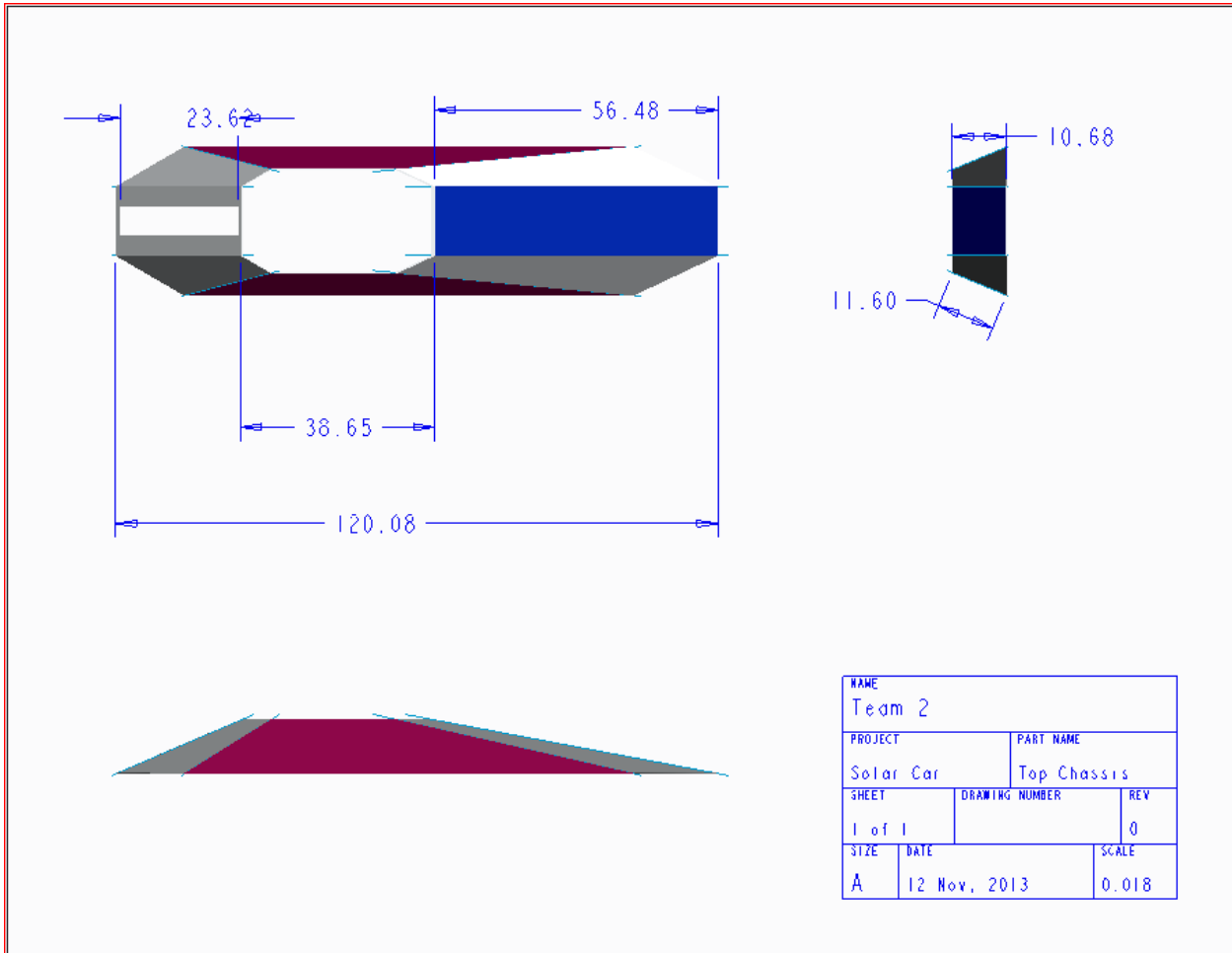
43	2.61	172	47.05	24.05	3.04	73.21	64.3
44	2.88	172	51.74	24.05	3.26	78.43	66.0
45	2.98	171	53.48	24.05	3.34	80.36	66.5
46	3.18	171	56.93	24.04	3.50	84.23	67.6
47	3.45	170	61.56	24.04	3.72	89.45	68.8
48	3.58	170	63.77	24.04	3.83	91.97	69.3
49	3.74	170	66.49	24.04	3.95	95.06	69.9
50	4.04	169	71.56	24.04	4.20	100.86	71.0
51	4.41	168	77.76	24.03	4.49	108.01	72.0
52	4.35	168	76.76	24.03	4.45	106.85	71.8
53	4.65	168	81.75	24.03	4.69	112.65	72.6
54	5.08	167	88.83	24.03	5.03	120.95	73.4
55	5.27	167	91.93	24.02	5.19	124.62	73.8
56	5.37	166	93.56	24.02	5.27	126.55	73.9
57	5.70	166	98.90	24.02	5.53	132.92	74.4
58	5.74	166	99.54	24.02	5.57	133.70	74.5
59	6.07	165	104.83	24.02	5.83	140.06	74.8
60	6.36	164	109.43	24.01	6.07	145.66	75.1
61	6.61	164	113.37	24.01	6.27	150.48	75.3
62	6.87	163	117.44	24.01	6.48	155.50	75.5
63	7.31	162	124.26	24.00	6.83	163.98	75.8
64	7.33	162	124.57	24.00	6.85	164.37	75.8
65	7.66	162	129.62	24.00	7.11	170.73	75.9
66	8.12	161	136.59	24.00	7.48	179.59	76.1
67	8.14	161	136.89	24.00	7.50	179.98	76.1
68	8.50	160	142.28	23.99	7.79	186.91	76.1
69	8.59	160	143.61	23.99	7.86	188.64	76.1
70	8.94	159	148.78	23.99	8.14	195.38	76.1
71	9.16	158	152.00	23.99	8.32	199.62	76.1

72	9.56	158	157.80	23.98	8.64	207.32	76.1
73	9.96	157	163.53	23.98	8.97	215.01	76.1
74	10.04	157	164.67	23.98	9.03	216.55	76.0
75	10.43	156	170.18	23.97	9.35	224.05	76.0
76	10.58	155	172.28	23.97	9.47	226.94	75.9
77	10.99	155	177.97	23.97	9.80	234.82	75.8
78	11.46	154	184.41	23.97	10.18	243.85	75.6
79	11.56	153	185.76	23.96	10.26	245.77	75.6
80	12.00	153	191.68	23.96	10.61	254.23	75.4
81	12.13	152	193.41	23.96	10.72	256.72	75.3
82	12.50	151	198.30	23.96	11.01	263.83	75.2
83	12.70	151	200.92	23.95	11.17	267.67	75.1
84	13.29	150	208.54	23.95	11.65	278.99	74.7
85	13.40	150	209.94	23.95	11.74	281.10	74.7
86	13.89	149	216.13	23.94	12.13	290.50	74.4
87	13.95	148	216.88	23.94	12.18	291.65	74.4
88	14.29	148	221.10	23.94	12.46	298.17	74.2
89	14.63	147	225.28	23.94	12.73	304.69	73.9
90	15.10	146	230.96	23.93	13.11	313.69	73.6
91	15.15	146	231.56	23.93	13.15	314.65	73.6

说明	转矩 (N.m)	转速 (r/min)	输出功率 (W)	电压 (V)	电流 (A)	输入功率 (W)	效率 (%)
92	15.42	145	234.78	23.93	13.37	319.82	73.4
93	15.82	145	239.48	23.92	13.69	327.49	73.1
94	16.12	144	242.97	23.92	13.93	333.23	72.9
95	16.46	143	246.87	23.92	14.20	339.74	72.7
96	16.78	143	250.50	23.91	14.46	345.86	72.4
97	17.32	141	256.51	23.91	14.90	356.19	72.0
98	17.37	141	257.06	23.91	14.94	357.15	72.0
99	17.64	141	260.02	23.91	15.16	362.31	71.8

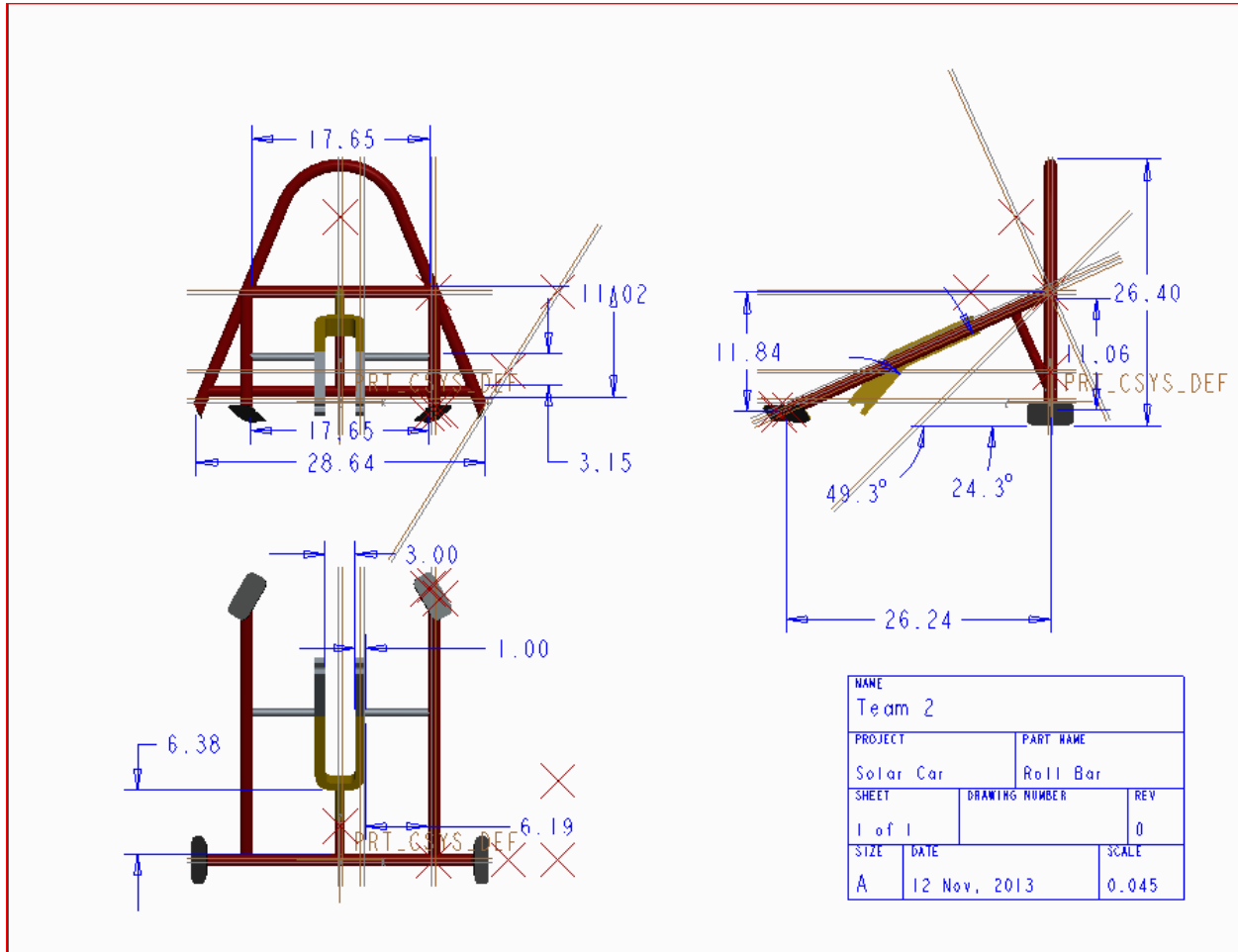
100	18.02	140	264.12	23.90	15.46	369.57	71.5
101	18.34	139	267.53	23.90	15.72	375.69	71.2
102	18.90	138	273.38	23.89	16.17	386.39	70.8
103	19.00	138	274.41	23.89	16.25	388.30	70.7
104	19.29	137	277.38	23.89	16.48	393.84	70.4
105	19.88	136	283.30	23.89	16.96	405.10	69.9
106	20.05	136	284.98	23.88	17.10	408.35	69.8
107	20.48	135	289.16	23.88	17.44	416.55	69.4
108	20.60	135	290.32	23.88	17.54	418.84	69.3
109	21.02	134	294.31	23.87	17.88	426.85	68.9
110	21.30	133	296.92	23.87	18.10	432.19	68.7
111	21.75	132	301.06	23.87	18.47	440.77	68.3
112	22.01	132	303.40	23.87	18.68	445.72	68.1
113	22.43	131	307.14	23.86	19.01	453.72	67.7
114	22.63	130	308.88	23.86	19.18	457.53	67.5

A5: Chassis

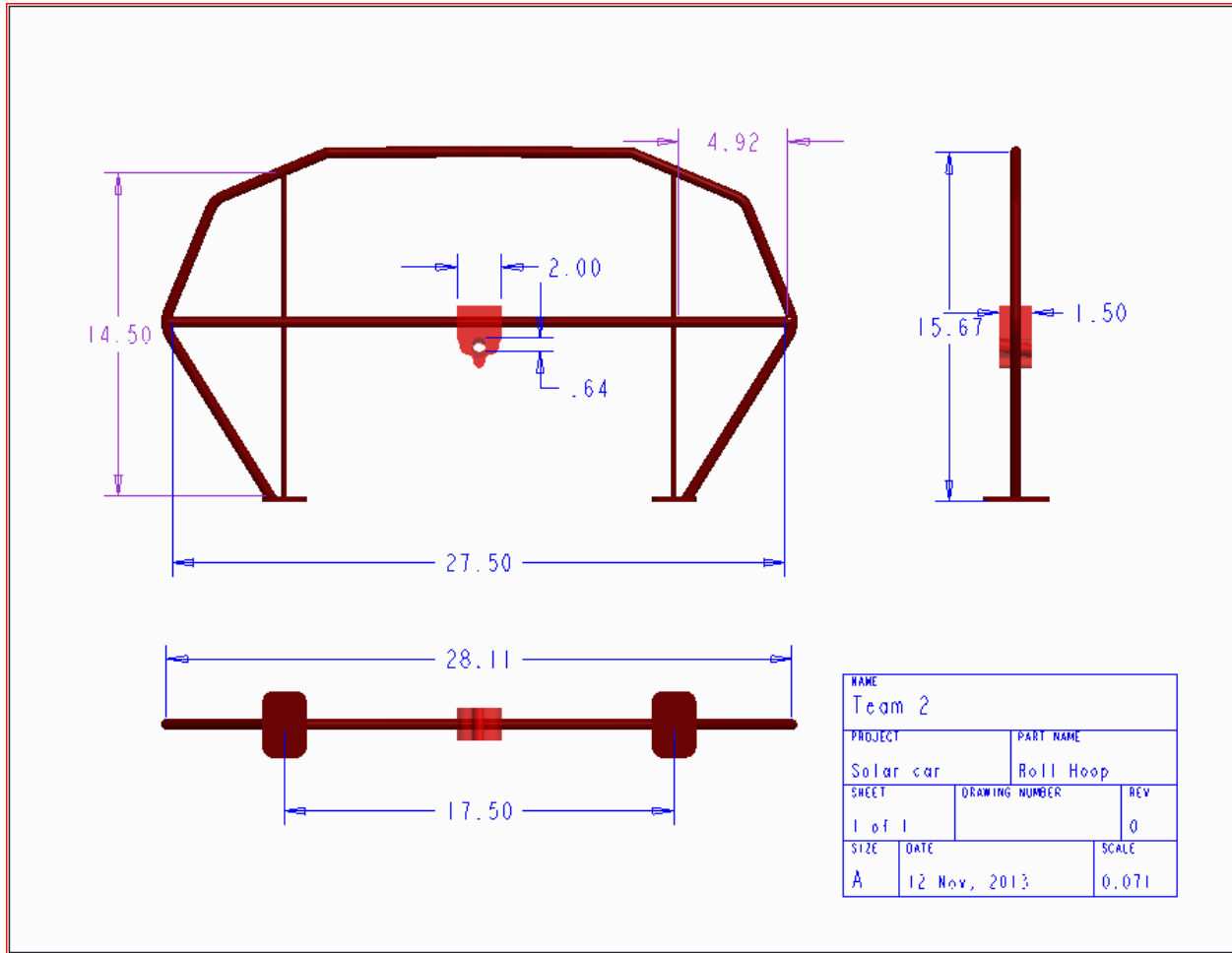


NAME		
Team 2		
PROJECT		PART NAME
Solar Car		Top Chassis
SHEET	DRAWING NUMBER	REV
1 of 1		0
SIZE	DATE	SCALE
A	12 Nov, 2013	0.018

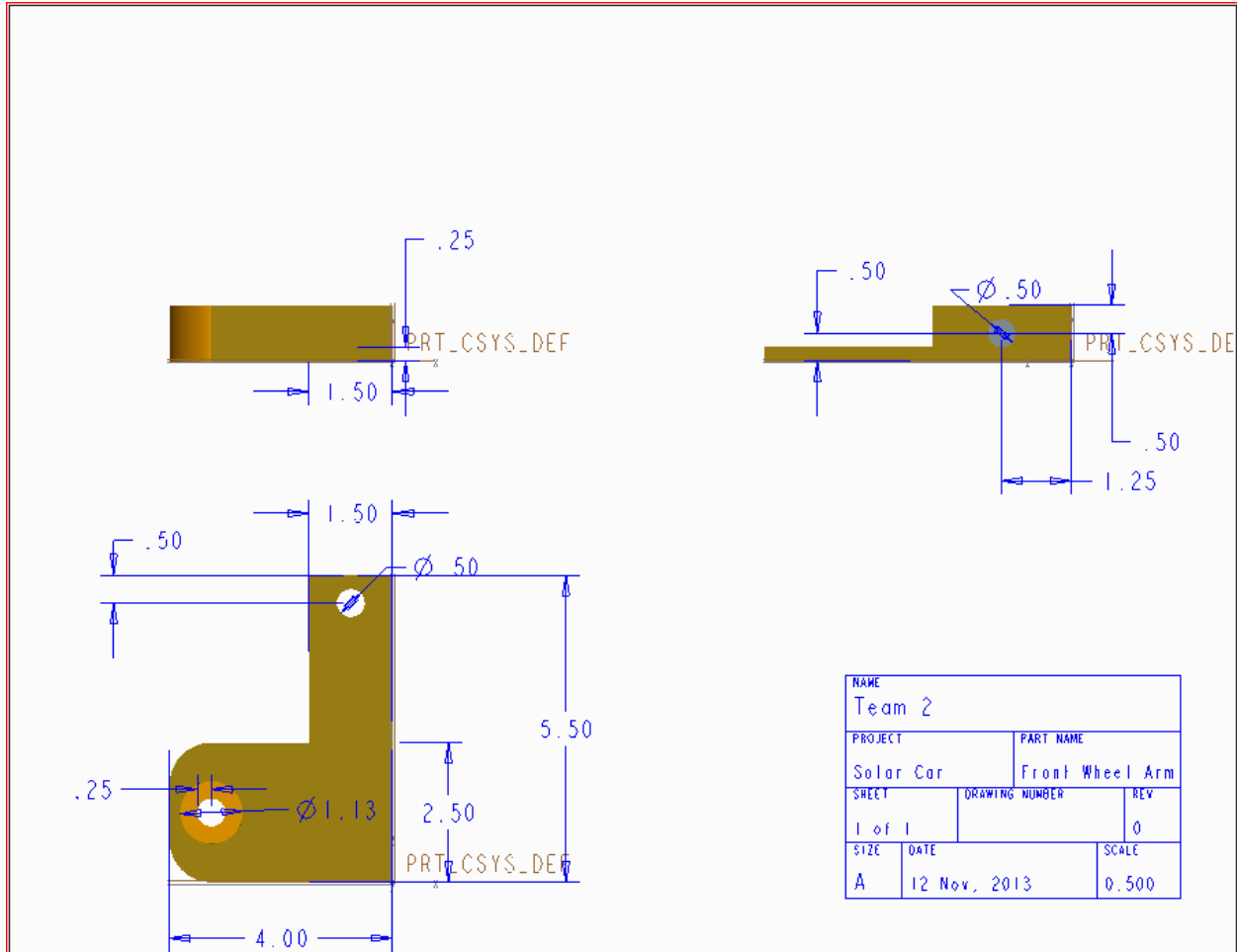
A6: Roll Bar and Rear Wheel Mount



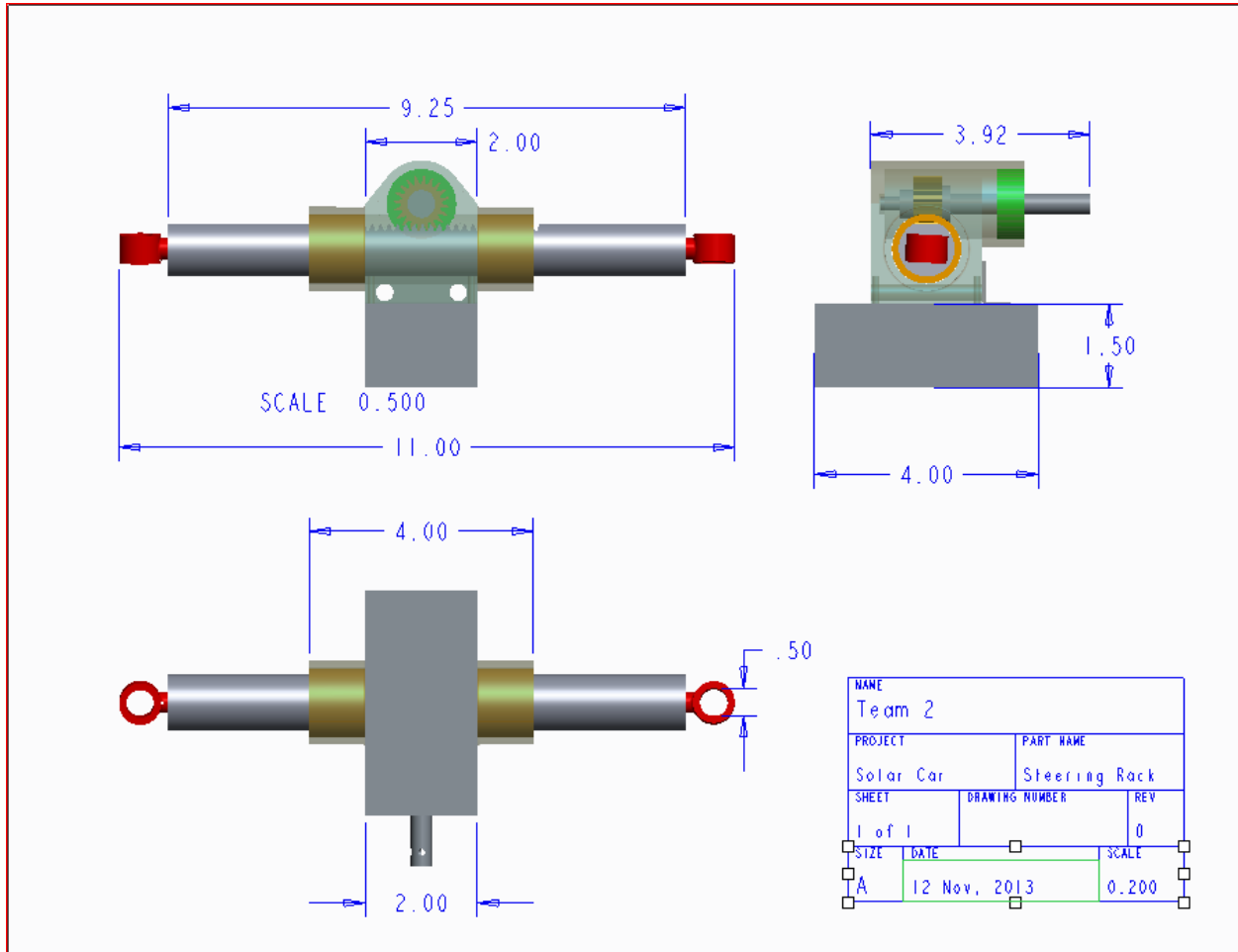
A7: Roll Hoop



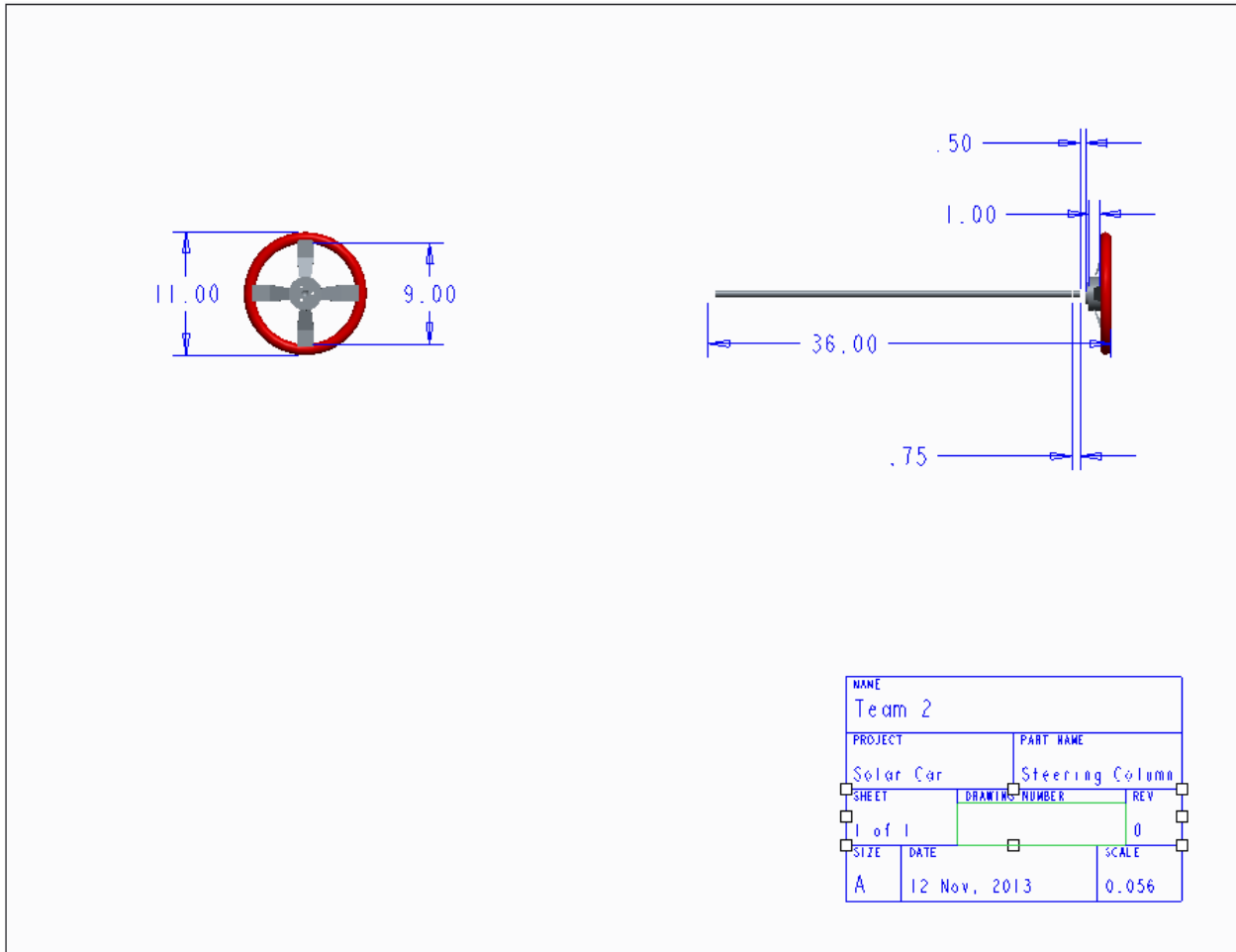
A8: Front Wheel Arm



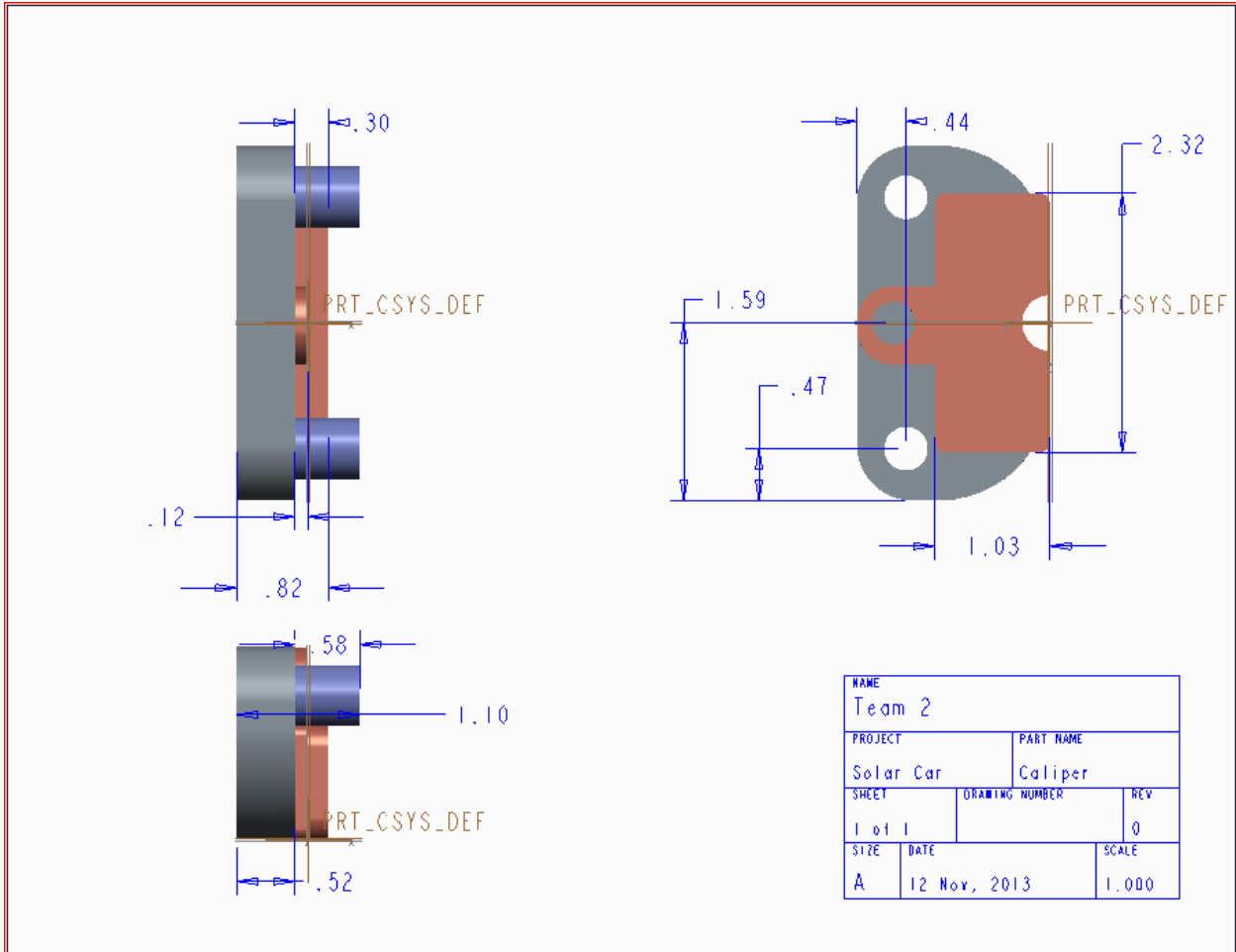
A9: Rack and Pinion



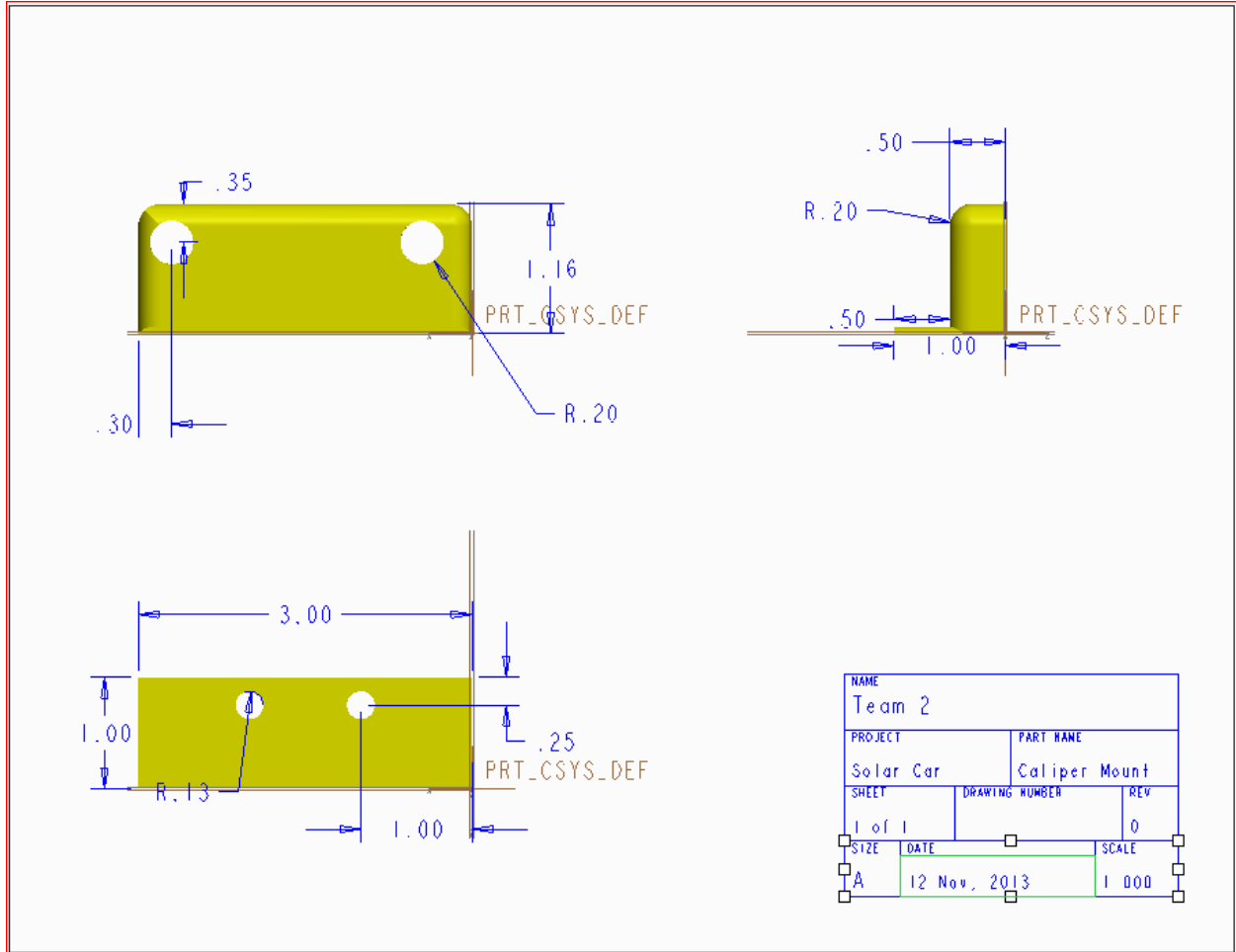
A10: Steering Wheel



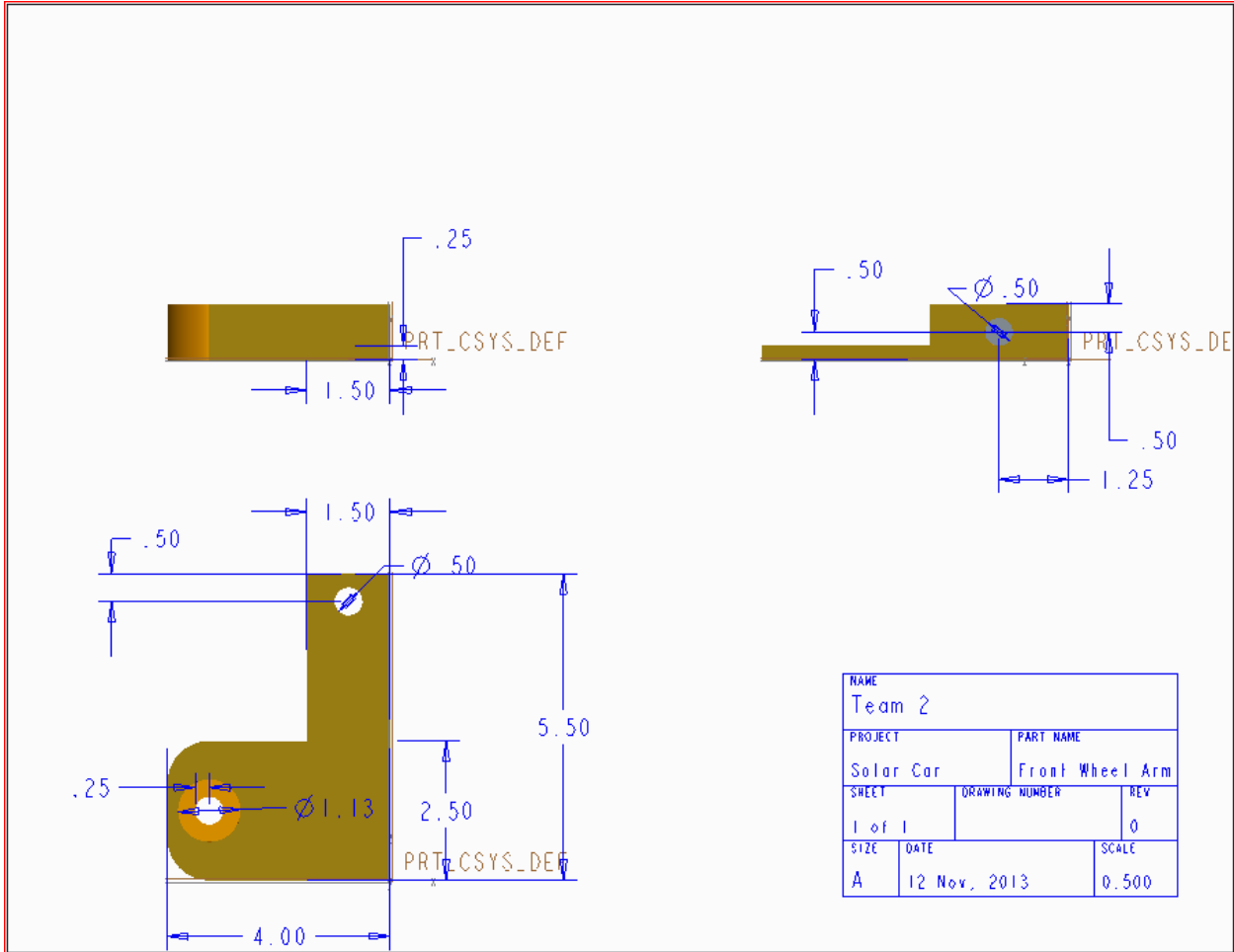
A11: Calipers



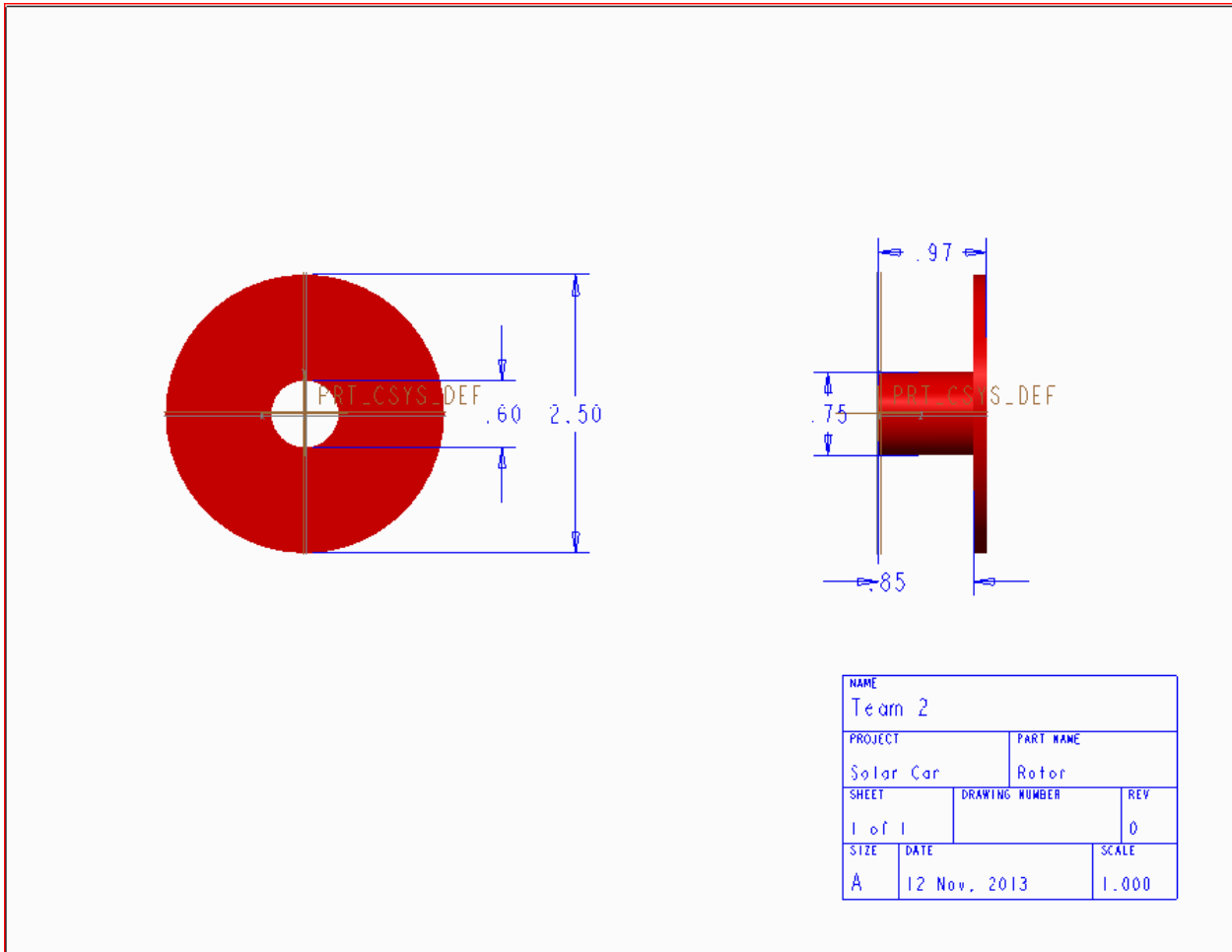
A12: Caliper Mounts



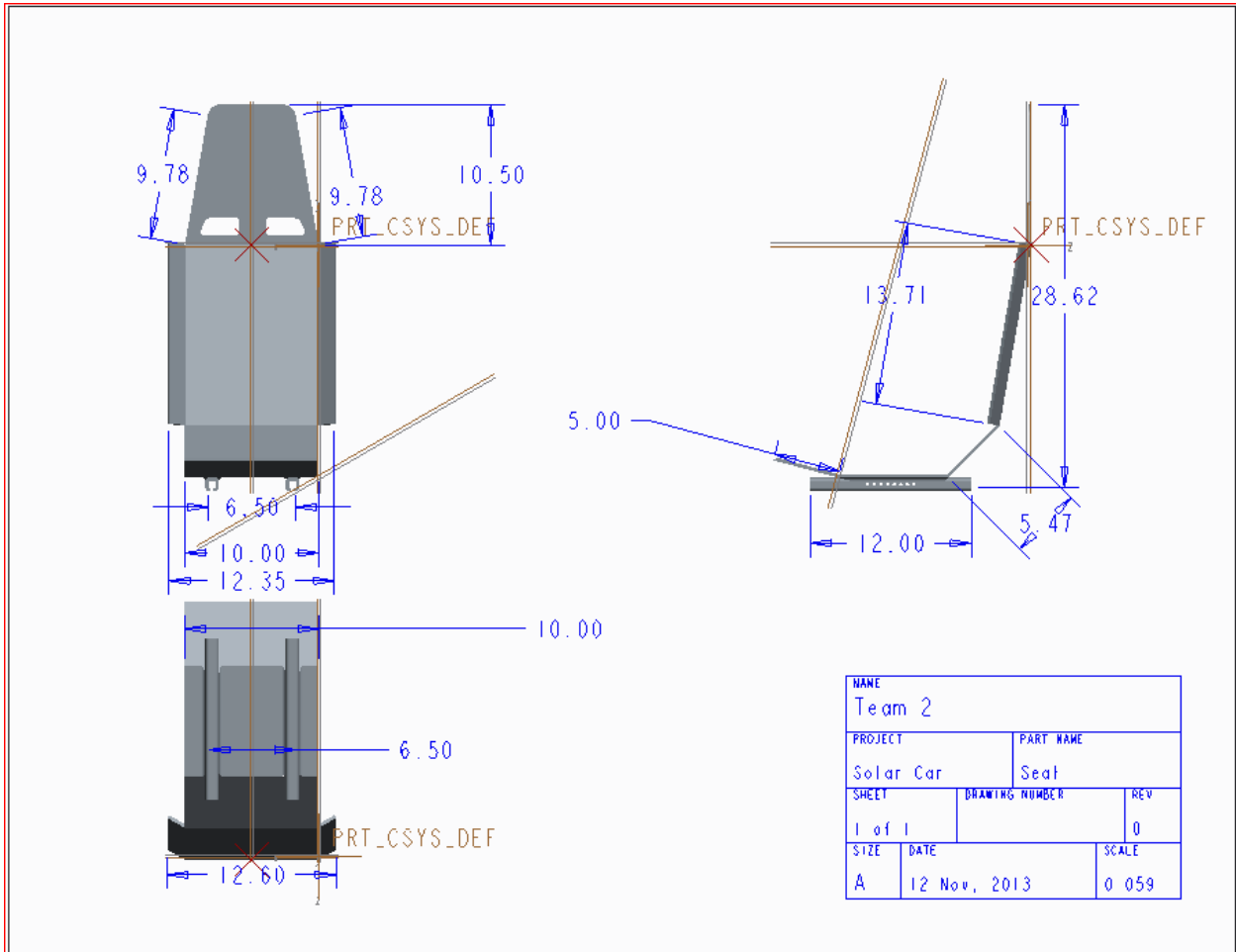
A13: Front Wheel Arm



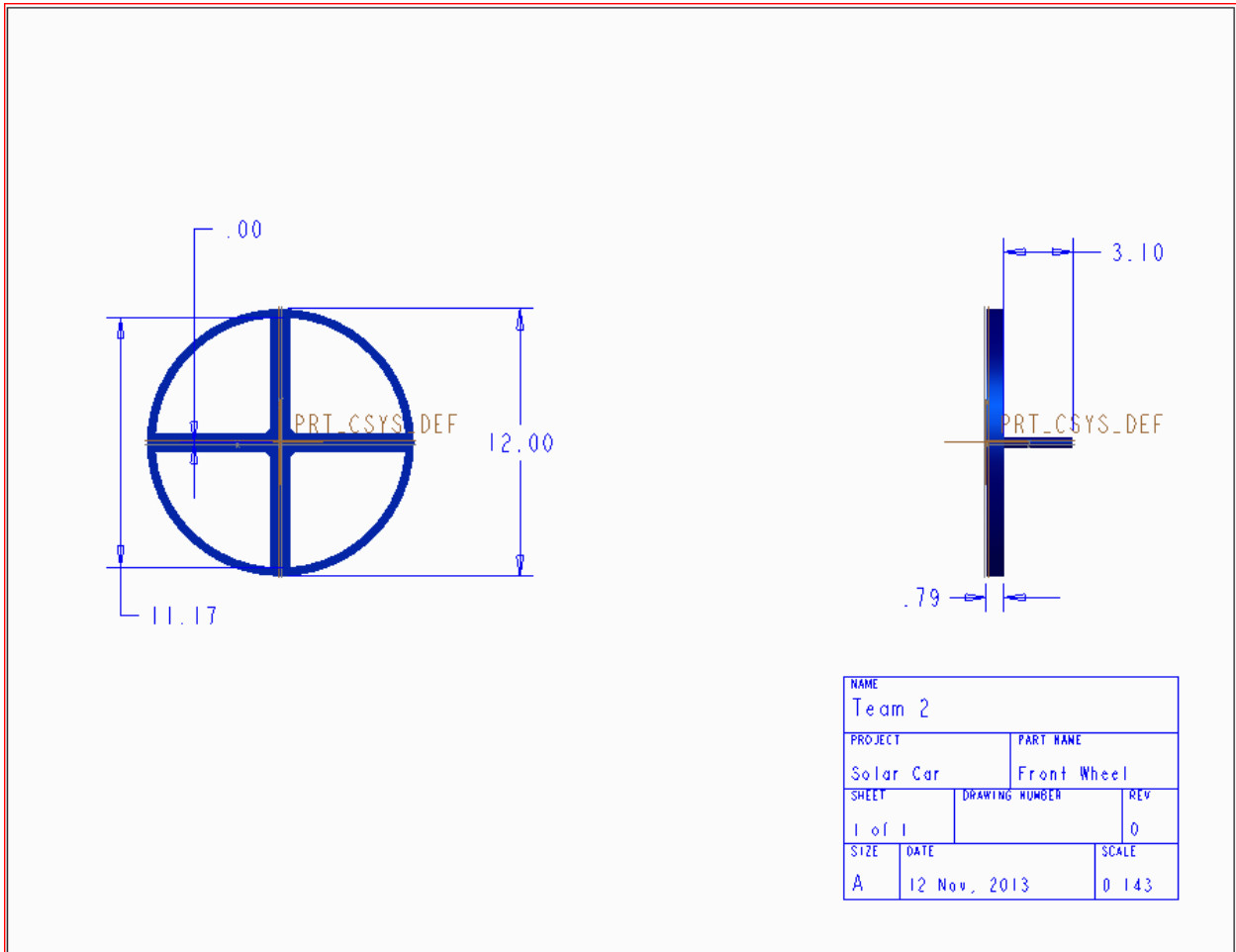
A14: Rotor



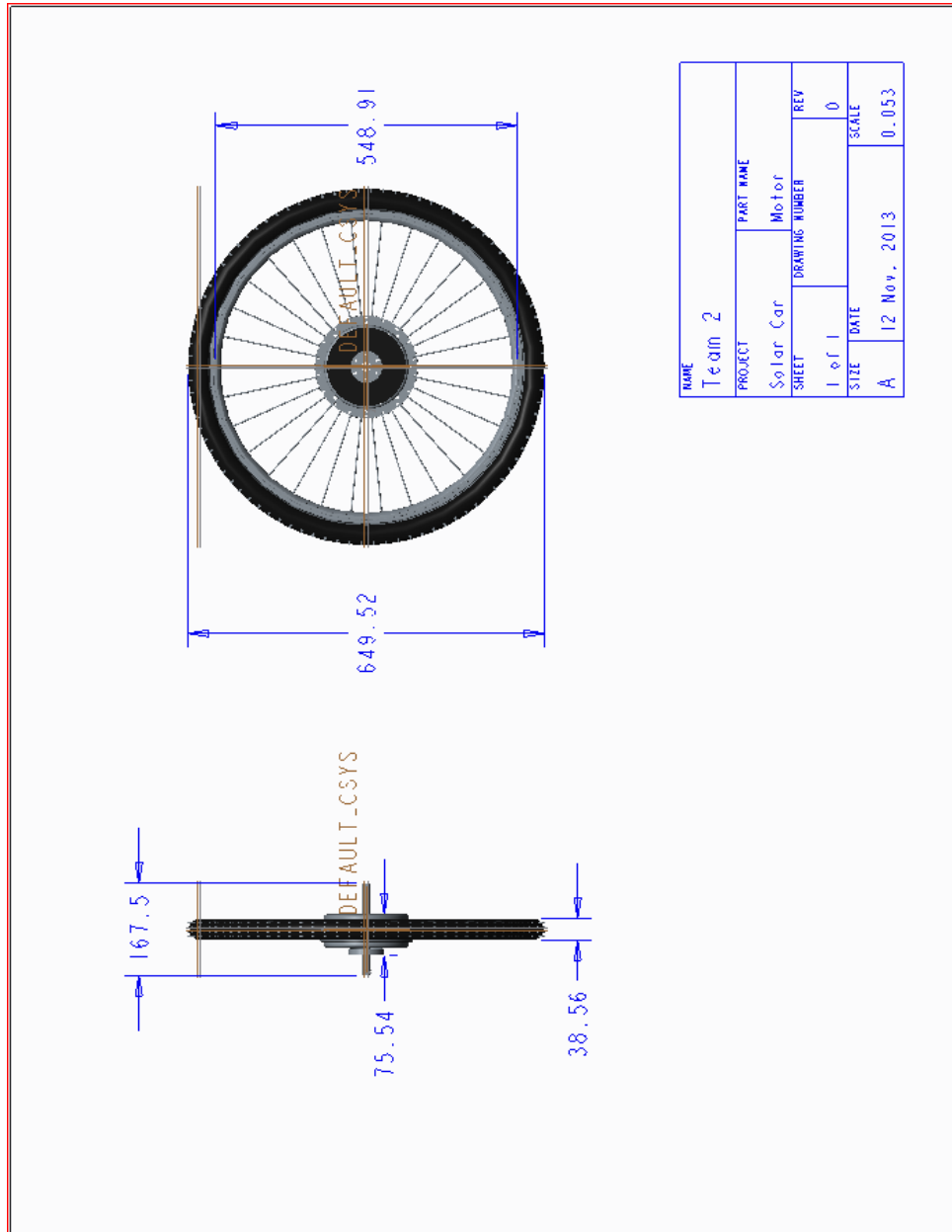
A15: Seat



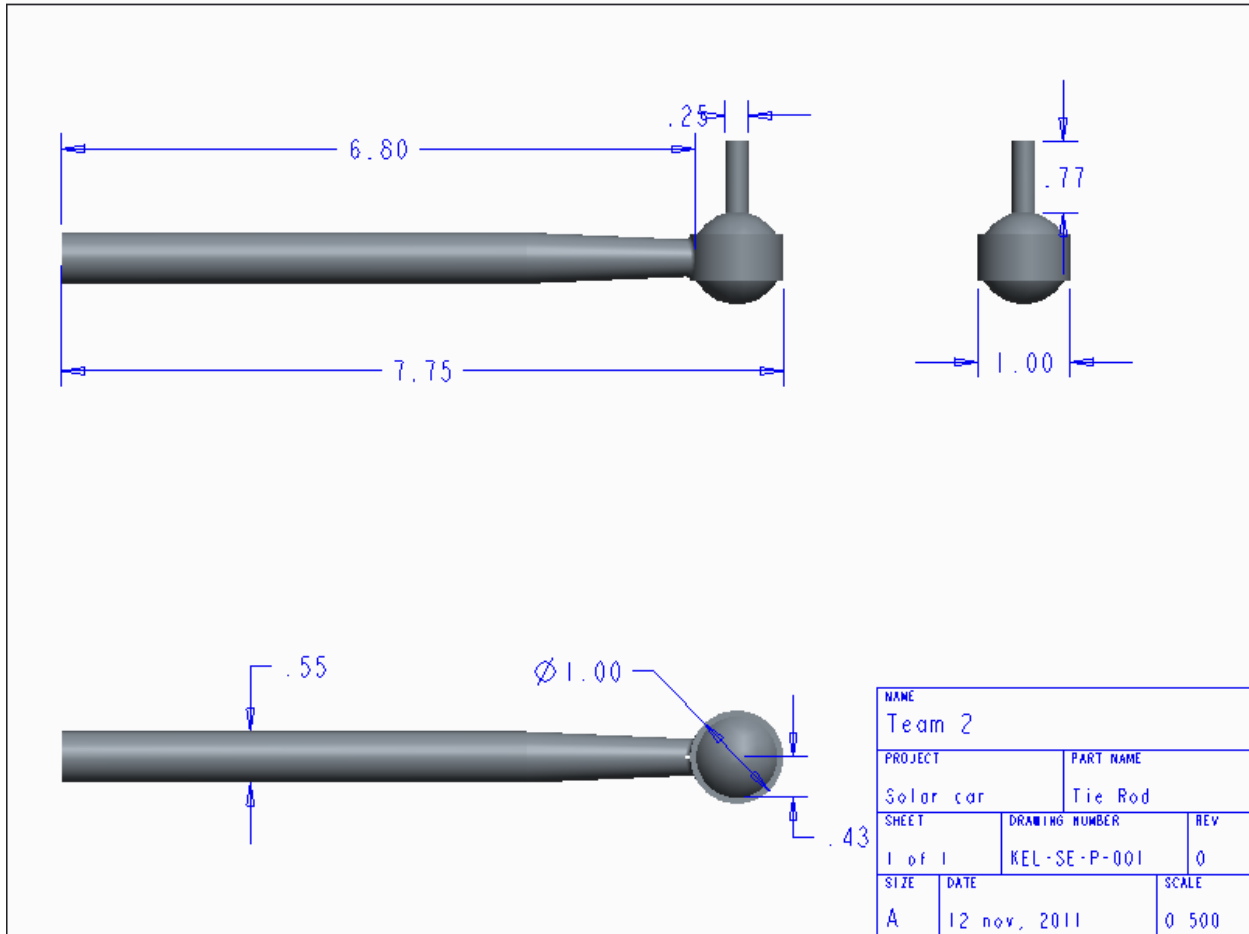
A16: Front Wheels



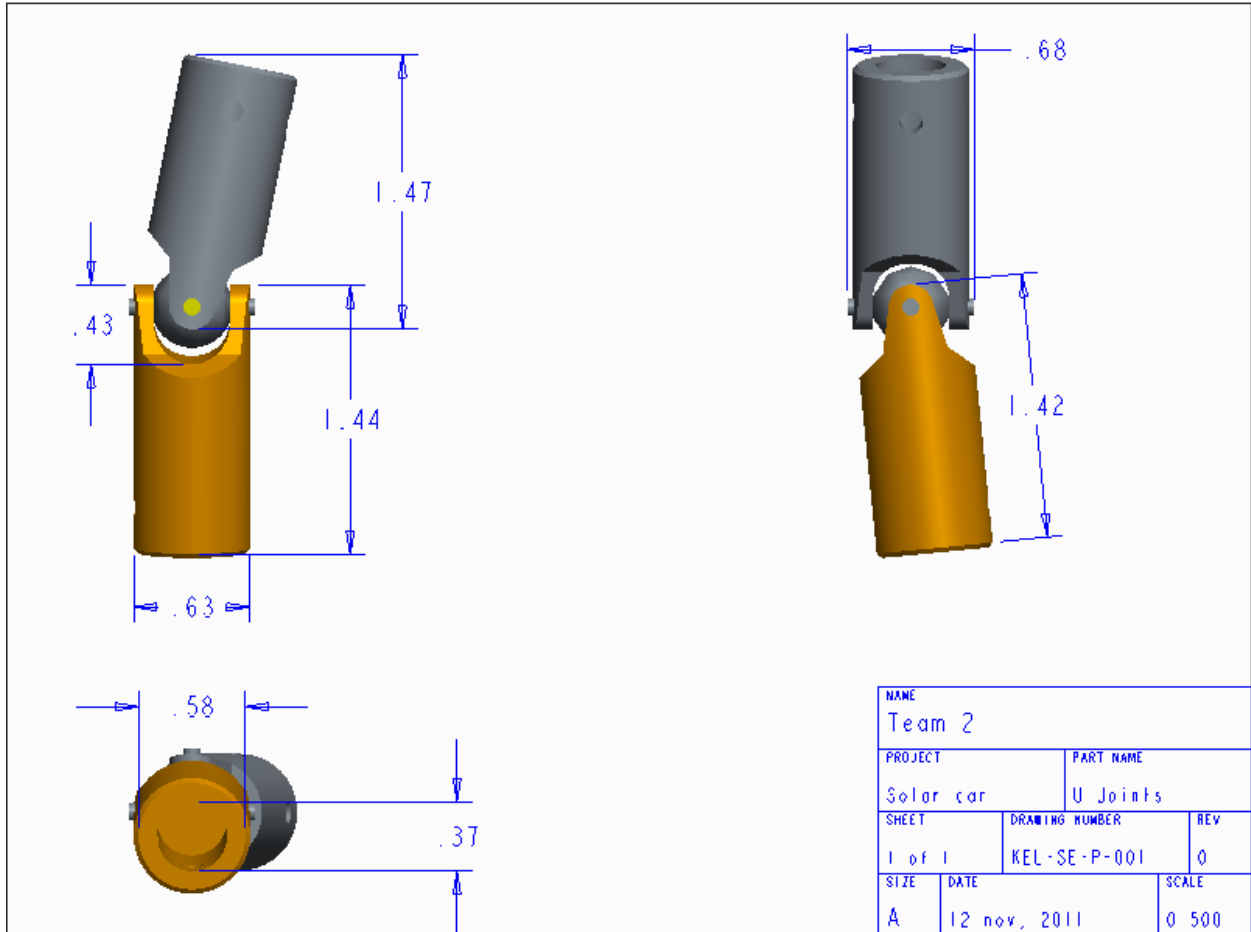
A17: Rear Wheel



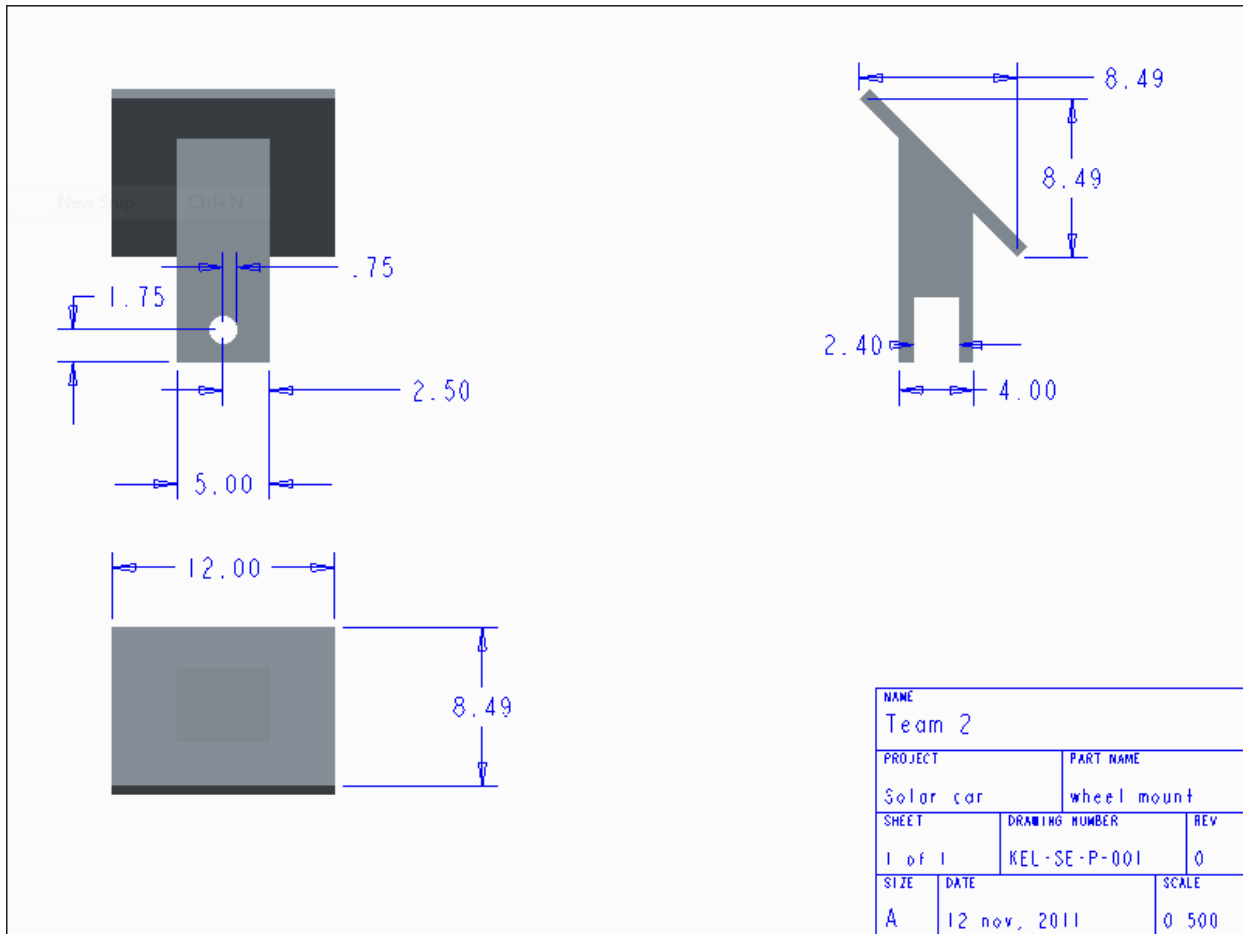
A18: Tie Rods



A19: Steering U-Joints



A20: Front Wheel Mounts



A21: Czochralski Process

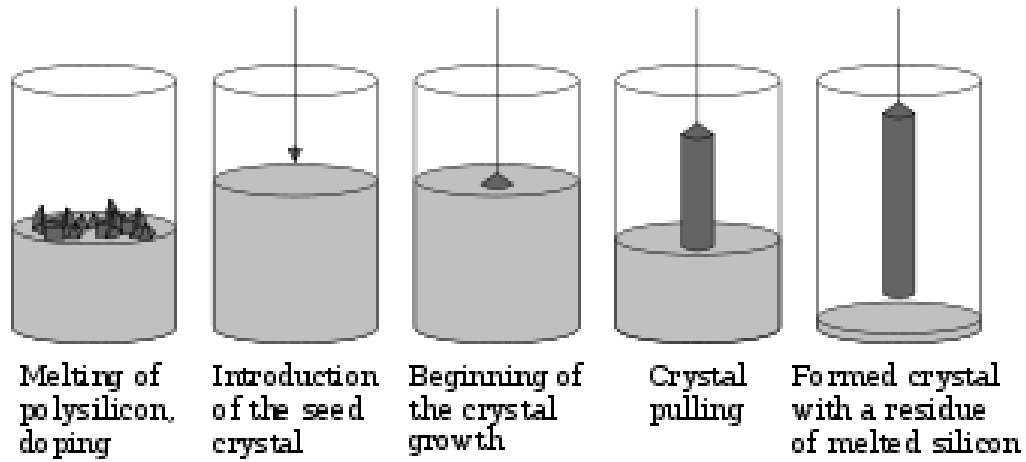


FIGURE 48 DIAGRAM DEMONSTRATING THE CZOCHRALSKI PROCESS

The Czochralski process is a process used in the production of monocrystalline solar cells. Briefly, the process consists of dissolving by melting the silicon in the crucible. The seed crystal used form the crystal is introduced in order to begin crystal growth. The seed is then pulled from the crucible which forms the silicon crystal.

A22 Solar Cell Technical Specifications

Irradiance (W/m^2)	$V_{p,m}$	$I_{p,m}$
1000	1.000	1.000
800	0.992	0.799
600	0.979	0.598
200	0.922	0.193

TABLE 19 SOLAR CELL IRRADIATION PROFILE

Current Temp Coefficients	$\alpha(I_{sc})$	0.03%/°C
Voltage Temp Coefficients	$\beta(V_{oc})$	-0.32%/°C
Power Temp Coefficients	$\gamma(P_{max})$	-0.42%/°C

TABLE 20 SOLAR CELL TEMPERATURE COEFFICIENTS

Efficiency Cell (%)	Power (W)	Max Current (A)	Min Current (A)	Short Circuit Current (A)	Max Voltage (V)	Open Circuit Voltage (V)
18-18.19%	2.67-2.7	5.07	4.19	5.42	0.53	0.628
17.8-17.00%	2.64-2.67	5.02	4.87	5.4	0.528	0.628
17.6-17.79%	2.61-2.63	5.02	4.86	5.37	0.524	0.625
17.4-17.59%	2.59-2.61	4.98	4.83	5.34	0.522	0.624
17.2-17.39%	2.56-2.59	4.93	4.79	5.3	0.522	0.623
17-17.19%	2.53-3.56	4.91	4.77	5.29	0.518	0.621
16.8-16.99%	2.5-2.53	4.88	4.73	5.26	0.516	0.620
16.6-16.79%	2.47-2.5	4.85	4.7	5.23	0.513	0.619
16.4-16.59%	2.44-2.47	4.82	4.67	5.21	0.511	0.618
16.2-16.39%	2.41-2.44	4.79	4.64	5.18	0.509	0.616
16-16.19%	2.38-2.41	4.76	4.61	5.15	0.506	0.615

TABLE 21 SOLAR CELL ELECTRICAL PERFORMANCE

A23: Sanyo Denki Fan and Specifications



FIGURE 49 SANYO DENKI FAN

Specifications									
Model No.	Rated Voltage (V)	Operating voltage range (V)	Rated current (A)	Rated input (W)	Rated speed (min ⁻¹)	Air flow (m ³ /min)	Static pressure (Pa)	Noise (dB[A])	Mass (g)
109BF12HC2	12	10.2 to 13.8	0.6	7.2	2,400	0.78 (27.5CFM)	175.4 (0.704inchH2O)	52	270

FIGURE 50 SANYO DENKI FAN SPECIFICATIONS

A24: Isolated DC-DC Converter Specifications

	LM25017
I _{out} (Max) (A)	0.65
V _{in} (Min) (V)	9
V _{in} (Max) (V)	48
V _{out} (Min) (V)	1.25
V _{out} (Max) (V)	40
I _q (Typ) (mA)	1.75
Switching Frequency (Max) (kHz)	1000
Switch Current Limit (Typ) (A)	1.3
Topology	Buck
Operating Temperature Range (C)	-40 to 125
Pin/Package	8SO PowerPAD 8WSON
Approx. Price (US\$)	1.25 1ku
Rating	Catalog
Duty Cycle (Max) (%)	90
Control Mode	Constant on-time (COT)
Regulated Outputs (#)	1

FIGURE 51 SPECIFICATIONS FOR THE LM25017 ISOLATED DC-DC CONVERTER

A25: LM5000 DataSheet

Absolute Maximum Ratings

V_{IN}		-0.3V to 40V
SW Voltage		-0.3V to 80V
FB Voltage		-0.3V to 5V
COMP Voltage		-0.3V to 3V
All Other Pins		-0.3V to 7V
Maximum Junction Temperature		150°C
Power Dissipation ⁽⁶⁾		Internally Limited
Lead Temperature		216°C
Infrared (15 sec.)		235°C
ESD Susceptibility ⁽⁴⁾	Human Body Model	2kV
	Machine Model	200V
Storage Temperature		-65°C to +150°C

A26: Bill of Materials

Solar Car Parts List:		
Quantity:	Type:	Name:
1	Part	Chassis Bottom
2	Part	Front Wheel Mount
1	Part	Roll bar
1	Part	Seat
1	Sub-Assembly	Rack and Pinion
1	Part	Motor
1	Part	Roll Hoop
1	Part	Chassis Top
2	Sub-Assembly	Front Steering Assembly
1	Part	Steering Housing
1	Sub-Assembly	Steering Column
1	Part	Intermediate Steering Shaft
2	Part	U-Joint
2	Part	U-Ball
2	Part	Front Wheel
2	Part	Front Brake Base
2	Part	Front Brake Caliper
2	Part	Front Wheel Rotor
2	Sub-Assembly	Tie Rod Set
2	Sub-Assembly	Brake Pedal
1	Part	Solar Panel Box

Steering Sub Assembly:		
Quantity:	Type:	Name:
1	Sub-Assembly	Front Steering Assembly
1	Part	Front Wheel
1	Part	Front Brake Base
1	Part	Rotor
2	Part	Front Brake Caliper
2	Part	Bearings

Brake Pedal Assembly:		
Quantity:	Type:	Name:
1	Sub-Assembly	Brake Pedal Assembly
2	Part	Brake Pedal Housing
2	Part	Brake Pedal

A27 Stress Calculation Results

Front Mount Stress Calculation Results and Constants

Rim/Pipe:	Normal Stress σ_y (psi):	Shear τ_{xy} (psi):	σ_1	σ_2	τ_{max} in plane	σ_{avg}	Shear Safety Factor AI 2014:	Shear Safety Factor AI 6061:
12 in Rims A piping	429.572	30.224	431.688	-2.116	216.902	214.786	115.259	87.537
12 in. Rims B piping	1647.102	47.494	1648.470	-1.368	824.319	823.551	30.306	23.033
12 in. Rims C piping	2720.876	88.656	2723.762	-2.886	1363.324	1360.438	18.338	13.937
12 in. Rims D piping	4434.505	66.492	4435.502	-0.997	2218.249	2217.252	11.270	8.565
16 in Rims A piping	763.684	30.224	764.878	-1.194	383.036	381.842	65.268	49.604
16 in. Rims B piping	2328.181	47.494	2328.951	-0.770	1464.861	1464.091	17.066	12.971
16 in. Rims C piping	4837.113	88.656	4838.738	-1.624	2420.181	2418.557	10.330	7.851
16 in. Rims D piping	7883.564	66.492	7884.125	-0.561	3942.343	3941.782	6.341	4.819
18 in Rims A piping	966.537	30.224	967.481	-0.944	484.213	483.269	51.630	39.239
18 in. Rims B piping	3705.979	47.494	3706.588	-0.609	1853.598	1852.990	13.487	10.250
18 in. Rims C piping	6121.971	88.656	6123.255	-1.284	3062.269	3060.986	8.164	6.205
18 in. Rims D piping	9977.636	66.492	9978.079	-0.443	4989.261	4988.818	5.011	3.808
20 in Rims A piping	1193.256	30.224	1194.021	-0.765	597.393	596.628	41.849	31.805
20 in. Rims B piping	4575.283	47.494	4575.776	-0.493	2288.134	2287.641	10.326	8.304
20 in. Rims C piping	7557.989	88.656	7559.029	-1.040	3780.034	3778.935	6.614	5.026
20 in. Rims D piping	12318.063	66.492	12318.428	-0.359	6159.394	6159.035	4.053	3.085

Front Mount Moment Calculation Results and Constants

Wheel Width (in):	Length from plate to kingpin (in):	Moment (lbs ² in):	Normal Force Per Wheel (lbs):	Length from Chassis to wheel mounting point
12.000	4.250	353.239	83.115	7.250
16.000	5.667	470.985		8.667
18.000	6.375	529.858		9.375
20.000	7.083	588.731		10.083
22.000	7.792	647.604		10.792

Square Tube Calculation Results and Constants

Square Tube (Outside length, Inside Length):	Moment of Inertia (in ⁴):	Neutral Axis (in):	Area of Square Tube (in ²):
A. 3x3x1/4 (3,2.5)	3.495	1.500	2.750
B. 2x2x1/4 (2, 1.5)	0.911	1.000	1.750
C. 2x2x1/8 (2, 1.75)	0.552	1.000	0.938
D. 1.5x1.5x1/4 (1.5, 1)	0.339	0.750	1.250

Wheel Hub Bolt Calculation Results and Constants

Diameter (in):	Area (in ²):	Inertia (in ⁴):	Direct Shear (psi):	Distance from Centroid (in):	Moment (lbs ² in):	Normal Stress σ_y (psi):
0.250	0.049	0.000	1634.064	0.000	602.584	1205.168
0.500	0.196	0.003	423.516	0.006	720.330	1440.660
0.750	0.442	0.016	188.229	0.031	779.203	1558.406
1.000	0.785	0.049	105.879	0.098	838.076	1676.153
τ_{xy} :	σ_y :	σ_x :	σ_1 :	σ_2 :	$\tau_{max \text{ in plane}}$:	σ_{avg} :
1634.064	1205.168	0.000	2400.627	-1195.459	1798.043	602.584
423.516	1440.660	0.000	1555.938	-115.278	835.608	720.330
188.229	1558.406	0.000	1580.819	-22.413	801.616	779.203
105.879	1676.153	0.000	1682.814	-6.662	844.738	838.076
Material:	Modulus of Rigidity (G) (ps	Yield Strength-Shear (psi):	Shear Safety Factor (0.25):	Shear Safety Factor (0.5):	Shear Safety Factor (0.75):	Shear Safety Factor (1.00):
Aluminum 2014-T6	3900.000	25000.000	13.904	29.918	31.187	29.595
Aluminum 6061-T6	3700.000	19000.000	10.567	22.738	23.702	22.492
Steel Structural A36	11000.000	20700.000	11.513	24.772	25.823	24.505
Steel Stainless 304	11000.000	17300.000	9.622	20.703	21.581	20.480
Steel Tool L2	11000.000	58800.000	32.702	70.368	73.352	69.607
Titanium Ti-6Al-4V	6400.000	77360.000	43.025	92.579	96.505	91.579